Tumor Suppression by ARF in Carcinogen-Exposed Mice

Stephanie E Busch

A dissertation

submitted in partial fulfillment of the

requirements for the degree of

Doctor of Philosophy

University of Washington

2012

Reading Committee:

Christopher J Kemp, Chair

William Grady

Bradley D Preston

Program Authorized to Offer Degree:

Molecular and Cellular Biology

University of Washington

Abstract

Tumor Suppression by ARF in Carcinogen-Exposed Mice

Stephanie E Busch

Chair of the Supervisory Committee:
Affiliate Professor Christopher J Kemp
Department of Pathology

The *ARF* tumor suppressor gene, encoded along with a second tumor suppressor, $p16^{INK4a}$, at the *CDKN2A* locus, is frequently inactivated in human cancers. However, the close proximity of *ARF* and $p16^{INK4a}$ lends itself to the concurrent loss of both genes, raising important questions about the specific contribution of ARF to tumor suppression *in vivo*. Multiple lines of evidence indicate that sustained signaling from oncogenes such as RAS or MYC induces the expression of ARF, which then stabilizes p53 activity to arrest cell proliferation. To address the role of ARF in RAS-driven cancers, we exposed wild-type and *Arf*-deficient mice to two separate carcinogens, ethyl carbamate (urethane) and 7,12-dimethylbenz[*a*]anthracene (DMBA). *Arf*-deficiency facilitated the growth and malignant progression of lung adenocarcinomas after urethane exposure. A subset of lung tumors in *Arf*-deficient animals presented as poorly differentiated and metastatic, with many characteristics of pulmonary sarcomatoid carcinoma, a transitional tumor type previously undocumented in mice. Unexpectedly, urethane injection also resulted in the development of hepatic vascular tumors in *Arf*-deficient animals. Suppression of hemangioma development by ARF was strongly

influenced by mouse genetic strain and was likely p53-dependent. Subjection of mice to the DMBA/TPA two-step skin carcinogenesis protocol further revealed that ARF inhibits the metastatic spread of carcinoma cells. The pro-invasion and metastasis phenotype of *Arf*-deficient carcinomas was apparent at the transcriptional level, and our data provide preliminary evidence of a role for ARF in regulating the epithelial-mesenchymal transition program. Taken together, these studies demonstrate that induction of ARF is an early response in carcinogenesis that mounts an effective barrier against tumor growth, invasion, and metastasis. For this reason, *ARF* status may have important implications for cancer patient prognosis and clinical management.

TABLE OF CONTENTS

LIST OF FIGURES

LIST OF TABLES

ACKNOWLEDGEMENTS

Many individuals have assisted in the completion of this work. First and foremost, I am grateful for the support of my graduate research supervisor, Chris Kemp. Without his counsel, this work would not exist.

I would also like to thank my doctoral supervisory committee: Katie Peichel, Wenqing Xu, Jonathan Cooper, and especially Bill Grady and Brad Preston, who served as readers.

Karen Kelly-Spratt has been a phenomenal mentor during my time in the Kemp lab. In many ways, my research is a continuation of her work, and the reagents and guidance she provided have been invaluable.

My research has been heavily reliant on histopathology, and most of the histochemistry included in this dissertation was performed by Kay Gurley, the Kemp lab manager and resident histology guru. Thanks for never clubbing me when I handed over "*just one more*" staining request sheet, Kay.

Russell Moser is the kind of coworker every graduate student wishes for. He knows something about everything, he is always willing to share what he knows, and if (by some chance) he doesn't know the answer to your question, he won't rest until he helps you find it. His ideas have helped shape many of my experiments, and I could not be more grateful.

My thanks to Denny Liggitt and Sue Knoblaugh for their assistance in analyzing tumor pathology, and to Julie Randolph-Habecker and Brian Johnson for chipping in with two special IHC stains. Elizabeth Jensen performs her job with professionalism and empathy, and I have often been the appreciative recipient of both. Also, my studies could not have been performed without the assistance of the staff and technicians in Comparative Medicine.

Susan Tilton analyzed the microarray data described in Chapter Four. Kyung Hoon-Kim performed some of the experiments on *Trp53*-deficient mice described in Chapter Three. Other past and affiliate members of the lab have provided supplies and advice, including Shawn Bailey, Anne Grosse-Wilde, and the teams under Alanna Ruddell and Gala Filippova.

I would also like to thank Don Anderson and the members of the Galloway, Porter, Grandori, and Taniguchi labs for their open doors, their expertise, their toolkits, and their laughter.

My graduate school tenure has been greatly simplified by the incredible administrative staff at the FHCRC and UW. I am much obliged to Marci Wright, Elizabeth Lynch, Laima Abele, Michele Karantsavelos, MaryEllin Robinson, the entire MCB Program, and the CMBTG.

Finally, I must acknowledge the contributions made to this work by my friends – who provided companionship, sanity, and proofreading – and my family. This work is the product of a lifetime of encouragement by my family to learn, to grow, and to give back. No words could ever suffice, and so I am left to say, inadequately, thank you.

DEDICATION

For my teachers, of whom many have waged their own wars against cancer.
Some won. Too many lost. All were dedicated and courageous.

For my grandparents, Everett and Jean Peterson.

And for Laura R –
I wish you could have made the journey with me.

Chapter One

Introduction

Cancer Genetics: A Primer

Although many biological factors contribute to tumor development, cancer is, in essence, a disease of uncontrolled cell proliferation. The loss of control occurs on two levels. First, the cell experiences near constant pro-growth signaling. Second, the cell can no longer stop itself from responding – a situation analogous to faulty brakes on a runaway car. The genes responsible for mediating these pro- and anti-proliferative phenomena are respectively referred to as oncogenes and tumor suppressor genes. In cancer oncogenes become activated, and tumor suppressor genes are silenced. These alterations form the crux of cancer genetics.

The *RAS* Family

The first oncogenes identified were of viral origin. *RAS*, shorthand for "rat sarcoma," was initially found in a family of retroviruses that induced sarcoma formation in infected animals (Harvey 1964; Kirsten and Mayer 1967). The transforming genetic element contained within the retroviral sequence had been transduced (i.e. "stolen") from the rat genome (Scolnick et al. 1973; Scolnick and Parks 1974). Over the next two decades of research, the cellular homologue for *RAS* was found in mammalian tissues (Ellis et al. 1981; Chang et al. 1982), the endogenous RAS protein was characterized as an effector of mitogenic signals (Kamata and Feramisco 1984; Mulcahy et al. 1985), and mutant *RAS* genes were identified in human cancer cells (Der et al. 1982; Parada et al. 1982; Santos et al. 1982). The verdict was in: *RAS* is a *bona fide* oncogene.

RAS is a small GTPase, a protein that fluctuates between an active, GTP-bound state and an inactive, GDP-bound state (Scolnick et al. 1979; Papageorge et al. 1982; Gibbs et al. 1984; Sweet et al. 1984). When activated, RAS initiates a signaling cascade that promotes cell proliferation, cell survival, and cell motility (Pylayeva-Gupta et al. 2011). Mutations at codons 12, 13, or 61 of *RAS* prevent the hydrolysis of GTP, thus locking the protein in its active state (Clark et al. 1985; Der et al. 1986; Scheffzek et al. 1997; Buhrman et al. 2010). All three mutations are considered oncogenic and have been identified in human cancer, although the extent to which specific residue substitutions contribute to the oncogenic behavior of *RAS* remains controversial (Pylayeva-Gupta et al. 2011).

The cellular *RAS* family includes three homologous members: Harvey (*H*-), Kirsten (*K*-) and *N-RAS*. In addition, *KRAS* encodes two alternate splice forms, *KRAS4A* and *KRAS4B*, bringing the total number of *RAS* family proteins to four. The proteins exhibit a high degree of sequence overlap (Karnoub and Weinberg 2008), diverging only at their C-termini, and display some functional redundancy (Johnson et al. 1997; Potenza et al. 2005). However, there is an unmistakably non-random distribution of mutant *RAS* isoforms in human cancer. For example, while *HRAS* mutations predominate in cancers of the bladder and head and neck, mutations of *KRAS* are more common in colorectal, lung, and pancreatic carcinomas (Karnoub and Weinberg 2008; Pylayeva-Gupta et al. 2011). The reasons for this tissue specificity are unclear, but may involve isoform-specific regulatory elements (To et al. 2008) or context-dependent oncogenic capacity (Haigis et al. 2008; Li et al. 2011).

Oncogenic Properties of RAS

RAS is a remarkably powerful oncogene. Even in the absence of growth factors, overexpression of mutant *RAS* forces quiescent NIH3T3 cells to re-enter the cell cycle (Feramisco et al. 1984; Stacey and Kung 1984). However, NIH3T3 cells are immortalized rodent fibroblasts, and primary human cells exhibit a more limited response to *RAS*. In the latter case, expression of mutant *RAS* triggers cell cycle arrest. For transformation to occur, mutant *RAS* must be accompanied by cooperating genetic events (Land et al. 1983; Ruley 1983; Hahn et al. 1999).

Upon activation, RAS signals through numerous downstream signaling pathways – most notably the RAF/MEK/ERK and PI3K/AKT pathways – to stimulate cell proliferation and survival (Pylayeva-Gupta et al. 2011). These pathways culminate in the up-regulation of several transcription factors, which, in turn, induce expression of Cyclin D1 (Filmus et al. 1994; Albanese et al. 1995; Lavoie et al. 1996). In this manner, RAS activity propels the cell into S phase. Persistent pro-mitogenic signaling from RAS to Cyclin D1 leads to DNA re-replication, replication stress, and DNA damage (Aggarwal et al. 2007; Blow and Gillespie 2008; Aggarwal et al. 2010). In cells with intact cell cycle checkpoints, the DNA damage response then triggers an irreversible growth arrest, termed oncogene-induced senescence (OIS) (Bartkova et al. 2005; Gorgoulis et al. 2005; Bartkova et al. 2006; Di Micco et al. 2006). OIS exists as a cellular circuit breaker, a fail-safe mechanism that switches off the "lights" when the oncogenic "current" reaches dangerous levels. However, in cells that lack a functional DNA damage checkpoint, proliferation continues unabated. This finding likely explains the previous observation that expression of *RAS* in primary human cells triggers

growth arrest, rather than transformation. Inactivation of the DNA damage checkpoint may be required for escape from *RAS*-induced senescence.

The *CDKN2A* Locus

In the early 1990's, a novel tumor suppressor gene was mapped to the short arm of human Chromosome 9 (Serrano et al. 1993; Xiong et al. 1993; Kamb et al. 1994; Nobori et al. 1994; Okamoto et al. 1995). To reflect its molecular weight and its cellular function as a cyclin-dependent kinase (CDK) inhibitor, the protein was named $p16^{INK4a}$ and the genetic locus *CDKN2A*. $p16^{INK4a}$ is a member of the INK4 family, which also includes $p15^{INK4b}$, $p18^{INK4c}$, and $p19^{INK4d}$. All four proteins inhibit CDK4 (and CDK6) to block cell progression into S phase (Ruas and Peters 1998). The $p16^{INK4a}$ gene most likely resulted from tandem duplication of $p15^{INK4b}$ (i.e. *CDKN2B*), which shares homology with and is located directly upstream from $p16^{INK4a}$ (Gil and Peters 2006). Unexpectedly, a third gene was soon discovered within the *CDKN2A*/*B* region of Chromosome 9 (Duro et al. 1995; Mao et al. 1995; Quelle et al. 1995; Stone et al. 1995). This gene, which resides in an alternate reading frame from $p16^{INK4a}$, was named *ARF*.

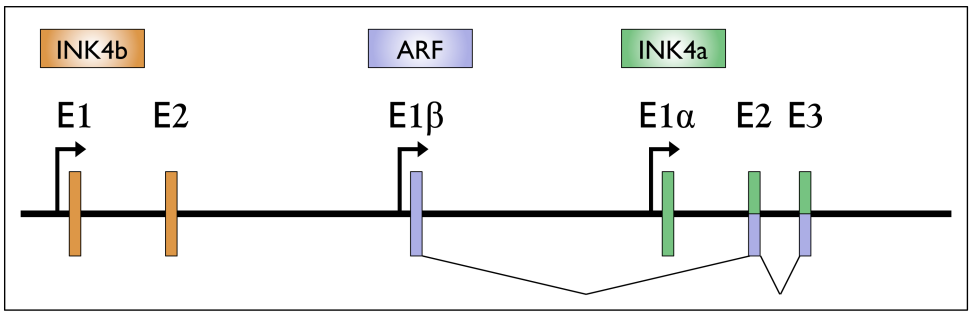

Figure 1.1: Organization of the *CDKN2B* and *CDKN2A* loci. Exon 1β of *ARF* is intercalated between exon 2 of $p15^{INK4b}$ and exon 1α of $p16^{INK4a}$. Figure is not drawn to scale. Adapted from (Sherr 2006).

ARF (*p14*^{ARF} in humans, *p19*^{Arf} in mice) and *p16*^{INK4a} have separate first exons (1β and 1α) and splice into exon 2 in alternate reading frames (Fig 1.1) (Quelle et al. 1995). Despite their disparate sequences, the protein products of *ARF* and *p16*^{INK4a} are both capable of inducing cell cycle arrest. Under conditions of cellular stress, p16^{INK4a} arrests cells at the G1/S checkpoint by inhibiting Cyclin D1-CDK4/6 complexes and preventing hyperphosphorylation of RB (Ruas and Peters 1998). RB thus remains bound to E2F, blocking entry into S phase. In contrast, ARF promotes arrest at both the G1/S and G2/M cell cycle checkpoints (Quelle et al. 1995; Kuo et al. 2003).

ARF Is a Tumor Suppressor *In Vivo*

Mice lacking both genes of the *CDKN2A* locus (i.e. *p16*^{Ink4a} and *p19*^{Arf} null) are prone to spontaneous tumor development and are highly susceptible to carcinogen-induced tumors (Serrano et al. 1996). The single knockout for *Arf* was constructed first. Surprisingly, mice deficient only for *Arf*, with *p16*^{Ink4a} intact, also exhibited a high incidence of spontaneous neoplasia (Kamijo et al. 1997; 1999). Indeed, the tumor spectrum for *Arf* $^{-/-}$ mice overlapped considerably with *Cdkn2a* $^{-/-}$ mice. Construction of the *p16*^{Ink4a} knockout mouse revealed a more limited contribution of the gene to tumor suppression (Krimpenfort et al. 2001; Sharpless et al. 2001). These unexpected findings have provoked many interesting discussions and heated debates about the specific contributions of each gene to tumor suppression in humans.

The *CDKN2A* locus is one of the most commonly altered genomic regions in human cancer. Nearly every neoplastic disease demonstrates a non-negligible rate of *CDKN2A* deletion,

mutation, or methylation (Saporita et al. 2007). The question of which product, ARF or $p16^{INK4a}$, is the target of this habitual silencing has been greatly complicated by the genes' close proximity (and by the presence of $p15^{INK4b}$, the third regional tumor suppressor gene). Clearly, $p16^{INK4a}$ plays a more vital role in suppressing tumor development in humans than in mice. Selective deletion or methylation of the gene has been identified in many cancers, and missense mutations in exon 1α of $p16^{INK4a}$ are also common (Ruas and Peters 1998). However, it is equally irrefutable that selective inactivation of *ARF* (with $p16^{INK4a}$ left intact) can and does occur in human cancer (Saporita et al. 2007). Mutations in *CDKN2A* exon 1β are infrequent, but germline deletions of exon 1β have been found in familial melanoma and astrocytoma kindreds (Randerson-Moor et al. 2001). Furthermore, selective methylation of the *ARF* promoter has been observed in multiple tumor types, including astrocytoma (Watanabe et al. 2003) and colorectal carcinoma (Esteller et al. 2000). Interestingly, missense mutations in exons 2 or 3 of *CDKN2A*, which would likely affect $p16^{INK4a}$, may not impact ARF protein function, as most of the essential properties of ARF are associated with amino acids encoded from exon 1β (Quelle et al. 1997; Midgley et al. 2000; Kim et al. 2003). In summary, loss of both $p16^{INK4a}$ and *ARF* likely contributes to carcinogenesis in humans, with different neoplastic disorders exhibiting different patterns of *CDKN2A* alteration.

ARF Expression Is Induced by Oncogenic Stress

The *CDKN2A* locus is a recent arrival on the evolutionary stage. The first *INK4* gene, a common ancestor of human $p15^{INK4b}$ and $p16^{INK4a}$, appeared in fish (Kazianis et al. 1999; Gilley and Fried 2001). Exon 1β of *ARF* most likely arose after the duplication of *INK4a/b* and has been identified in birds and mammals (Kim et al. 2003; Di Tommaso et al. 2004;

Sherr 2006). The absence of the genes in lower organisms suggests that the regulatory activities of ARF and $p16^{INK4a}$ were acquired to protect against uncontrolled proliferation in mutlicellular, long-lived vertebrates, but are not essential for normal development or everyday cell cycle control. The (mostly) unremarkable development of *Arf* and $p16^{Ink4a}$ knockout mice substantiates this claim (Kamijo et al. 1997; Krimpenfort et al. 2001; Sharpless et al. 2001), as do observations from several *Arf*-reporter constructs (Zindy et al. 2003; Freeman-Anderson et al. 2009; Gromley et al. 2009). ARF protein expression is rarely detected in normal cells *in vivo*. Instead, expression of ARF occurs in response to abnormal cellular stresses.

As described above, healthy cells have the ability to sense and counteract oncogenic signaling. This intrinsic tumor suppression proceeds through two pathways: apoptosis and senescence (Lowe et al. 2004). Apoptosis, a form of programmed cell death, is a radical solution to oncogenic stress that permanently removes the problem cell from the population. In contrast, oncogene-induced senescence spares the cell but forces its (presumably irreversible) exit from the cell cycle (Serrano et al. 1997; Collado and Serrano 2010). Mounting evidence suggests that ARF makes a vital contribution to OIS signaling *in vitro* and *in vivo*. In wild-type mouse embryonic fibroblasts (MEFs), oncogenic RAS induces ARF expression and triggers a p53-dependent arrest (Palmero et al. 1998; Ferbeyre et al. 2002). Escape from RAS-induced senescence in culture typically requires inactivation of the ARF-p53 pathway (Lin et al. 1998; Lin and Lowe 2001; Ferbeyre et al. 2002). Thus, unsurprisingly, $Arf^{-/-}$ MEFs evade senescence and are readily transformed by oncogenic RAS (Kamijo et al. 1997).

The connection between mutant *RAS* and ARF expression is complicated and has not yet been fully elucidated, but may involve the DMP1 or E2F transcription factors. DMP1 (cyclin D-binding Myb-like protein) is perhaps the best-understood link between ARF and RAS in mouse cells. Oncogenic RAS signaling increases binding of DMP1 to the *Arf* promoter, activating *Arf* gene expression and producing a p53-dependent cell cycle arrest (Inoue et al. 1999; Sreeramaneni et al. 2005). Furthermore, DMP1 is required for the induction of ARF by RAS, and *Dmp1* $^{-/-}$ cells escape RAS-induced senescence (Inoue et al. 2000; Sreeramaneni et al. 2005).

The E2F1, -2, and -3 proteins are activated by Cyclin D-CDK4/6 complexes downstream of RAS (Chen et al. 2009) and have been shown to arrest proliferation by directly promoting *ARF* transcription in human cells (Bates et al. 1998; Dimri et al. 2000; Parisi et al. 2002; Komori et al. 2005). However, the relationship between ARF and the E2F family is a tangled one. In some contexts E2F down-regulates ARF expression (Rowland et al. 2002; Aslanian et al. 2004), ARF can inhibit the growth-promoting activity of E2F (Eymin et al. 2001; Martelli et al. 2001; Mason et al. 2002; Rizos et al. 2007; Zhang et al. 2010a), and E2F is not required for induction of ARF or OIS in mouse fibroblasts (Palmero et al. 2002; Rowland et al. 2002). To confuse matters even further, E2F has been shown to efficiently repress expression from the *Dmp1* promoter (Mallakin et al. 2006). To summarize these bewildering findings, E2F activates ARF, represses ARF, represses an activator of ARF, and is functionally inhibited by ARF; moreover, many of these events may be species and cell-type specific.

Induction of ARF is not limited to RAS, E2F, and DMP1. The MYC (Eischen et al. 1999), E1A (de Stanchina et al. 1998), β-catenin (Damalas et al. 2001) and v-ABL (Radfar et al. 1998) oncogenes have all been shown to turn on ARF expression in mouse cells. However, several important functional distinctions exist between mouse $p19^{Arf}$ and human $p14^{ARF}$. Most notably, RAS has not been shown to induce $p14^{ARF}$ expression in human cells (Wei et al. 2001; Brookes et al. 2002; Voorhoeve and Agami 2003), except in the context of E2F deregulation (Berkovich et al. 2003). The relationship between MYC and $p14^{ARF}$ is still uncertain, as one group observed increased ARF expression in c-MYC-expressing human fibroblasts (Benanti et al. 2007), while another group did not (Lindstrom and Wiman 2003). Further complicating matters, most studies of *ARF* in humans have, by necessity, been conducted *in vitro*. As the very act of placing a cell in artificial tissue culture conditions can turn on ARF expression (Zindy et al. 1998; Sherr and DePinho 2000), these studies should be interpreted with caution. Based on evidence from *in vivo* mouse tumor studies and from examinations of the frequency of *CDKN2A* and/or $p14^{ARF}$ loss in human tumors, it remains likely that ARF contributes to OIS and tumor suppression in at least some human cell types.

$p16^{INK4a}$ and *ARF* have separate promoter elements, and transcriptional regulation and epigenetic silencing of the two genes can be highly selective (Esteller et al. 2000). However, the close proximity of $p16^{INK4a}$ and *ARF* (as well as $p15^{INK4b}$) hint at a biological need for coordinated regulation of the tumor suppressor gene loci (Gil and Peters 2006). In support of this argument, a conserved *cis*-acting regulatory domain has been identified upstream of $p15^{INK4b}$ (Gonzalez et al. 2006). Binding of the replication-licensing factor CDC6 to this regulatory domain causes transcriptional repression of the entire *CDKN2A/B* region. There is

also strong evidence that Polycomb group proteins, such as BMI1, can repress transcription of all three genes at the loci (Jacobs et al. 1999; Gil and Peters 2006; Agherbi et al. 2009). These joint regulatory mechanisms are still being elucidated, but the findings go a long way toward explaining the seemingly dangerous clustering of three important tumor suppressor genes in such a small genomic space. Coordinated activation/repression of the *CDKN2A/B* loci might allow for a more rapid, switch-like response to certain cellular stimuli (Gil and Peters 2006).

Additional mechanisms for regulating ARF expression exist beyond Polycomb. Pokemon (ZBTB7A) (Maeda et al. 2005), Twist (Maestro et al. 1999), and TBX2 and -3 (Jacobs et al. 2000; Brummelkamp et al. 2002; Lingbeek et al. 2002) are all implicated in the repression of *ARF* transcription. Furthermore, p53 binds to the *ARF* promoter and inhibits its transcription (Robertson and Jones 1998; Zeng et al. 2011), explaining initial observations that cells lacking wild-type *TP53* express ARF at high levels (Quelle et al. 1995; Kamijo et al. 1997).

The Canonical ARF-MDM2-p53 Axis

Many of the anti-proliferative activities of ARF have been attributed to its regulation of the p53 tumor suppressor pathway (Fig. 1.2). In oncogene-stressed cells, ARF antagonizes the MDM2 E3 ubiquitin ligase, thereby stabilizing cellular p53 levels (Pomerantz et al. 1998; Zhang et al. 1998; Tao and Levine 1999). The precise mechanism by which ARF inhibits MDM2 function remains controversial – sequestration of MDM2 by ARF in the nucleolus may (Weber et al. 1999; Zhang and Xiong 1999; Weber et al. 2000b) or may not (Llanos et al. 2001; Korgaonkar et al. 2002) be required – but it is clear that the three proteins compose an important signaling axis in mammalian cells.

Studies of mouse genetics provide the strongest evidence of the interplay between ARF, MDM2, and p53. Loss of *Mdm2* is embryonic lethal in mice, but the lethality is rescued by concurrent deletion of *Trp53*, strongly implicating p53 as a downstream mediator of MDM2 function (Jones et al. 1995; Montes de Oca Luna et al. 1995). Deletion of *Arf* from *Trp53* heterozygote animals significantly accelerates tumor development and removes the selective pressure to silence the remaining wild-type *Trp53* allele, but co-deletion of *Arf* and *Trp53* produces a tumor phenotype similar to that of the *Trp53* single knockout (Moore et al. 2003). Again, these results suggest that the major functions of ARF are mediated by p53. Notably, however, triple knockout mice with simultaneous loss of *Arf*, *Mdm2*, and *Trp53* exhibit an expanded tumor spectrum compared to all single- and double-knockout animals (Weber et al. 2000a), leaving open the possibility of some p53-independent tumor suppression by ARF.

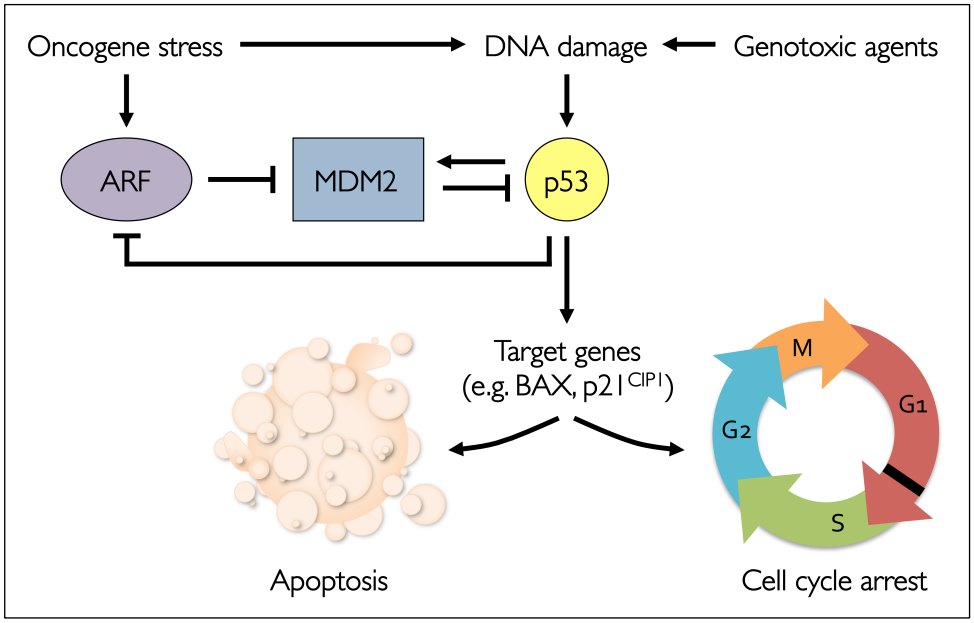

Figure 1.2: The canonical ARF-MDM2-p53 axis. Cellular p53 levels can be stabilized by oncogenic signaling through ARF or by a DNA damage response. The functional consequence of p53 activation is the initiation of a transcriptional program that produces pro-apoptotic and anti-proliferative responses. Figure adapted from (Sherr 2006).

TP53 is, arguably, the most important tumor suppressor gene in the cellular armory, as loss of p53 function occurs in a vast majority of human cancers (Olivier et al. 2010). Two roads lead to p53 activation: oncogenic stress signaling through ARF and a DNA damage response through ATM/ATR and CHK2/CHK1 (Efeyan and Serrano 2007). However, these signaling inputs may not be functionally equivalent. A pair of landmark papers recently demonstrated that the short-term DNA damage response of p53 does not contribute to tumor suppression. Instead, long-term stabilization of p53 by ARF is required for cancer protection after exposure to genotoxic agents (Christophorou et al. 2006; Efeyan et al. 2006). These studies will need to be repeated in additional cell types and under different conditions, but for now it appears likely that ARF acts as a critical conduit for p53-mediated death and growth arrest in stressed cells.

p53-Independent Functions of ARF

As described above, genetic studies of triple knockout *Arf* $^{-/-}$; *Mdm2* $^{-/-}$; *Trp53* $^{-/-}$ animals demonstrated that ARF likely possesses some MDM2- and p53-independent functions. Much effort has gone into identifying these non-canonical roles of ARF, yielding several surprising discoveries.

ARF exerts its anti-proliferative effect by arresting cells at the G1/S and G2/M checkpoints. Although growth arrest by ARF is often mediated by p53, overexpression of ARF also triggers a G1 phase arrest in cells lacking functional p53 (Weber et al. 2000a). ARF has been shown to down-regulate expression of Cyclin D1, the major G1 cyclin responsible for driving cells into S-phase. This transcriptional repression by ARF occurs through both direct

(D'Amico et al. 2004) and indirect (Andrique et al. 2012) mechanisms, and may partially account for p53-independent G1 arrest downstream of ARF. Early studies found that ARF was not required for p53 activation by ionizing radiation (IR) (Kamijo et al. 1997; Sherr 2006), fostering the widely held belief that ARF does not participate in the DNA damage response. However, subsequent work has identified multiple roles for ARF in DNA damage signaling and DNA repair. Sustained induction of p53 after IR requires ARF expression, and *Arf* $^{-/-}$ MEFs exhibit an impaired DNA damage checkpoint response after IR (Khan et al. 2000). In addition, ARF contributes to DNA damage signaling through p53-independent mechanisms. ARF triggers G2/M arrest in *p53*-deficient cells, both by impairing function of the CDC25C phosphatase and CDC2 kinase (Normand et al. 2005) and by activating the ATM/CHK2 pathway (Eymin et al. 2006).

Given the defining relationship between ARF and cellular stress, one of the most unexpected discoveries on ARF function has been its role in regulating the normal development of the hyaloid vasculature system in the mouse eye (McKeller et al. 2002; Martin et al. 2004; Silva et al. 2005; Thornton et al. 2005). In the absence of *Arf*, a large retrolental mass of cells accumulates in the eye vitreous. The mass, which is composed of both endothelial cells and pericytes, prevents the regression of the hyaloid vascular system and ultimately destroys the retina and the lens, causing blindness in *Arf* $^{-/-}$ animals. This ARF activity is independent of p53 and exclusive of oncogenic signaling. Instead, expression of ARF is controlled by the TGFβ2-SMAD signaling pathway (Gromley et al. 2009), prompting speculation that TGFβ might also regulate ARF expression in tumors. Another intriguing question raised by these findings is whether ARF might regulate angiogenesis in cancer. Indeed, two recent studies

have found inhibition of angiogenesis to be an important component of tumor suppression by ARF (Kawagishi et al. 2010; Zerrouqi et al. 2012).

Non-Small Cell Lung Carcinoma

Lung cancer is the leading cause of cancer-related death in the United States and the world (Jemal et al. 2011; SEER Cancer Statistics Review, 1975-2008). The disease is divided into two main subtypes – small cell (SCLC) and non-small cell lung carcinoma (NSCLC) – that differ in morphology, epidemiology, prognosis, and treatment. The majority of lung cancer cases (85.3%) are classified as NSCLC. In addition, NSCLC is, itself, subdivided into adenocarcinoma (45.1%), squamous cell carcinoma (23.4%), and large cell carcinoma (3.4%) (SEER Cancer Statistics Review, 1975-2008). Despite recent pharmacological success stories (Janku et al. 2010), NSCLC has largely remained an intractable disease. Patients diagnosed with localized NSCLC have a somewhat promising 5-year relative survival rate of 53.6%. Unfortunately, however, the majority of patients (54%) first present with distant metastatic disease, and only 3.8% of these patients will survive at least 5 years beyond their diagnosis (SEER Cancer Statistics Review, 1975-2008). These daunting statistics highlight the urgency of developing innovative treatments for NSCLC.

Pathology of NSCLC

As initially described by Fearon and Vogelstein (1990), cancer generally develops in a step-wise manner, with temporal accumulation of genetic alterations driving tumorigenesis through a sequence of precursor lesions. Accordingly, preinvasive lesions (atypical adenomatous

hyperplasia (AAH) and adenocarcinoma *in situ* (AIS)) have been identified in the pulmonary epithelia of smokers prior to diagnosis of overt cancer and are frequently observed in resected lung from NSCLC patients (Westra 2000; Travis et al. 2011). These precursor lesions typically harbor genetic abnormalities also found in malignant lung tumors (Westra et al. 1996; Kitaguchi et al. 1998; Selamat et al. 2011), strongly arguing that they represent early stages of a clonal tumor development continuum.

Because it has been challenging to identify and study pulmonary adenocarcinoma precursors in humans, many researchers have investigated lung tumor evolution in mice. However, there are important differences in the classification schema for preinvasive lesions from the two species (Nikitin et al. 2004). In mice, benign tumors, termed "adenomas," are considered part of an AAH-adenoma-adenocarcinoma tumor progression spectrum, whereas in humans, the term "adenoma" is applied to tumors that rarely or never progress to malignancy. While innate differences in pulmonary tumor evolution between humans and mice remain possible, it is likely that the human AAH and AIS designations cover tumor stages that, in mice, would be classified as adenomas. Murine adenomas are typically small (< 5mm) nodules consisting of a uniform population of cuboidal to columnar epithelial cells with round nuclei and eosinophilic cytoplasm. Adenomas exhibit low mitotic activity, have well-defined borders, and are non-invasive. Murine adenocarcinomas are large (> 5mm) tumors that display cellular and nuclear atypia, vacuolated or basophilic cytoplasm, and regional variation in growth patterns. Adenocarcinomas exhibit frequent mitoses and invade neighboring lung parenchyma, airways, and blood/lymphatic vessels. Notably, large adenomas can be difficult to distinguish from well-differentiated adenocarcinomas (Nikitin et al. 2004).

Most murine lung tumors are believed to derive from type II pneumocytes (Belinsky et al. 1992; Mason et al. 2000), although derivation from bronchiolar Clara cells has not been excluded (Gunning et al. 1991; Thaete and Malkinson 1991). Several studies have also highlighted the existence of a bronchioalveolar stem cell (BASC) that may be a common progenitor of Clara cells and type II pneumocytes and the cell of origin of mouse lung adenocarcinoma (Kim et al. 2005; Yanagi et al. 2007; Regala et al. 2011). The BASC model is not without controversy, however (Xu et al. 2012). Meanwhile, the cell of origin for human pulmonary adenocarcinoma is still unknown, and it remains to be determined whether cellular origin has clinical significance for lung adenocarcinoma.

Established Molecular Alterations in NSCLC

Ding et al. produced the seminal work on genetic alterations in lung adenocarcinoma (2008). The group identified 26 genes commonly mutated in patients, including *KRAS*, *TP53*, *CDKN2A*, *RB1*, *ATM*, and multiple receptor tyrosine kinases (e.g. *EGFR*, *ERBB4*, *KDR*, *FGFR4*, *PDGFRA*, and *LTK*). Copy number gains or losses were also frequently observed in the identified genes. In addition to highlighting several novel somatic mutations, these findings substantiated earlier, individual studies on oncogenes and tumor suppressor genes in lung adenocarcinoma.

The contributions of EGFR (Lynch et al. 2004; Paez et al. 2004; Pao et al. 2004) and KRAS (Rodenhuis et al. 1988; Westra et al. 1993) to lung carcinogenesis have been well described. Typically, *EGFR* and *KRAS* mutations are mutually exclusive (Pao et al. 2005; Zhu et al.

2008). *EGFR* mutations preferentially arise in never-smokers and are initially responsive to therapy with gefitinib or erlotinib (Lynch et al. 2004; Paez et al. 2004; Pao et al. 2004). Conversely, *KRAS* mutations are associated with cigarette exposure (Slebos et al. 1991; Ahrendt et al. 2001) and demonstrate a poor response to tyrosine kinase inhibitors (Pao et al. 2005). All told, *KRAS* mutations occur in approximately 35% of lung adenocarcinoma patients (Ding et al. 2008). Unfortunately, unlike EGFR, little progress has been made in the pharmacologic targeting of mutant KRAS (Cox and Der 2010; Janku et al. 2010).

TP53 (Takahashi et al. 1989) and *CDKN2A* (Packenham et al. 1995) are important lung tumor suppressor loci, estimated by Ding et al. to be mutated or deleted in 36% and 15% of lung adenocarcinoma cases, respectively (2008). Other groups have found *TP53* alterations in up to 70% of adenocarcinoma cases, depending on smoking history (Herbst et al. 2008). The inclusion of data on hypermethylation may also significantly raise the overall frequency of *CDKN2A* silencing in lung adenocarcinoma (Zhang et al. 2011). Most lung adenocarcinomas with *CDKN2A* alterations exhibit simultaneous loss of ARF and $p16^{INK4a}$ expression (Vonlanthen et al. 1998), precluding analysis of the contribution of *ARF* loss to adenocarcinoma development. Overexpression of *MDM2* and inactivation of *ARF* appear to be mutually exclusive events in NSCLC (Eymin et al. 2002), but inactivation of *TP53* and *ARF* can occur in the same tumor (Sanchez-Cespedes et al. 1999). Studies have observed loss of ARF expression in 92%, 54%, and 47% of adenocarcinoma specimens examined (Xue et al. 2002; Mori et al. 2004; Wang et al. 2005), and there is some indication that *ARF* loss may correlate with *EGFR* mutations in never-smoker patients (Mounawar et al. 2007).

Mouse Models of *Kras*-Driven NSCLC

Multiple mouse models have been developed to study *Kras*-driven NSCLC. The majority of models are mice genetically engineered to bear activating mutations in codon 12 of *Kras* (Farago et al. 2012). Indeed, recent technological advances have enabled the development of several remarkably elegant genetic mouse models for lung cancer research. However, one of the oldest and best-studied models of NSCLC utilizes the chemical carcinogen urethane (i.e. ethyl carbamate) to induce pulmonary tumor development.

The urethane model of lung carcinogenesis has been well established over nearly seven decades of research (Zimmerli and Schlatter 1991; Malkinson 2001; Forkert 2010). A component of cigarette smoke and alcoholic beverages (Schmeltz et al. 1978; Battaglia et al. 1990), urethane is a potent mutagen in rodents whose metabolism to vinyl carbamate epoxide is catalyzed by cytochrome P450 2E1 (Ghanayem 2007; Forkert 2010). Mice exposed to urethane develop lung tumors with *Kras* codon 61 missense mutations at high frequency (You et al. 1989; Cazorla et al. 1998). Only about half of urethane-induced pulmonary lesions progress beyond the benign adenoma stage (Tannenbaum and Maltoni 1962), making this model an ideal system in which to assay tumor suppressor gene loss during malignant progression.

Although primarily utilized in pulmonary tumorigenesis studies, urethane is a multipotential carcinogen, and exposure to urethane produces additional, lower frequency neoplasms. Hepatocellular carcinoma, mammary gland adenocarcinoma, and Harderian gland tumors are all associated with long-term exposure to urethane (Tannenbaum and Maltoni 1962;

Vesselinovitch and Mihailovich 1968a, 1968b). Of particular note, when administered at high doses or with recurrent low dose application, urethane induces hepatic vascular lesions in wild-type mice (Tannenbaum and Silverstone 1958; Kawamoto et al. 1961; Inai et al. 1991; Beland et al. 2005).

Aims of Dissertation Research

The overarching goal of my thesis research was to identify and elucidate tumor suppression by ARF in multiple mouse models of carcinogenesis. To that end, I examined the effect of *Arf* loss on carcinogen-induced tumor development in three tissues: lung, liver, and skin. First, I investigated the role of ARF in urethane-induced, *Kras*-driven non-small cell lung carcinoma. I describe my findings on the inhibition of NSCLC growth and invasion by ARF in Chapter Two. I further studied the effect of *Arf* loss on the development of hepatic vascular lesions after urethane exposure, work described in Chapter Three. Finally, using the DMBA/TPA model of skin carcinogenesis, I analyzed regulation of malignant progression, epithelial-mesenchymal transition, and metastasis by ARF in squamous cell carcinoma. A brief account of this research is provided in Chapter Four.

Chapter Two

ARF Inhibits the Growth and Malignant Progression of Non-Small Cell Lung Carcinoma

Stephanie E Busch[1,3], Kay E Gurley[1], Russell D Moser[1], Karen S Kelly-Spratt[1], Christopher J Kemp[1,2]

[1]Division of Human Biology, [2]Division of Public Health Sciences, Fred Hutchinson Cancer Research Center, Seattle, Washington 98109

[3]Molecular and Cellular Biology Graduate Program, University of Washington, Seattle, Washington 98195

Manuscript in Preparation

Summary

Non-small cell lung carcinoma (NSCLC) is among the deadliest of human cancers. The *CDKN2A* locus, which houses the *INK4a* and *ARF* tumor suppressor genes, is frequently altered in NSCLC. However, the specific role of ARF in pulmonary tumorigenesis remains unclear. Several lines of evidence indicate that oncogenic KRAS induces the expression of ARF, thus stabilizing p53 activity and arresting cell proliferation. To address the role of ARF in *Kras*-driven NSCLC, we injected wild-type and *Arf*-deficient mice with the pulmonary carcinogen urethane. Lung tumor size and associated morbidity were significantly increased in $Arf^{-/-}$ animals compared to $Arf^{+/+}$. Pulmonary lesions from $Arf^{+/+}$ mice were typically benign, while tumors from $Arf^{-/-}$ mice rapidly progressed to malignancy. A subgroup of lung tumors in $Arf^{-/-}$ mice presented as dedifferentiated and metastatic, with many characteristics of pulmonary sarcomatoid carcinoma, a tumor type previously undocumented in mice. Benign adenomas from $Arf^{+/+}$ mice robustly expressed ARF, but ARF expression was markedly reduced in malignant adenocarcinomas. *Arf*-deficient tumors also exhibited increased cell proliferation and DNA damage. These findings demonstrate that induction of ARF is an early response in lung tumorigenesis that mounts a strong barrier against tumor growth and malignant progression.

Introduction

Non-small cell lung carcinoma (NSCLC) is the leading cause of cancer-related death in the United States and the world, with a five-year relative survival rate of only 17% (SEER Cancer Statistics Review, 1975-2008). Lung adenocarcinoma, the predominant histological subtype of NSCLC (SEER Cancer Statistics Review, 1975-2008), commonly harbors genetic alterations in *KRAS* (38%), *TP53* (36%) and *CDKN2A* (15%) (Ding et al. 2008). However, the timing, impact, and clinical significance of these changes are not yet fully understood.

The *CDKN2A* locus houses both the *ARF* ($p14^{ARF}$ in humans, $p19^{Arf}$ in mice) and *INK4a* ($p16^{INK4a}$) tumor suppressor genes. ARF, so named because it is transcribed from an alternate reading frame, shares no homology with INK4a and is controlled by a separate promoter (Quelle et al. 1995). Both proteins induce cell cycle arrest, albeit by regulating different signaling pathways. Under conditions of cellular stress, INK4a promotes G1 arrest by inhibiting Cyclin D-Cdk4/6 complexes and preventing hyperphosphorylation of RB (Serrano et al. 1993; Xiong et al. 1993; Kamb et al. 1994; Nobori et al. 1994). In contrast, ARF triggers arrest at the G1 and G2 checkpoints (Quelle et al. 1995; Kuo et al. 2003), in part by antagonizing the MDM2 ubiquitin ligase and stabilizing cellular p53 levels (Pomerantz et al. 1998; Zhang et al. 1998; Tao and Levine 1999; Lin and Lowe 2001). Although p53-independent tumor suppression by ARF has been demonstrated (Sherr 2006), these activities are not as well elucidated as the canonical ARF-MDM2-p53 signaling axis.

Several recent studies examining tumor suppression by ARF in NSCLC have yielded contradictory results. While ARF expression was found to be elevated in pre-malignant lung

lesions in *Kras*^{G12V} animals and, indeed, considered to be a marker of oncogene-induced senescence (Collado et al. 2005), expression of ARF was primarily restricted to high-grade adenocarcinomas in two mouse models of *Kras*^{G12D}-driven lung cancer (Feldser et al. 2010; Junttila et al. 2010). In addition, *Arf* loss did not significantly impact lung tumor progression in *Kras*^{G12D} mice (Young and Jacks 2010). These latter results are surprising, given the established relationship between KRAS, ARF, and p53 (Sherr 2006) and the observation that *Trp53* loss of function cooperates with mutant *Kras* in multiple mouse models of lung adenocarcinoma (Fisher et al. 2001; Johnson et al. 2001; Jackson et al. 2005; Wang et al. 2006; Zheng et al. 2007; Feldser et al. 2010; Junttila et al. 2010). Moreover, loss of ARF expression has been observed in lung tumors in mice (Tam et al. 2003) and in humans (Vonlanthen et al. 1998; Sanchez-Cespedes et al. 1999; Nicholson et al. 2001; Xue et al. 2002; Park et al. 2003), and restoration of ARF expression arrests the growth of patient-derived lung cancer cell lines (Gao et al. 2001; Eymin et al. 2003; Zhang et al. 2010b). As *ARF* status may have important implications for NSCLC patient prognosis and clinical management, further examination of the role of ARF in lung tumorigenesis is warranted. Herein we identify ARF as a major suppressor of the growth and malignant progression of carcinogen-induced, *Kras*-driven NSCLC.

Results

Arf Deficiency Leads to Increased Lung Tumor Size and Associated Morbidity

To examine the role of ARF in lung tumorigenesis, we injected cohorts of *Arf* $^{+/+}$, *Arf* $^{+/-}$ and *Arf* $^{-/-}$ mice with urethane. Kaplan-Meier analysis indicated that urethane-exposed *Arf* $^{-/-}$

animals experienced significantly increased overall mortality (Fig. 2.2A) and lung-tumor associated morbidity (Fig. 2.1A) compared to their *Arf* $^{+/+}$, *Arf* $^{+/-}$ and unexposed *Arf* $^{-/-}$ littermates (log-rank test for trend, $P < 0.0001$). By 25 weeks post-injection, 68.2% of *Arf* $^{-/-}$ mice exposed to urethane succumbed to lung tumors, whereas all *Arf* $^{+/+}$, *Arf* $^{+/-}$ and unexposed *Arf* $^{-/-}$ mice remained viable. *Arf* $^{-/-}$ mice also presented with lymphomas and sarcomas (data not shown) at a rate similar to that previously reported (Kamijo et al. 1999), and two-thirds of *Arf* $^{-/-}$ animals developed hepatic vascular lesions after urethane exposure. As described previously, these lesions were typically small and had a limited impact on overall survival (Busch et al. 2012).

At necropsy, *Arf* $^{-/-}$ animals presented with substantial pulmonary tumor burden (Fig. 2.1B, bottom). Although tumor multiplicity did not vary between genotypes (Fig. 2.1C), tumor size was greatly increased in *Arf* $^{-/-}$ mice ($P < 0.0001$; Fig. 2.1D). Notably, while *Arf* $^{+/+}$ and *Arf* $^{+/-}$ mice rarely developed tumors exceeding 3mm in diameter, *Arf* $^{-/-}$ mice routinely developed tumors between 4 and 17mm diameter (Fig. 2.2B). This marked increase in tumor size corresponded with a nearly three-fold increase in lung mass in *Arf*-deficient mice (Fig. 2.1E). In summary, while homozygous loss of *Arf* did not affect lung tumor initiation after carcinogen exposure, it greatly increased the rate of lung tumor growth and associated morbidity and mortality.

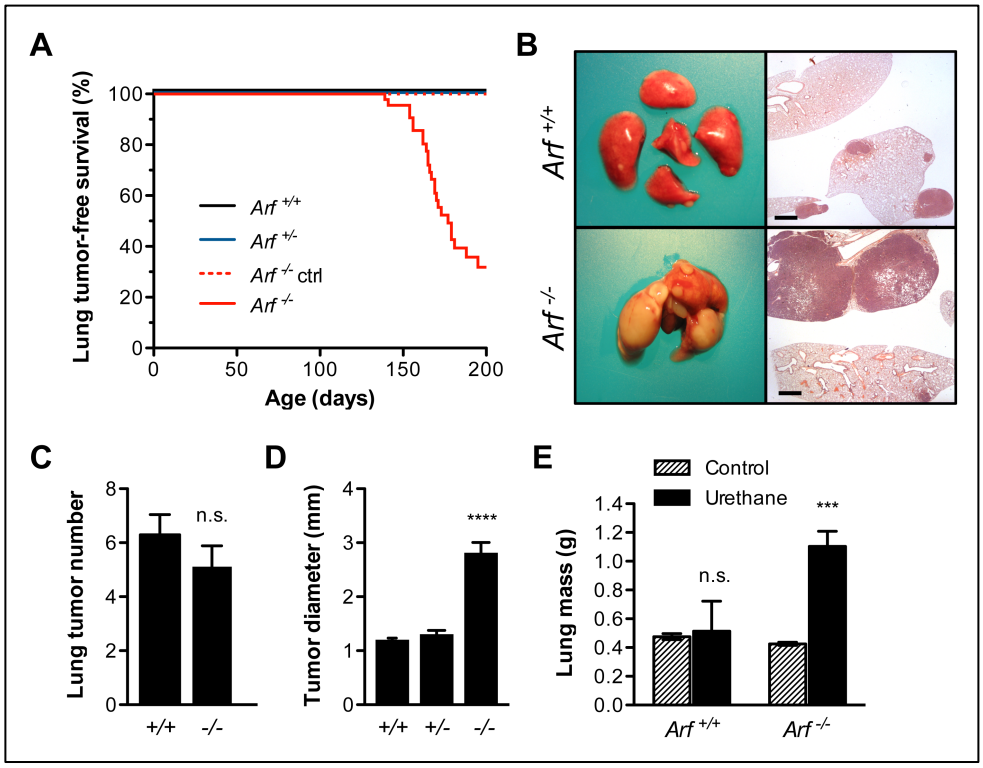

Figure 2.1: *Arf* loss accelerates tumor growth and morbidity in urethane-exposed mice. **[A]** *Arf* loss led to accelerated lung tumor-associated morbidity after urethane exposure (logrank test for trend, $P < 0.0001$). **[B]** At necropsy, *Arf*$^{-/-}$ mice (bottom) bore massive lung tumors compared to *Arf*$^{+/+}$ mice (top). H&E images shown on right; scale bar 1mm. **[C]** At 17 weeks post-exposure, an equivalent number of tumors were visible on the surface of *Arf*$^{+/+}$ and *Arf*$^{-/-}$ lungs ($P = 0.2840$; $n = 10$ *Arf*$^{+/+}$ and 9 *Arf*$^{-/-}$). **[D]** Mean tumor diameter. Tumors were measured with calipers; largest diameter was used for analysis. Mean values differed significantly between genotypes (**** $P < 0.0001$; $n = 351$ *Arf*$^{+/+}$, 196 *Arf*$^{+/-}$, and 211 *Arf*$^{-/-}$ tumors). **[E]** Mass of lungs from non-tumor bearing control and urethane-exposed male mice. *Arf*$^{-/-}$ mice carried a significantly greater lung tumor burden than *Arf*$^{+/+}$ (***$P = 0.0007$; $n \geq 4$ each condition). Note that all lungs were inflated with a set volume of fixative prior to being weighed.

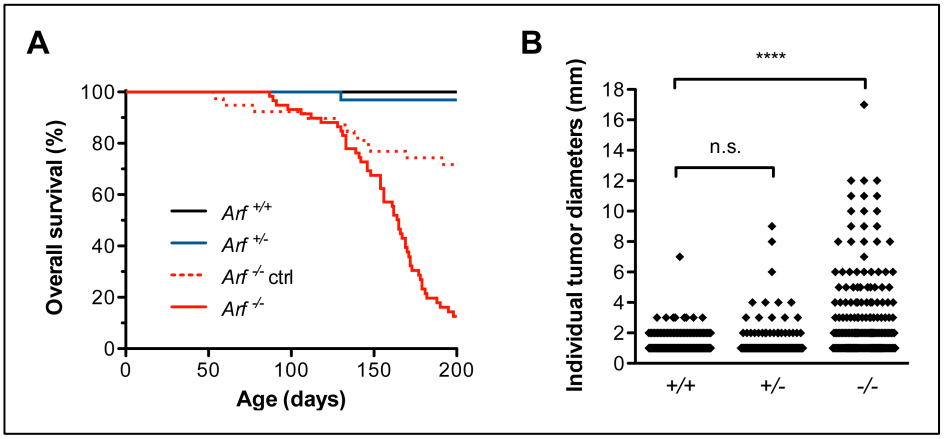

Figure 2.2: *Arf* loss accelerates disease. **[A]** *Arf*$^{-/-}$ mice exhibited significantly reduced overall survival after urethane injection (logrank test for trend, $P < 0.0001$). **[B]** Plot of individual tumor diameters (**** $P < 0.0001$).

Loss of *Arf* Facilitates Malignant Progression

The urethane model of mouse lung carcinogenesis captures a tumor development spectrum that proceeds from hyperplasia to benign adenomas and, infrequently, to malignant adenocarcinomas (Tannenbaum and Maltoni 1962). At 25 weeks post-urethane, the majority of tumors present in *Arf* $^{+/+}$ (65.9%) and *Arf* $^{+/-}$ (72.5%) animals were identified as pulmonary adenomas (Fig. 2.3A, top, B). The incidence of adenocarcinomas was significantly greater (79.5%) in *Arf* $^{-/-}$ animals ($P < 0.0001$; Fig. 2.3B). Pulmonary adenocarcinomas were characterized by pleomorphic nuclei, abundant mitotic activity, and invasion into adjacent parenchyma and airways (Fig. 2.3A, bottom). Intravasation of adenocarcinoma cells was also observed (Fig. 2.3C).

A subset of adenocarcinomas in *Arf* $^{-/-}$ mice exhibited exceptionally poor differentiation (Fig. 2.3D, E) and metastasized to both intra- and extra-thoracic sites (Fig. 2.3F, H). These tumors displayed histopathological characteristics typical of pulmonary sarcomatoid carcinoma (Pelosi et al. 2010), an aggressive tumor type that, to our knowledge, has not previously been observed in mice. Of note, although the metastatic lesions most closely resembled undifferentiated spindle cell tumors, regions of the metastases that retained epithelial differentiation expressed pro-Surfactant Protein C (Fig. 2.3G, H), consistent with lung epithelial origin.

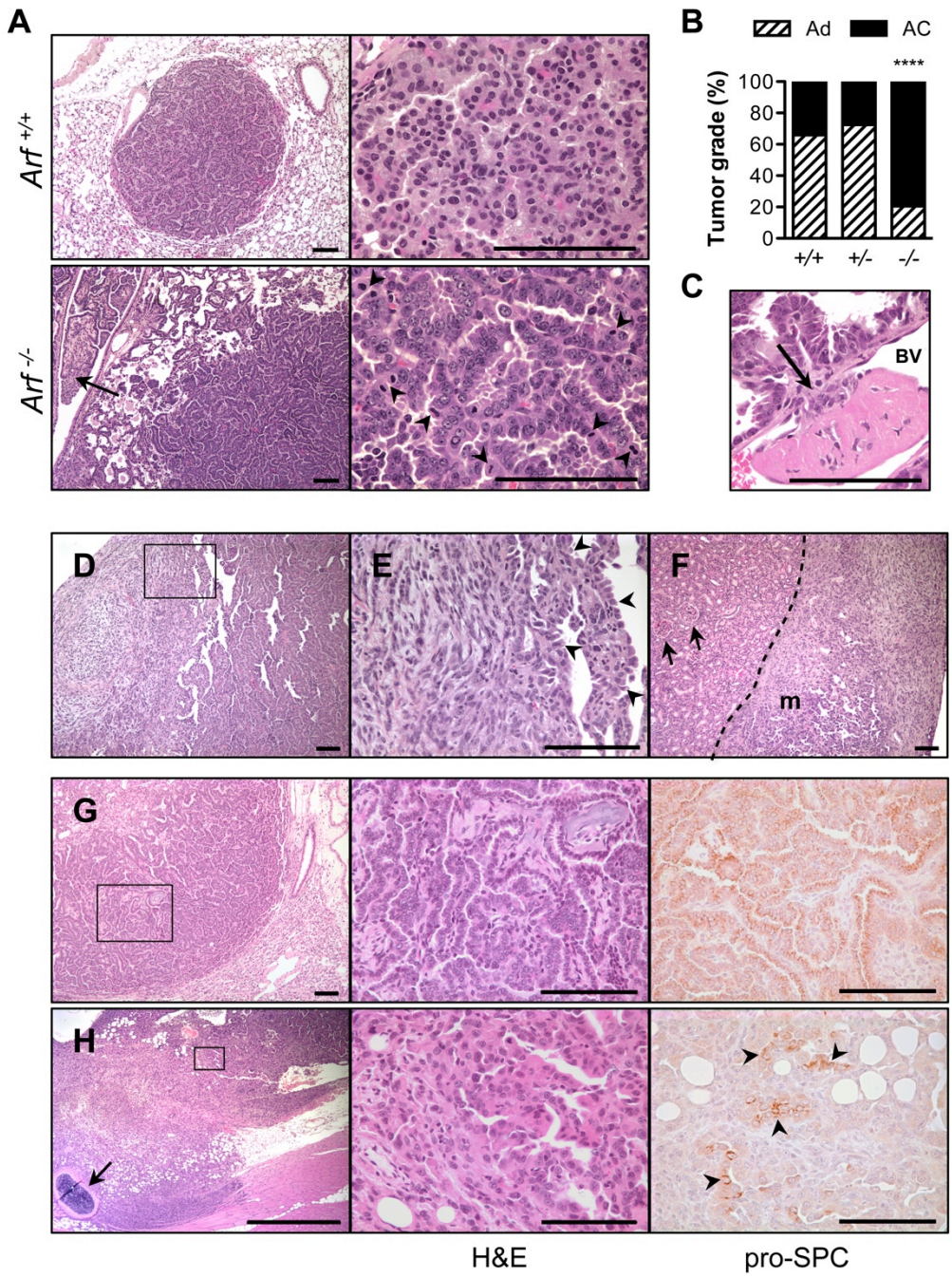

Figure 2.3: *Arf* loss increases incidence of malignant, poorly differentiated tumors. **[A]** Adenomas occurred primarily in *Arf* $^{+/+}$ mice (top). Tumors had discrete borders and were composed of a uniform cell population with small, round nuclei and moderate amounts of eosinophilic cytoplasm. Mitotic figures were rare. Adenocarcinomas predominated in *Arf* $^{-/-}$ mice (bottom). They invaded the surrounding lung parenchyma and airways (arrow), and exhibited cellular atypia, pleomorphic nuclei, and cytoplasmic vacuoles. Mitotic figures (arrowheads) were frequent. **[B]** Incidence of lung adenomas (Ad) and adenocarcinomas (AC) across three genotypes (**** $P < 0.0001$; $n = 44$ *Arf* $^{+/+}$, 40 *Arf* $^{+/-}$ and 39 *Arf* $^{-/-}$ tumors examined). **[C]** Intravasation of *Arf* $^{-/-}$ adenocarcinoma. Tumor cells have broken through the basement membrane (arrow) to invade the neighboring blood vessel (BV). An endothelialized thrombus, in pink, has formed at the site. **[D]** Pulmonary sarcomatoid carcinoma-like lesions formed in the lung. **[E]** Magnification of boxed region in [D]. Arrowheads point to epithelial regions of sarcomatoid carcinoma. **[F]** Metastasis (m) of mixed epithelial and sarcomatoid components to kidney. Arrows indicate normal kidney glomeruli. **[G-H]** Adenocarcinomas [G] and sarcomatoid metastases [H] from the same mouse exhibited immunoreactivity for pro-surfactant protein C (pro-SPC), a marker of lung epithelial cells. Invasion of the pleura and chest wall is shown in [H]. Arrow indicates rib. The metastatic sarcomatoid tumor maintained regions of epithelial differentiation (boxed region, magnified in middle panel) that expressed pro-SPC (arrowheads). Scale bars 100μm, except panel [H] (1mm).

ARF Expression Is Induced Early in Tumor Development

Having found that homozygous *Arf* loss enhances the progression of urethane-induced lung tumors, we hypothesized that ARF may act as a barrier to malignancy during tumor development. We therefore examined ARF expression in early and late-stage tumors from *Arf* $^{+/+}$ mice. Early-stage adenomas exhibited prominent ARF expression (Fig. 2.4A, middle), while expression of ARF in adenocarcinomas was restricted to small, sporadic foci (Fig. 2.4A, bottom). Consequently, the number of ARF^{+} cells per field was significantly reduced in malignant (17.39 ± 1.59) compared to benign (35.07 ± 3.12) tumors ($P < 0.0001$; Fig. 2.4B). ARF expression was thus triggered early and silenced late during pulmonary tumor development.

We also assayed loss of heterozygosity of *Arf* during tumor progression. The wild-type *Arf* allele underwent partial deletion in all adenocarcinomas examined from *Arf* $^{+/-}$ mice (Fig. 2.4C). Taken together with the observation that *Arf* $^{+/-}$ mice exhibited a tumor phenotype similar to *Arf* $^{+/+}$mice (Fig. 2.1D and 2.3B), the selection against the wild-type *Arf* allele suggests that tumor suppression by ARF in this model is not haploinsufficient. Furthermore, these findings indicate that tumor suppression by ARF is a potent barrier to malignant progression *in vivo*.

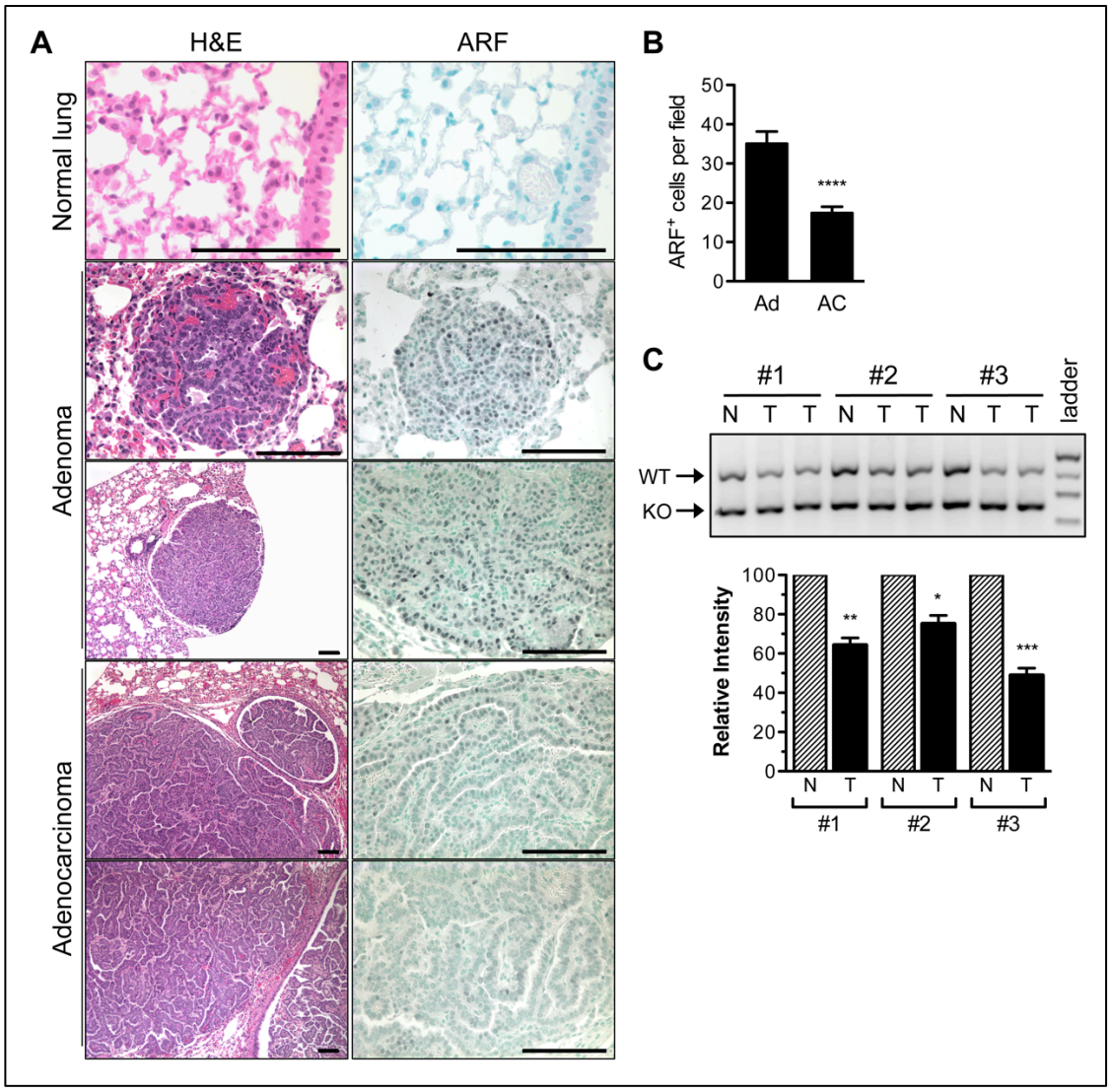

Figure 2.4: ARF expression is induced early in tumor development. [A] Adenomas (Ad) from *Arf* $^{+/+}$ mice robustly expressed ARF, but adenocarcinomas (ACs) frequently lost ARF expression. [B] Quantification of ARF positive cells (**** $P < 0.0001$; $n = 46$ adenoma and 145 AC fields examined). [C] Loss of the wild-type (WT) allele in lung adenocarcinomas from *Arf* $^{+/-}$ mice. Relative intensities of WT and knock-out (KO) DNA bands are quantified (* $P = 0.0103$; ** $P = 0.0023$; *** $P = 0.0008$).

ARF Induction by Mutant KRAS Activates the p53 Pathway

Many of the tumor suppressive activities previously ascribed to ARF are linked to its role in stabilizing p53 in oncogene-stressed cells (Lin and Lowe 2001; Sherr 2006). Consistent with previous reports on urethane carcinogenesis (You et al. 1989), activating *Kras* mutations were identified in all lung tumors examined ($n = 4$ each genotype; Fig. 2.5). To investigate whether ARF blocks *Kras*-driven pulmonary tumor growth and progression through a p53-dependent

pathway, we examined expression of the prototypical p53 transcriptional target $p21^{CIP1}$ (i.e. p21), a cyclin-dependent kinase inhibitor. ARF frequently co-localized with p21 in adenomas and mixed-grade tumors from wild-type mice (Fig. 2.6, top). Notably, $ARF^{+}p21^{+}$ tumor regions were largely negative for phosphorylated Histone H2A.X, a sensitive indicator of DNA damage. These results indicate that expression of ARF triggers an anti-proliferative response through p53 that does not require concomitant DNA damage signaling.

Although $p21^{CIP1}$ expression was also observed in tumors from *Arf* $^{-/-}$ mice, the pattern of immunoreactivity differed appreciably. In *Arf*-deficient tumors, unlike in wild-type, p21 expression was frequently associated with expression of phospho-H2A.X and nuclear phospho-ERK1/2, markers of DNA damage and cellular proliferation, respectively (Fig. 2.6, bottom). It is possible that induction of p21 in *Arf* $^{-/-}$ animals reflects activation of p53 by DNA damage, a cellular response that does not require ARF (Kamijo et al. 1997). p53-independent expression of p21 in cancer cells has also been demonstrated (Macleod et al. 1995; Marchetti et al. 1996; Aliouat-Denis et al. 2005). We attempted to genetically assay the p53-dependence of pulmonary tumor suppression by ARF by repeating the urethane carcinogenesis study in *Trp53* $^{-/-}$ mice. Unfortunately, all animals died from lymphoma by 15 weeks post exposure, precluding analysis of lung tumor growth (data not shown). In summary, the co-expression of $p21^{CIP1}$ and ARF strongly supports the argument that ARF suppresses *Kras*-driven lung tumorigenesis through a p53-dependent pathway. Remnant p21 expression in tumors from *Arf*-deficient mice may signify the activation of an alternative p53 pathway downstream of DNA damage.

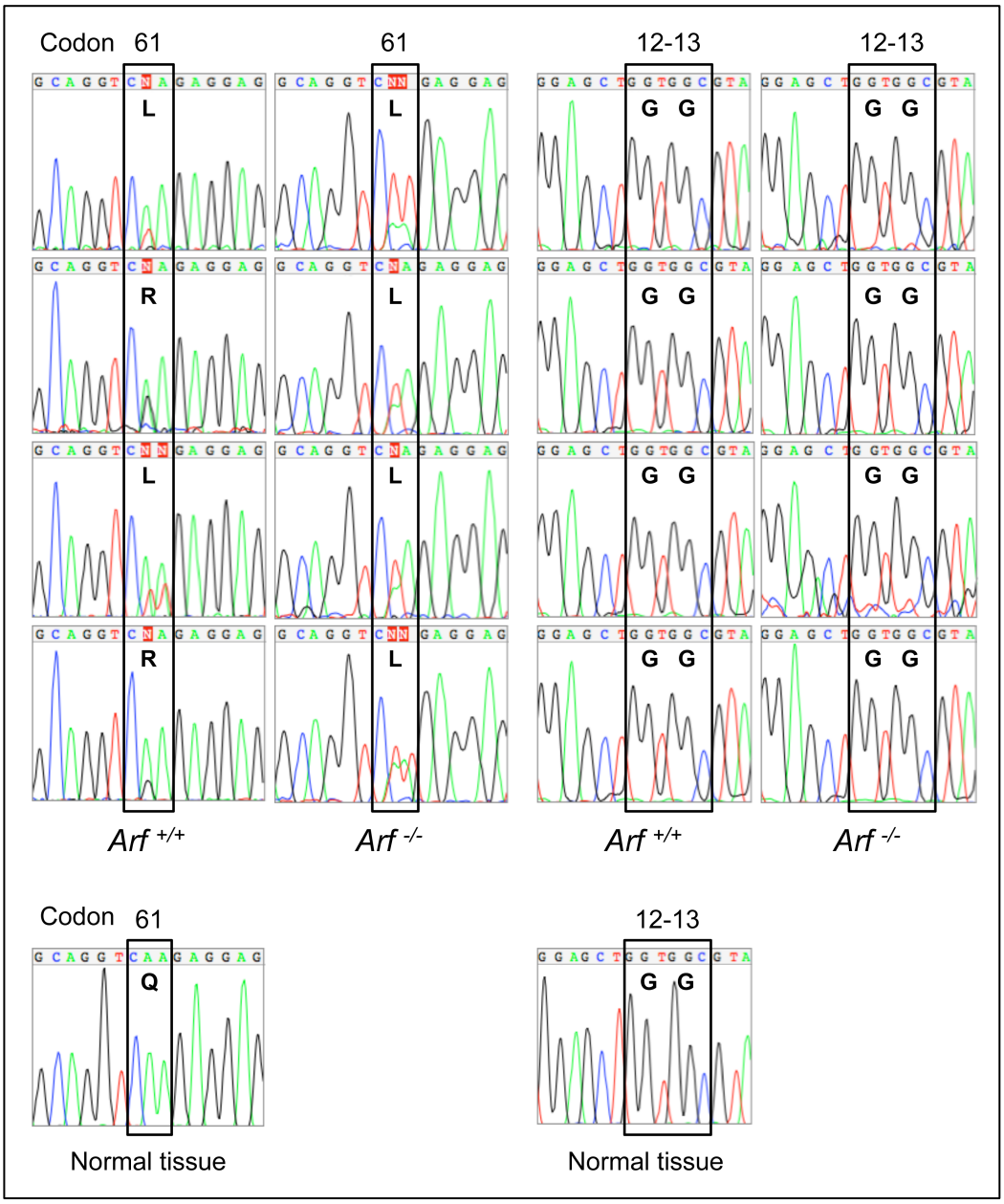

Figure 2.5: Activation of the RAS pathway in urethane-induced tumors. The codon 61 glutamine (Q) residue of *Kras* in both *Arf* $^{+/+}$ and *Arf* $^{-/-}$ lung tumors was mutated to leucine (L) or arginine (R). The glycine (G) 12 and 13 amino acids were unaffected ($n = 4$ each genotype).

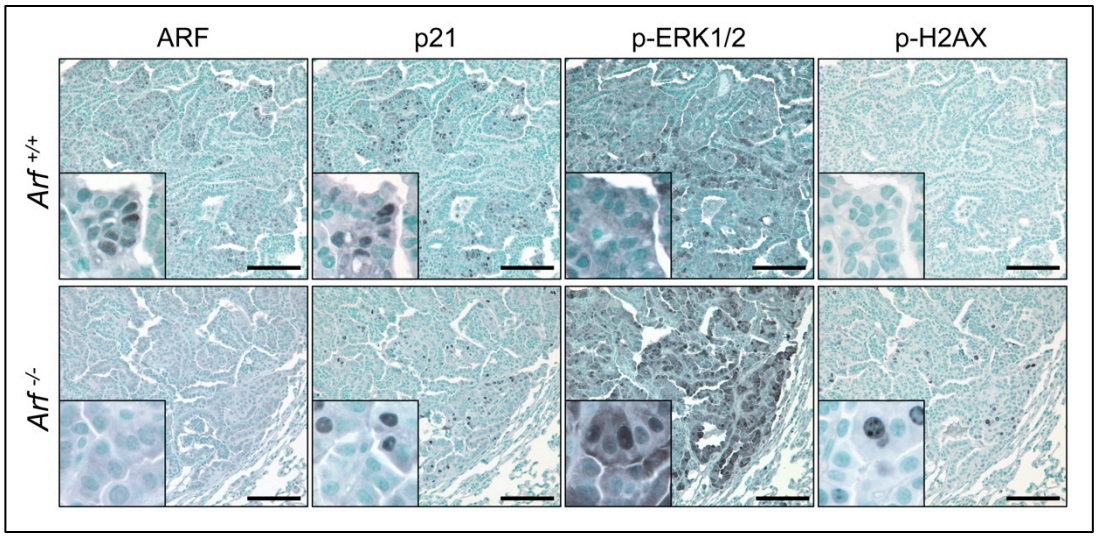

Figure 2.6: ARF, p21, and phosphorylated ERK1/2 co-localized in tumors from *Arf* $^{+/+}$ mice (top), but staining for phosphorylated histone H2A.X was largely negative. In *Arf* $^{-/-}$ adenocarcinomas (bottom), p21 staining correlated with H2AX^{+} tumor regions. Magnified, matched regions of staining are shown in the insets. All scale bars 100μm.

RAS-ERK Signaling and Nuclear Cyclin D1 Are Elevated in *Arf*-Deficient Mice

Based on the abundance of mitotic figures in *Arf* $^{-/-}$ tumors (Fig. 2.3A), we speculated that *Arf*-deficiency might confer a proliferative advantage to *Kras*-transformed pulmonary cells. To address this hypothesis, we examined the expression of cell cycle markers in tumors from *Arf* $^{+/+}$ and *Arf* $^{-/-}$ mice. Adenocarcinomas from *Arf*-deficient animals exhibited significantly elevated expression of the mitotic marker phospho-Histone H3 compared to *Arf* $^{+/+}$ adenocarcinomas (Fig. 2.7A), indicating that *Arf* loss is accompanied by an increase in cell proliferation. Immunoblot analysis further revealed up-regulation of nuclear Cyclin D1 and nuclear phospho-ERK1/2 expression in adenomas and adenocarcinomas from *Arf* $^{-/-}$ mice compared to *Arf* $^{+/+}$ (Fig. 2.7B). A marked increase in expression of the DNA damage marker phospho-Histone H2A.X was also observed in *Arf* $^{-/-}$ lung tumors compared to wild-type (Fig. 2.7C). Tumors from both genotypes expressed little detectable cleaved Caspase 3 at all stages of tumor development (Fig. 2.8), indicating that the pro-tumorigenic effect of *Arf* loss cannot be explained by differences in apoptotic rate. From these findings, we conclude that *Arf*

deficiency potentiates unrestrained cell proliferation and genomic instability. These signaling alterations likely account for the increased lung tumor growth and accelerated tumor progression observed in *Arf*-deficient animals.

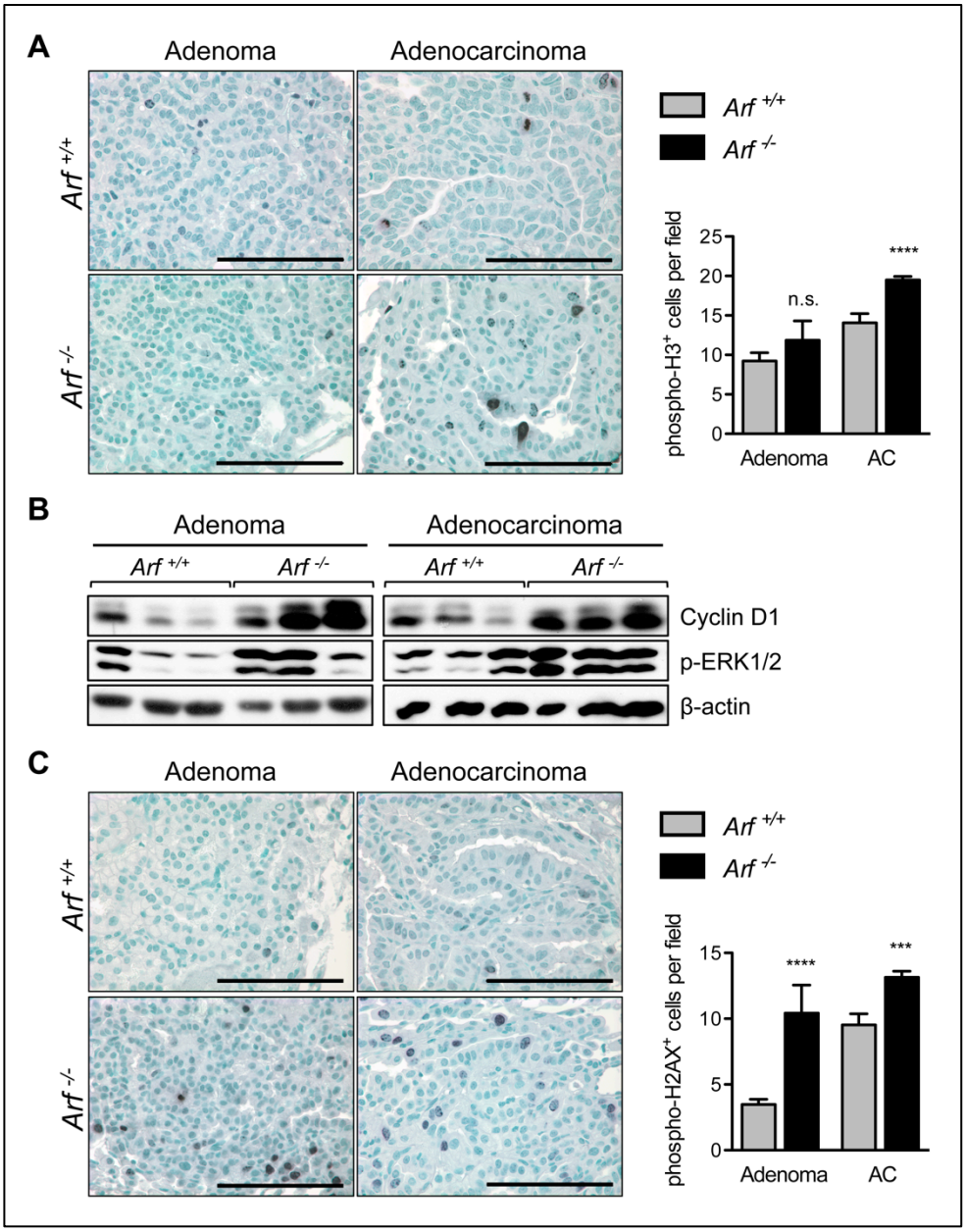

Figure 2.7: *Arf* loss accelerates cell proliferation. **[A]** *Arf* $^{-/-}$ ACs exhibited higher proliferation than tumors from *Arf* $^{+/+}$ mice, as shown by phospho-histone H3 staining (**** $P < 0.0001$; $n = 119$ adenoma and 220 AC fields counted from *Arf* $^{+/+}$; $n = 22$ and 829 fields *Arf* $^{-/-}$ mice). **[B]** Nuclear Cyclin D1 and phospho-ERK1/2 expression were strongly up-regulated in both adenomas and ACs in *Arf*-deficient compared to wild-type mice. Loading control β-actin. **[C]** Phospho-histone H2A.X staining illustrates an increase in DNA damage in tumors from *Arf*-deficient mice (**** $P < 0.0001$; *** $P = 0.0001$; $n = 85$ adenoma and 307 AC fields counted from *Arf* $^{+/+}$; $n = 31$ and 788 fields *Arf* $^{-/-}$ mice). Damage foci were also larger and more numerous per cell in *Arf* $^{-/-}$ mice compared to *Arf* $^{+/+}$. Note that the paucity of adenomas in *Arf* $^{-/-}$ animals prevented inclusion of additional fields in the statistical analysis of p-H3 and p-H2AX staining. Scale bars 100μm.

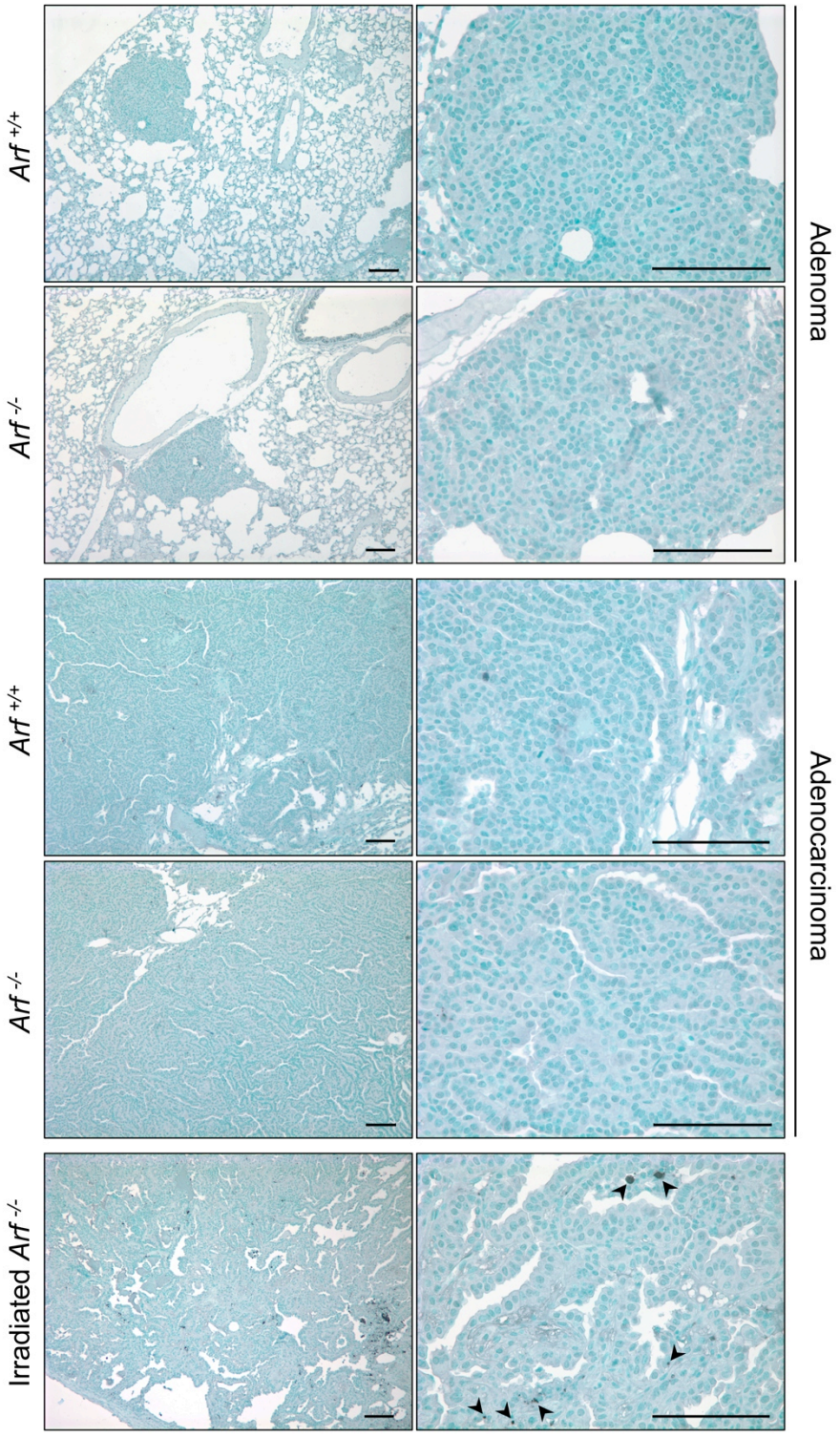

Figure 2.8: Absence of apoptosis in tumors of all genotypes. Cleaved Caspase 3 staining of adenomas and adenocarcinomas from *Arf* $^{+/+}$ and *Arf* $^{-/-}$ mice. All fields examined were largely or entirely negative for immunoreactivity. A lung adenocarcinoma from an irradiated (4Gy/4hr) *Arf* $^{-/-}$ mouse serves as positive control. Scale bars 100μm.

Discussion

Although ARF serves as a major regulator of p53 stability in oncogene-stressed cells and is frequently silenced in cancer, the contribution of ARF to tumor suppression in the lung remains controversial. Herein we tested the hypothesis that *Arf* suppresses carcinogen-induced, *Kras*-driven lung adenocarcinoma. ARF expression in wild-type mice was typically confined to benign adenomas and co-localized with $p21^{CIP1}$ expression, suggesting that tumor suppression by ARF is an early response in lung tumorigenesis that proceeds through a p53-dependent pathway. *Arf* loss resulted in the formation of large, poorly differentiated, and metastatic lung tumors. Elevated expression of nuclear Cyclin D1 and phospho-ERK1/2 in tumors from *Arf*-deficient mice, accompanied by increased proliferation and DNA damage, indicate that ARF induction restrains hyperproliferation and genomic instability in a *Kras*-mutant lung environment.

The *Cdkn2a* locus, which houses both *Arf* and *Ink4a*, has been proposed as a candidate for the *Papg-1* (i.e. pulmonary adenoma progression 1) susceptibility locus in mice. The *Papg-1* locus maps to mouse Chromosome 4 and was so named because of its significant association with lung tumor size (Manenti et al. 1997). A previous study investigating this connection employed the double knockout $Arf^{-/-};Ink4a^{-/-}$ mouse, precluding direct analysis of the contributions of each gene to pulmonary tumor suppression *in vivo* (Zhang et al. 2002). However, based on strain-specific variation in INK4a function, but not in ARF, the authors deduced that *Ink4a* is the major lung tumor suppressor gene encoded from *Cdkn2a*. Our findings reveal that *Arf* loss plainly facilitates the progression of lung adenocarcinoma. Nevertheless, there is strong evidence that *Ink4a* deficiency also contributes to the disease

(Sharpless et al. 2001; Gu et al. 2006; Zhang et al. 2010b). As in mice, parsing the tumor suppressive activities of ARF and INK4a in humans has proven difficult. Selective inactivation of *ARF* does occur in human cancers, but deletion of the entire *CDKN2A* locus is a far more common event (Saporita et al. 2007). It is likely that both products of the *CDKN2A* locus play an important role in suppressing lung adenocarcinoma development.

Arf-deficient mice unexpectedly presented with lung tumors that were markedly de-differentiated and, at times, sarcomatoid in appearance. These lesions exhibited many of the characteristics of pulmonary sarcomatoid carcinoma (PSC), a rare neoplasm in humans that has not previously been described in rodents (Nikitin et al. 2004; Pelosi et al. 2010). PSC is believed to be a "transitional" tumor type, with the sarcomatoid elements of the lesion deriving from epithelial carcinoma cells through the activation of an epithelial-mesenchymal transition (EMT) program (Wick and Swanson 1993; Thompson et al. 1996; Pelosi et al. 2010). The development of PSC lesions in *Arf*-deficient animals argues that ARF may regulate the *in vivo* differentiation of cancer cells. In support of this, loss of heterozygosity at Chromosome 9p21 (i.e. *CDKN2A*) has been reported in human PSC cases (Dacic et al. 2002), and *Arf*-deficiency has been shown to promote EMT in a breast cancer model (Debies et al. 2008). Additional investigation of the contribution of ARF to the EMT program in carcinogenesis is clearly warranted. In addition, our model provides a unique platform on which to conduct future examinations of PSC pathogenesis.

Cyclin D1 is a crucial regulator of CDK4 and CDK6 kinase activity during the G1 phase of the cell cycle (Quelle et al. 1993). RAS and other mitogenic signals drive expression of

Cyclin D1, resulting in progression to S phase (Lavoie et al. 1996). Gene amplification and elevated transcription of Cyclin D1 (i.e. *CCND1*) both occur in cancer, but the oncogenic properties of Cyclin D1 are linked to its persistent localization in the nucleus (Alt et al. 2000). Alterations in the transport and degradation of Cyclin D1 (Pontano and Diehl 2008), as well as certain missense mutations in *CCND1* itself, lead to its nuclear accumulation, promoting DNA re-replication and associated genomic instability (Aggarwal et al. 2007; Pontano et al. 2008). For this reason, increased nuclear Cyclin D1 is a poor prognostic indicator in NSCLC (Gautschi et al. 2007). In light of the established connection between nuclear Cyclin D1 accumulation and genomic instability, it is tempting to speculate that the high levels of DNA damage observed in *Arf*-deficient animals result from misregulation of Cyclin D1. However, although ARF has been shown to inhibit transcription of Cyclin D1 (D'Amico et al. 2004; Andrique et al. 2012), a mechanistic link between ARF and Cyclin D1 localization has yet to be demonstrated.

Alternatively, ARF may directly contribute to DNA damage signaling in NSCLC through both p53-dependent and -independent mechanisms. *Arf* $^{-/-}$ mouse embryonic fibroblasts exhibit an impaired DNA damage checkpoint response after ionizing radiation (IR), and sustained induction of p53 after IR requires ARF expression (Khan et al. 2000). Moreover, ARF triggers G2/M arrest in *p53*-deficient cells, both by impairing function of the CDC25C phosphatase (Normand et al. 2005) and by activating the ATM/CHK2 pathway (Eymin et al. 2006). Loss of *Arf* may also indirectly inhibit DNA repair by increasing the cellular pool of unbound MDM2. MDM2 has been shown to bind and inhibit NBS1, a component of the Mre11/Rad50/Nbs1 DNA repair complex, thus delaying repair of DNA double strand breaks

(Alt et al. 2005). It is conceivable that MDM2-mediated inhibition of DNA repair is elevated in an *Arf*-null tumor environment. In summary, multiple pathways connect ARF to the DNA damage response and DNA repair, and *Arf* loss may have profound consequences for genomic integrity. The degree to which increased DNA damage and impaired checkpoint control drive transformation in *Arf*-deficient cells, as well as the p53-dependency of these events, will be the subject of future investigation.

Recently, there have been conflicting reports regarding the timing of ARF expression during lung tumorigenesis. While ARF induction was observed in pulmonary adenomas from $Kras^{G12V}$ mice (Collado et al. 2005), two additional studies examining ARF in $Kras^{G12D}$-driven lung tumorigenesis found that ARF expression was largely restricted to high-grade adenocarcinomas (Feldser et al. 2010; Junttila et al. 2010). Notably, the latter investigations examined ARF expression in the context of *Trp53* nullizygosity. It is perhaps not surprising that regulation of ARF expression is altered in a *Trp53*-deficient environment, given that p53 represses ARF transcription (Zeng et al. 2011). Our findings clearly demonstrate that, in a pulmonary environment without *ab initio* alteration of tumor suppressor pathways, induction of ARF expression is an early event in neoplastic development.

There is also evidence to suggest that tumor suppression by *Arf* may greatly depend on the mouse model utilized. *Arf* loss did not significantly impact lung tumor progression in mice genetically engineered to bear a $Kras^{G12D}$ mutation (Young and Jacks 2010). Although we observed similar trends in lung tumor size as Young and Jacks, the extent of tumor growth, progression, and metastasis in $Arf^{-/-}$ mice compared to $Arf^{+/+}$ was considerably increased in

our investigation. The reasons for this are unclear, but the two models differ in several important ways. First, our study employed the urethane model of chemical carcinogenesis. Urethane primarily generates activating mutations in *Kras* codon 61, rather than codon 12 (Fig. 2.5), and the pulmonary cell lineage targeted by urethane may differ from that targeted in the genetic model. Second, the studies were performed in mice of dissimilar genetic backgrounds (NIH/Ola versus mixed C57Bl/6 x 129/SvJ), which could influence tumor phenotype. Many factors likely shape tumor suppression by ARF, both in mice and in humans. While our findings strongly implicate *Arf* loss in lung carcinogenesis, the precise conditions under which ARF exerts its anti-proliferative effect remain to be determined.

The tumor suppressor gene *ARF* has proven mysterious and controversial from its first identification. Although recent studies have raised questions regarding the contribution of ARF to lung tumor suppression, our findings clearly indicate a tumor suppressive function for ARF in NSCLC. Taken together with our previous report on tumor suppression by ARF in cutaneous squamous cell carcinoma (Kelly-Spratt et al. 2004), our results argue that induction of ARF is an early response to oncogenic signaling that erects a barrier against tumor growth and invasion. *ARF* status may therefore have important implications for lung cancer patient prognosis and clinical management.

Materials and Methods

Animal Model

All animal experiments were approved by the Institutional Animal Care and Use Committee of the Fred Hutchinson Cancer Research Center. *Arf*-deficient mice (Kamijo et al. 1997) were backcrossed onto the NIH/Ola strain (Harlan Olac, Oxfordshire, UK) for 20 generations. *Arf* $^{+/-}$ breeder mice were intercrossed and lung carcinogenesis studies performed on littermates of each genotype: *Arf* $^{-/-}$ (n = 59), *Arf* $^{+/-}$ (n = 33), and *Arf* $^{+/+}$ (n = 56). DNA for genotyping was isolated by digestion of ear tissue with proteinase K in InstaGene Matrix solution (Bio-Rad). Each mouse was genotyped as described (Kamijo et al. 1997). Mice were subjected to a single intraperitoneal injection of urethane (Sigma) in a PBS vehicle (1 mg/g bodyweight) between 21 and 28 days of age. A cohort of uninjected *Arf* $^{-/-}$ (n = 39), *Arf* $^{+/-}$ (n = 14), and *Arf* $^{+/+}$ (n = 33) mice was included for control. Animals were euthanized by CO_2 asphyxiation at indicated time points or when moribund. Lungs were filled with fixative before excision. Tumors macroscopically visible on the pleural surface were counted, and microcalipers were used to measure tumor diameter. Normal and tumor tissues were snap-frozen in liquid nitrogen and/or fixed in neutral buffered formalin.

Immunohistochemistry and Histopathology

Formalin-fixed tissues were processed to paraffin. For analysis, 4µm-thick sections were stained for either hematoxylin and eosin (H&E) or a specific protein. Immunostaining was performed using standard methods for the following proteins: phospho-Histone H3 (Ser10),

phospho-Histone H2A.X (Ser139), cleaved Caspase 3 (Asp175), phospho-p44/42 MAP Kinase (Thr202/Tyr204), i.e. ERK1/2, (all from Cell Signaling), $p19^{Arf}$ (Santa Cruz), and p21 (BD Biosciences). Staining for pro-Surfactant Protein C (Millipore) was completed by the Univ. of Washington Histology and Imaging Core Research Laboratory using the Leica Bond Automated Immunostainer.

Serial sections stained with H&E were analyzed and diagnosed as described (Kelly-Spratt et al. 2009). In order to match the original stained slide, global adjustments to white balance, brightness, and/or color saturation were made to copies of some photomicrographs using Adobe Photoshop. To calculate labeling indices for phospho-H3, phospho-H2A.X, and ARF, at least 10 fields at 600X magnification were counted for each individual tumor, where possible ($n \geq 3$ mice for each genotype and/or stage). To control for differences in staining between edge and interior fields of large-diameter tumors, only immunoreactive cells within two fields of the tumor perimeter were counted for all samples.

Western Blot Analysis

Frozen lung tumor tissues were used to prepare nuclear and cytoplasmic protein lysates, as described (Schreiber et al. 1989), with modifications (Philipp-Staheli et al. 2002). Buffers were supplemented with standard protease and phosphatase inhibitors. Proteins were quantified using the Bradford assay (Bio-Rad), diluted in loading buffer, run on SDS-PAGE gels, and transferred to PVDF membranes. Primary antibodies included Actin (Santa Cruz), Cyclin D1 and phospho-ERK1/2 (Cell Signaling), and β-actin (BioVision). HRP-conjugated

secondary antibodies (Santa Cruz) were used together with SuperSignal West detection substrate (Thermo Scientific).

Semi-Quantitative PCR

Genomic DNA was isolated from frozen *Arf* $^{+/-}$ lung adenocarcinomas and matched normal kidney tissue using the DNeasy Blood & Tissue Kit (Qiagen). DNA concentrations were measured in triplicate using the NanoDrop 1000 spectrophotometer (Thermo Scientific). Genotyping primers for exon 1β of *Arf*, as referenced above, were used to amplify equivalent amounts of genomic DNA over a 32 cycle PCR. Amplification reactions for the wild-type and knockout alleles were performed in separate tubes, and the products pooled and run jointly on an agarose gel. All samples were normalized to the knockout allele (i.e. loading control) band using Quantity One Software (Bio-Rad). Normal kidney tissue intensity levels were set at 100% for each animal. Tumor samples were run in duplicate in two independent experiments and averaged (n = 4). Mean band intensity was compared to the theoretical mean (100%) using the one-sample t test.

Kras Sequence Analysis

Total RNA was isolated from lung tumors using TRIzol reagent (Invitrogen) and subsequently purified with the RNeasy Mini Kit (Qiagen) according to the manufacturer's instructions. cDNA synthesis was performed with SuperScript II Reverse Transcriptase using oligo(dT) primers (Invitrogen). Amplification of *Kras* exons 1 and 2 was performed using primers 5'-AGGCCTGCTGAAAATGACTG-3' and 5'-CCAGGACCATAGGCACATCT-3'.

The BigDye Sequencing protocol (PE Applied Biosystems) was used to sequence *Kras* codons 12 and 13 (5'-CTCTATCGTAGGGTCGTAC-3'), and 61 (5'-GACTCCTACAGGAAACAAGT-3').

Statistical Methods

Time until development of pulmonary lesions causing death or requiring euthanasia was graphically summarized using the Kaplan-Meier method, and survival differences were analyzed for significance using the log-rank test for trend. Animals euthanized for reasons other than the presentation of pulmonary lesions were included in the analysis of overall mortality but were considered censored observations in the second log-rank analysis. The incidence of lung tumors by 17 weeks post urethane-injection was compared between genotypes; differences were analyzed for significance using the unpaired t test. Differences in mean tumor diameter and lung mass were analyzed using the unpaired t test. Animals who died before 20 weeks post-injection were excluded from analysis of tumor size. Individual tumor diameters were graphically summarized in a scatter plot, and variations between genotypes were statistically assessed using the Mann Whitney test. Incidence of benign and malignant lesions was compared between genotypes using the Fisher's exact test. Immunoreactive cell counts were graphed and analyzed for significant differences between groups using the unpaired t test. All values given represent mean ± SEM. All *P* values were two-tailed. *P* values < 0.05 were considered significant. Statistical analyses were performed using GraphPad Prism software.

Acknowledgements

This work was supported by the NCI Mouse Models of Human Cancer Consortium, U01 CA141550, and by NIEHS 5 R01 ES020116. SEB was supported by Public Health Service, National Research Service Award, T32 GM007270 from the NIGMS.

Chapter Three

ARF Suppresses Hepatic Vascular Neoplasia in a Carcinogen-Exposed Murine Model

Stephanie E Busch[1,3], Kay E Gurley[1], Russell D Moser[1], and Christopher J Kemp[1,2]

[1]Division of Human Biology, [2]Division of Public Health Sciences, Fred Hutchinson Cancer Research Center, Seattle, Washington 98109, USA

[3]Molecular and Cellular Biology Graduate Program, University of Washington, Seattle, Washington 98195, USA

modified from Busch, S. E., et al. 2012. ARF Suppresses Hepatic Vascular Neoplasia in a Carcinogen-Exposed Murine Model. *J. Pathol.* 227 (3):298-305.

Summary

Hepatic hemangiosarcoma is a deadly malignancy whose etiology remains poorly understood. Inactivation of the *CDKN2A* locus, which houses the *ARF* and $p16^{INK4a}$ tumor suppressor genes, is a common event in hemangiosarcoma patients, but the precise role of ARF in vascular tumorigenesis is unknown. To determine the extent to which ARF suppresses vascular neoplasia, we examined the incidence of hepatic vascular lesions in *Arf*-deficient mice exposed to the carcinogen urethane (i.p. 1 mg/g). Loss of *Arf* resulted in elevated morbidity and increased the incidence of both hemangiomas and incipient hemangiosarcomas. Suppression of vascular lesion development by ARF was heavily dependent on both *Arf* gene-dosage and the genetic strain of the mouse. *Trp53*-deficient mice also developed hepatic vascular lesions after exposure to urethane, suggesting that ARF signals through a p53-dependent pathway to inhibit the development of hepatic hemangiosarcoma. Our findings provide strong evidence that inactivation of *Arf* is a causative event in vascular neoplasia and suggest that the ARF pathway may be a novel molecular target for therapeutic intervention in hemangiosarcoma patients.

Introduction

Hemangiosarcoma is a rare but deadly disease that accounts for approximately one percent of all sarcoma cases and two percent of all primary liver malignancies in people (Budd 2002; Weihrauch et al. 2002; Koch et al. 2008). Hepatic hemangiosarcoma development has been associated with occupational exposure to a number of environmental toxins, and presentation of both cutaneous and visceral hemangiosarcomas after radiotherapy is also common (Robinson et al. 1987; Lee et al. 1996; Mark et al. 1996; Hozo et al. 2000; Cha et al. 2004). Despite the aggressive nature of this disease, there are few treatment options for patients presenting with hemangiosarcoma of the liver or other internal sites. Aggressive surgical resection is the standard form of treatment, but post-operative chemotherapy regimens are limited in both number and efficacy. Consequently, five-year survival rates for hemangiosarcoma patients are generally poor (Budd 2002; Koch et al. 2008). The limited success of adjuvant therapy reflects a fundamental lack of insight into the etiology of hemangiosarcoma. An enhanced understanding of the molecular mechanisms underlying this disease will identify novel targets for clinical intervention.

The *CDKN2A* locus, which houses the *ARF* ($p14^{ARF}$ in humans, $p19^{Arf}$ in mice) and $p16^{INK4a}$ tumor suppressor genes (Quelle et al. 1995), is frequently inactivated in hepatic hemangiosarcoma (Weihrauch et al. 2002). Epigenetic silencing of *ARF* occurs in 26% of cases (Weihrauch et al. 2002), but a direct, causative role for *ARF* in hemangiosarcoma formation has yet to be established. ARF is best known for stabilizing p53 activity in oncogene-stressed cells (Pomerantz et al. 1998; Tao and Levine 1999; Lin and Lowe 2001). In recent years, additional functions of ARF have also been described (Sherr 2006), such as

controlling the regression of the hyaloid vasculature system in the developing mouse eye (McKeller et al. 2002; Martin et al. 2004; Silva et al. 2005; Thornton et al. 2005; Gromley et al. 2009). However, the extent to which ARF regulates the proliferation or transformation of endothelial cells in adult mice and humans remains poorly studied.

Urethane (ethyl carbamate) is a chemical carcinogen frequently utilized in mouse pulmonary tumorigenesis studies. Occurring naturally in many foods and beverages as a fermentation by-product (Zimmerli and Schlatter 1991), urethane is metabolized by cytochrome P450 2E1 to form vinyl carbamate epoxide, which in turn produces potentially mutagenic DNA adducts (Forkert 2010). Notably, urethane's metabolites produce the same DNA adducts as vinyl chloride (Barbin 2000), a chemical known to induce angiosarcoma of the liver in humans (Creech and Johnson 1974). When administered at high doses or with recurrent low dose application, urethane induces long-latency hepatic vascular lesions in wild-type mice (Tannenbaum and Silverstone 1958; Kawamoto et al. 1961; Inai et al. 1991; Beland et al. 2005). One case of urethane-associated hepatic hemangiosarcoma in a human patient has also been reported (Cadranel et al. 1993).

Here we show that *Arf*-deficient mice exposed to urethane exhibited a significantly increased incidence of hepatic hemangiomas and incipient hemangiosarcomas. *Arf* loss contributed to multiple stages of vascular tumorigenesis, from early, preneoplastic angiectasis to the ultimate formation of hemangiomas with cellular atypia and hemangiosarcomatous differentiation. We further demonstrate that suppression of vascular neoplasia by ARF is heavily influenced by genetic strain, is *Arf* gene-dose-dependent, and likely proceeds through a p53-dependent

pathway. Our findings present strong evidence that ARF suppresses the formation of vascular tumors in adult mice and, furthermore, provide a model in which to study the etiology of vascular neoplasia.

Materials and Methods

Animal Model

All experiments were approved by the FHCRC Institutional Animal Care and Use Committee. *Arf*-deficient mice (Kamijo et al. 1997) were backcrossed separately onto C57BL/6 (The Jackson Laboratory, Bar Harbor, ME, USA) and NIH/Ola (Harlan Olac, Oxfordshire, UK) strains for 16 and 20 generations, respectively. *Arf* $^{+/-}$ mice were intercrossed and carcinogenesis studies performed on resultant littermates of each genotype: *Arf* $^{-/-}$ (n = 69 for C57BL/6; n = 59 for NIH/Ola), *Arf* $^{+/-}$ (n = 42 C57BL/6; n = 33 NIH/Ola), and *Arf* $^{+/+}$ (n = 30 C57BL/6; n = 56 NIH/Ola). Mice deficient for *Trp53* (Donehower et al. 1992) were backcrossed onto the C57BL/6 strain for 20 generations, and carcinogenesis studies were performed on male mice of each genotype: *Trp53* $^{-/-}$ (n = 11), and *Trp53* $^{+/-}$ (n = 22). DNA for genotyping was isolated by digestion of ear tissue with proteinase K in InstaGene Matrix solution (Bio-Rad, Hercules, CA, USA). Each mouse was genotyped as described (Donehower et al. 1992; Kamijo et al. 1997).

Arf- and *Trp53*-deficient mice were subjected to a single injection of urethane (Sigma, St. Louis, MO, USA) in a PBS vehicle (i.p. 1 mg/g bodyweight) between 21 and 28 days of age. An additional cohort of *Trp53* $^{+/-}$ mice (n = 12) was injected with urethane at 14 days of age.

A cohort of unexposed C57BL/6 strain *Arf* $^{-/-}$ (*n* = 25), *Arf* $^{+/-}$ (*n* = 23), and *Arf* $^{+/+}$ mice (*n* = 22) was included for control. Animals were euthanized by CO_2 asphyxiation at indicated time points or when moribund. All tissues were examined for the presence of lesions during necropsy. Normal and pathological tissues were frozen in liquid nitrogen and/or fixed for subsequent analysis.

Histopathology and Immunohistochemistry

Tissues were fixed in 10% neutral buffered formalin for at least 4 hrs, then processed and embedded in paraffin. 4-μm-thick tissue sections were cut, mounted on glass slides, and stained with H&E. Tissue samples were submitted to the FHCRC institutional histopathology core for von Willebrand Factor staining (#A0082; Dako, Glostrup, Denmark). A small set of tissue sections was also stained for phosphorylated p42/44 MAPK (pERK) (#4376; Cell Signaling Technology, Danvers, MA, USA). Controls included mouse kidney and rabbit IgG isotype control. All H&E slides were analyzed by a veterinary pathologist blind to genotype. Diagnosis of angiectasis was based on dilatation of the liver sinusoids in the absence of proliferating endothelial cells. Diagnosis of hemangioma was determined by the presence of abnormal vascular spaces lined by proliferating endothelial cells. A subset of more aggressive hemangiomas presented with cellular atypia, regions of solid growth, and incipient hemangiosarcomatous differentiation (Thoolen et al. 2010). In order to match the original stained slide, global adjustments to white balance, brightness, and/or color saturation were made to copies of some photomicrographs using Adobe Photoshop.

Statistical Methods

Time until development of hepatic vascular lesions causing death or requiring euthanasia was graphically summarized in a Kaplan-Meier plot, and survival differences were analyzed for significance using the log-rank test. Animals euthanized for reasons other than presentation of vascular lesions were considered censored observations in the second log-rank analysis. These animals were included in the analysis of overall mortality for *Arf* mice. The incidence of lesions by 25 weeks post urethane-injection was compared between strains for each genotype, and between *Arf*- and *Trp53*-deficient animals; differences were analyzed for significance using the Fisher's exact test. Mice who died before 25 weeks and did not present with macroscopic hepatic vascular lesions were excluded from the Fisher's exact test analyses.

Results

Accelerated Morbidity of *Arf*-Deficient Mice after Urethane Exposure

To investigate the tumor suppressive role of ARF in vascular neoplasia, we exposed *Arf*-deficient mice to the carcinogen urethane. Kaplan-Meier analysis demonstrated that C57BL/6 $Arf^{-/-}$ mice injected with urethane suffered significantly shortened lifespans compared to their $Arf^{+/+,}$ $Arf^{+/-}$ and untreated $Arf^{-/-}$ littermates (Fig. 3.1A). The median life expectancy of urethane-exposed $Arf^{-/-}$ mice was reduced to 262 days from greater than 400 days for all other genotypes. Both $Arf^{-/-}$ and $Arf^{+/-}$ mice also developed lymphomas and sarcomas (data not shown) at a rate similar to that previously reported (Kamijo et al. 1999). Moribund $Arf^{-/-}$ mice frequently presented with lethargy, swollen abdomens, and symptoms of anemia (e.g. pale ears and digits). During necropsy these animals were found to have grossly diseased livers

bearing multifocal, massive thromboses (Fig. 3.1B). Rupture of these thromboses resulted in abdominal hemorrhaging that caused near-immediate death. In contrast to the marked lethality of urethane to C57BL/6 *Arf* $^{-/-}$ mice, no *Arf* $^{+/+}$ or *Arf* $^{+/-}$ littermates or unexposed *Arf* $^{-/-}$ mice succumbed to hepatic vascular lesions by 50 weeks post-injection (Fig. 3.1C). Lesion incidence and associated lethality were statistically similar between genders (data not shown).

Susceptibility to Vascular Lesions Is Strain-Specific

Tumor susceptibility in mice is strongly influenced by genetic background. To investigate the effect of genetic background on urethane-induced vascular lesions, we examined tumor incidence in NIH/Ola strain *Arf*-deficient mice (Fig. 3.1D). As in the C57BL/6 *Arf* $^{+/+}$ mice, urethane injection did not yield gross hepatic lesions in NIH/Ola *Arf* $^{+/+}$ mice. However, in contrast to the 40.9% (9 of 22) of C57BL/6 *Arf* $^{+/-}$ mice that exhibited macroscopic hepatic vascular lesions by 25 weeks, no NIH/Ola *Arf* $^{+/-}$ mice (0 of 32) bore lesions at this age. Furthermore, only 66.7% of NIH/Ola *Arf* $^{-/-}$ mice (12 of 18) developed lesions by 25 weeks, compared to 91.7% of C57BL/6 *Arf* $^{-/-}$ mice (44 of 48). Hepatic vascular lesions that did develop in NIH/Ola strain mice were typically smaller and less physically deleterious than lesions in C57BL/6 mice. Therefore, the susceptibility of *Arf*-deficient animals to vascular carcinogenesis is modified by genetic background, with the relative risk of C57BL/6 strain exceeding NIH/Ola.

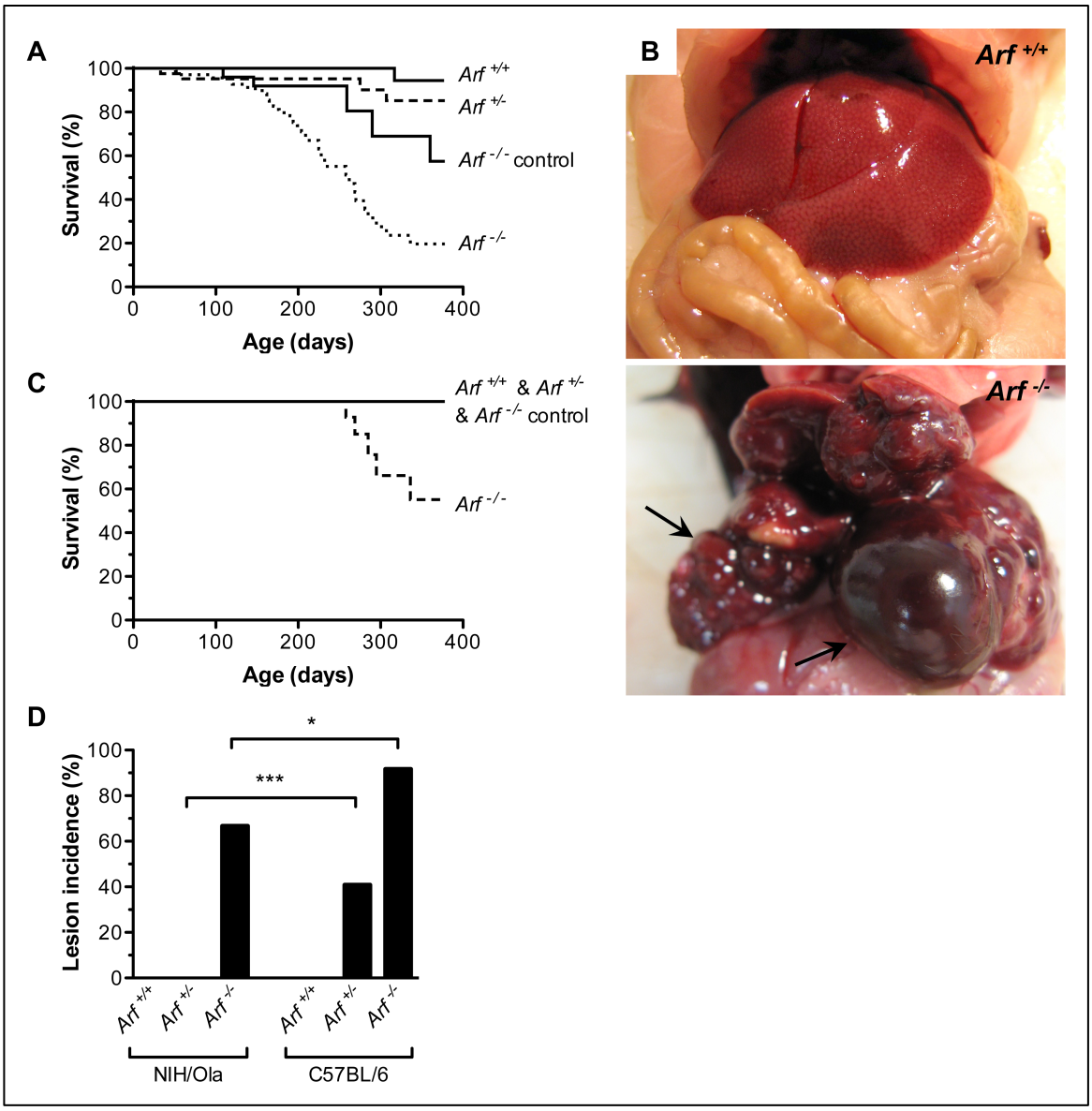

Figure 3.1: *Arf*-deficient mice developed lethal vascular tumours after urethane exposure. **A:** The overall mortality of *Arf* $^{-/-}$ mice was increased relative to *Arf* $^{+/+}$ and *Arf* $^{+/-}$ littermates and untreated *Arf* $^{-/-}$ mice (log-rank test, two-tailed; $P < 0.0001$). **B:** Representative images of livers from urethane exposed *Arf* $^{+/+}$ (top) and *Arf* $^{-/-}$ (bottom) mice. Massive, multifocal, blood-filled lesions (arrows) covered the liver surface in *Arf*-deficient mice. **C:** The incidence of lethal hepatic vascular lesions increased in *Arf* $^{-/-}$ mice compared to *Arf* $^{+/+}$, *Arf* $^{+/-}$, and untreated *Arf* $^{-/-}$ littermates. Data were censored to include only animals whose deaths were attributed to vascular lesions (log-rank test, two-tailed; $P = 0.0005$). **D:** Incidence of macroscopic hepatic vascular lesions observed 25 weeks post-urethane exposure in NIH/Ola and C57BL/6 strain *Arf* $^{+/+}$, *Arf* $^{+/-}$, and *Arf* $^{-/-}$ mice (Fisher's exact test, two-tailed; * $P = 0.02$, *** $P < 0.0001$).

Loss of *Arf* Facilitates the Malignant Progression of Vascular Neoplasia

To determine the histopathological basis of the hepatic lesions, H&E stains for a subset of samples collected at 25 and 50 weeks post-exposure were examined by a veterinary pathologist. The analysis uncovered a tumor progression spectrum of vascular neoplasia in *Arf*-deficient mice, with lesions ranging from angiectasis to benign hemangioma to hemangioma with cellular atypia (Table 3.1). Low magnification views of representative wild-type and *Arf*-deficient liver lobes are shown in Figure 3.2 (A, B), and characteristic images of the tumor diagnostic criteria are provided (Fig. 3.2C-E). By 50 weeks post-exposure, 40% of *Arf* $^{+/+}$ mice exhibited focal angiectasis but were otherwise unaffected compared to *Arf*-deficient mice. At 25 weeks, all *Arf* $^{+/-}$ mice examined presented with angiectasis of the liver. By 50 weeks, 80% of *Arf* $^{+/-}$ mice exhibited hemangioma lesions, with one mouse displaying multifocal cellular atypia and hemangiosarcomatous differentiation. A nearly identical rate of hemangioma incidence (75%) was observed in *Arf* $^{-/-}$ mice, but at the earlier time point of 25 weeks post-urethane exposure. 38% and 40% of *Arf* $^{-/-}$ mice presented with incipient hemangiosarcomas at the 25 and >25 week time points, respectively. One unexposed *Arf* $^{-/-}$ mouse (n = 3) developed a small hemangioma by 50 weeks, and no vascular lesions were observed in unexposed *Arf* $^{+/-}$ mice at the same time point (n = 5; data not shown).

The diagnosis of vascular neoplasia was substantiated by immunohistochemical analysis with von Willebrand Factor (vWF) antibody, an established marker of endothelial cells (Fig. 3.2F-H). While vWF staining was restricted to the endothelial cells lining hepatic blood vessels in unexposed mice (Fig. 3.3A), abundant vWF positive cells were present in urethane-induced

tumors (Fig. 3.2G, H), confirming the endothelial nature of the hepatic lesions. Vascular lesions that developed in urethane-exposed, *Arf*-deficient animals – including a cardiac hemangioma – were also focally positive for phosphorylated ERK, an indicator of RAS pathway activation (Fig. 3.3A, B). Taken together, these findings suggest that suppression of vascular tumor development by ARF in this model is time- and *Arf* gene-dose-dependent, in that *Arf* $^{+/-}$ mice demonstrated both delayed neoplastic formation and malignant progression compared to their *Arf* $^{-/-}$ littermates.

Table 3.1: Vascular tumor progression is *Arf* gene-dosage and time-dependent. [a] An insufficient number of C57BL/6 *Arf* $^{-/-}$ mice survived to 50 weeks post-urethane exposure, necessitating the inclusion of samples collected at any time after 25 weeks in the analysis. [b] A subset of liver samples from urethane-exposed, female mice of each genotype was selected at random for scoring. H&E stained sections were diagnosed blind to genotype by a veterinary pathologist. [c] Diagnosis indicates presence of hemangioma with cellular atypia and hemangiosarcomatous differentiation.

	Arf $^{+/+}$		***Arf*** $^{+/-}$		***Arf*** $^{-/-}$	
	25wk	**50wk**	**25wk**	**50wk**	**25wk**	**> 25wk[a]**
Lesion grade	Lesion incidence % (number of cases/total # tissues examined[b])					
Angiectasis	0 (0/5)	40 (2/5)	100 (4/4)	80 (4/5)	88 (7/8)	80 (4/5)
Hemangioma	0 (0/5)	0 (0/5)	0 (0/4)	80 (4/5)	75 (6/8)	80 (4/5)
Hemangioma w/atypia[c]	0 (0/5)	0 (0/5)	0 (0/4)	20 (1/5)	38 (3/8)	40 (2/5)

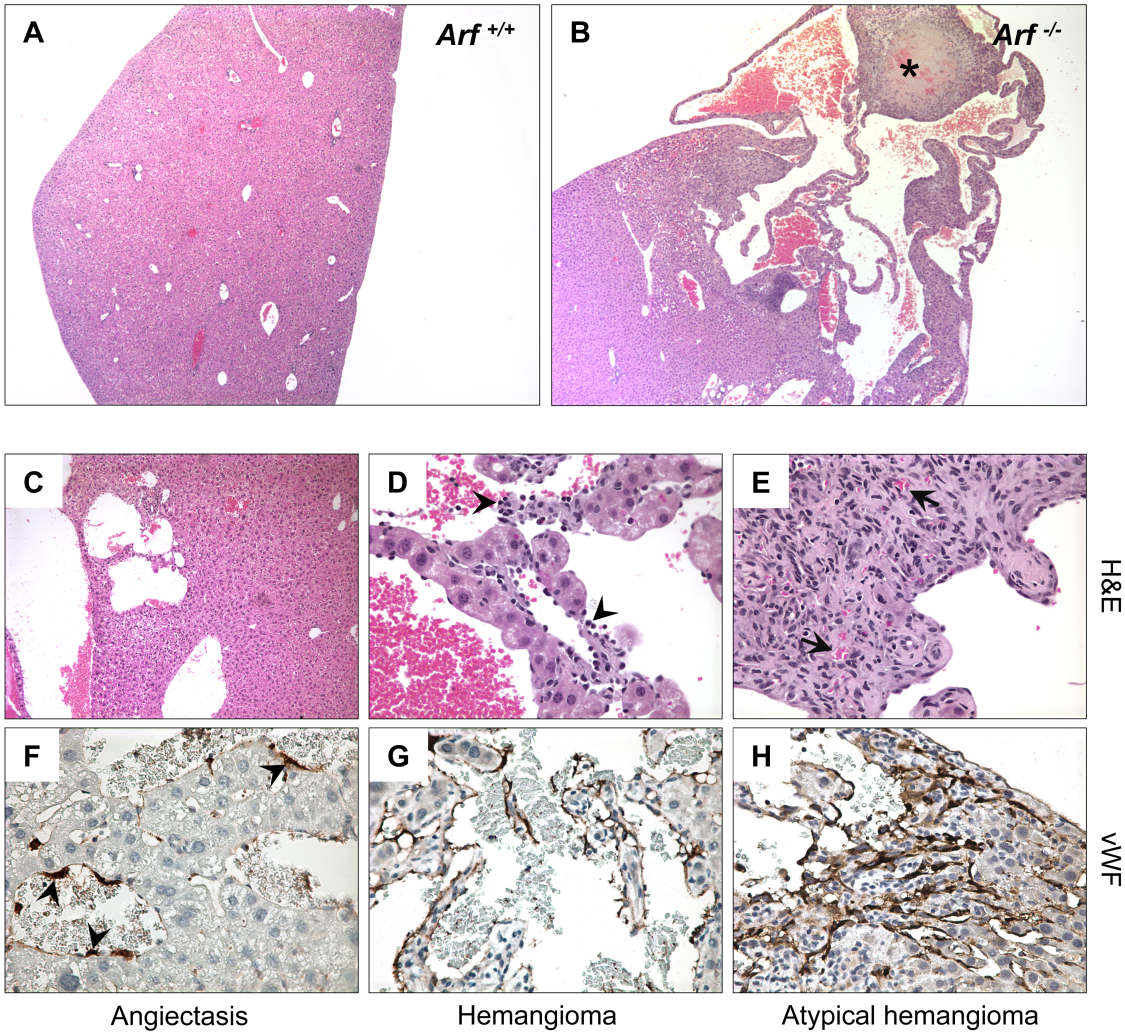

Figure 3.2: Pathology of urethane-induced vascular lesions. **A-B:** Representative images of liver lobes from urethane-exposed mice (40X magnification). The hepatic parenchyma in *Arf* $^{+/+}$ mice (**A**) remained largely unaffected. Vascular lesions on the hepatic surface in *Arf* $^{-/-}$ mice (**B**) disrupted the hepatic architecture and caused substantial secondary change, including thrombosis and associated fibrosis (asterisk). Regions of dark background shading in the upper corners of (**A**) and (**B**) were removed using Adobe Photoshop®. **C:** Angiectasis. A single layer of endothelial cells lined the enlarged sinusoids (100X). **D:** Uniform, proliferating endothelial cells (arrowheads) formed irregular vascular channels characteristic of hemangioma (400X). **E:** Multifocally, some hemangiomas exhibited cellular atypia and incipient hemangiosarcomatous differentiation. Plump-to-elongated endothelial cells formed small vascular channels (arrows) and appeared clustered and multilayered (400X). **F-H:** vWF staining (400X) highlights the normal sinusoidal endothelial cells in angiectasis (arrowheads, **F**), shows proliferating endothelial cells lining abnormal vascular spaces in hemangioma (**G**), and reveals atypical endothelial cells aligning in sheets in an incipient hemangiosarcoma (**H**).

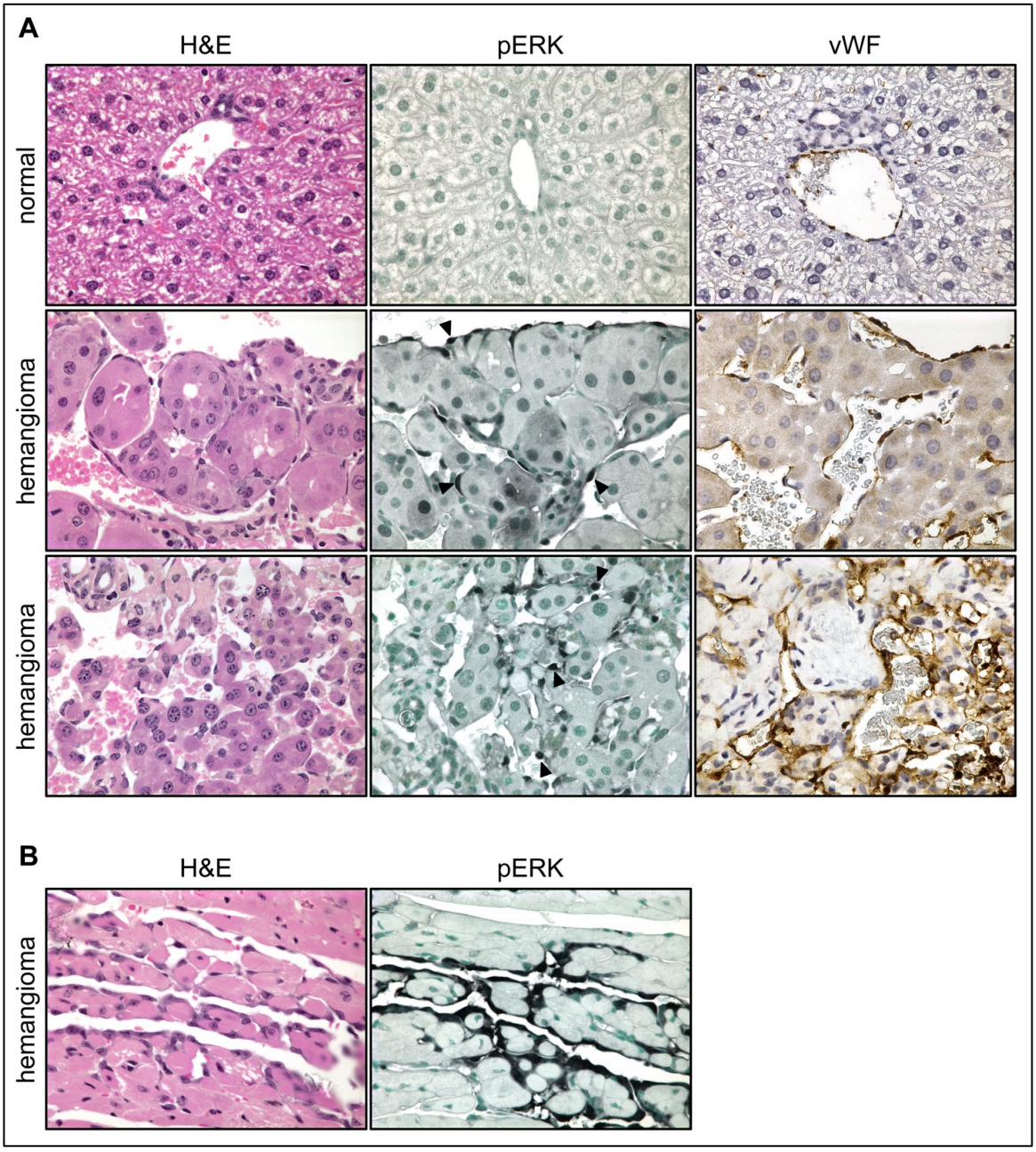

Figure 3.3: Hepatic vascular lesions exhibit activation of the RAS-ERK pathway. **A:** Proliferating endothelial cells, highlighted with vWF (right) were focally positive for phospho-ERK in the hepatic hemangiomas (600X). Arrowheads indicate positive cells. **B:** A urethane-induced cardiac hemangioma was strongly positive for phosopho-ERK (600X).

Incidence of Vascular Lesions in *Trp53*-Deficient Mice

Many of the tumor suppressive activities previously attributed to ARF are related to its role in stabilizing cellular p53 levels (Sherr 2006), and *Trp53* loss has been implicated in

hemangiosarcoma development in mice and humans (Hollstein et al. 1994; Kemp 1995; Naka et al. 1997; Zietz et al. 1998; Carmichael et al. 2000). These facts prompted us to determine the extent to which suppression of vascular neoplasia by ARF is p53-dependent. We analyzed the effect of urethane exposure on C57BL/6 *Trp53*-deficient male mice. All *Arf* $^{+/+}$;*Trp53* $^{-/-}$ animals (n = 11) succumbed to thymic lymphomas by 15 weeks post-exposure, and none exhibited hepatic vascular lesions at necropsy. However, 9.5% of *Arf* $^{+/+}$;*Trp53* $^{+/-}$ mice (2 of 21) developed hepatic vascular lesions by 25 weeks (Fig. 3.4A), and a small cohort of mixed-gender *Arf* $^{+/+}$;*Trp53* $^{+/-}$ mice exposed to urethane at an earlier time point (14 days) and allowed to age up to 58 weeks post-injection presented with malignant hepatic vascular lesions (3 of 12; 25%; Fig. 3.4A, B). Although the 25-week lesion incidence rate for *Trp53* $^{+/-}$ mice (9.5%) was lower than that observed in *Arf* $^{+/-}$ mice (3 of 12 male mice; 25%), this difference was not statistically significant (P = 0.3275). The development of vascular tumors in urethane-exposed *Trp53*-deficient mice supports the argument that tumor suppression by ARF in this model is likely mediated by p53.

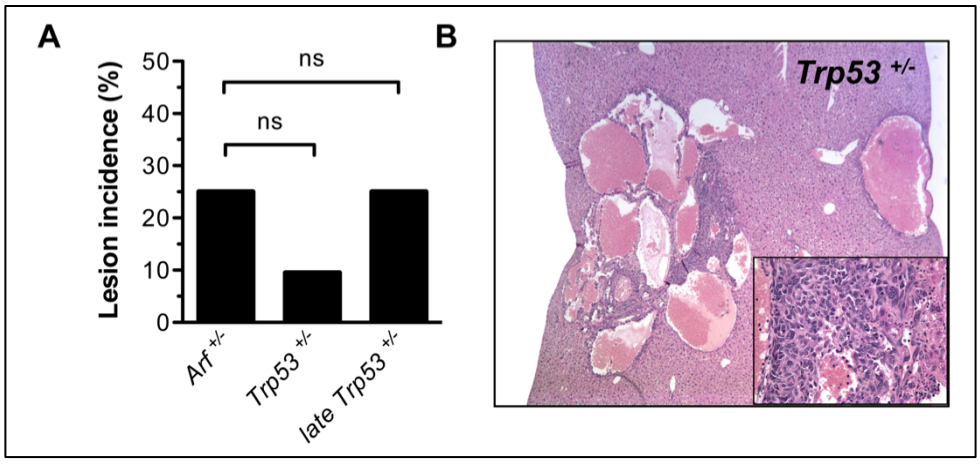

Figure 3.4: Hepatic vascular neoplasia in *Arf*-deficient mice resembles lesions observed in urethane-exposed *Trp53*-deficient mice. **A:** Incidence of hepatic vascular lesions observed 25 weeks post-urethane exposure in male C57BL/6 *Arf* $^{+/-}$ (3 of 12; 25.0%) and *Trp53* $^{+/-}$ (2 of 21; 9.5%) mice (Fisher's exact test, two-tailed; P = 0.3275). Incidence of lesions in *Trp53* $^{+/-}$ mice rose at later time points, as 3 of 12 (25.0%) mice sacrificed between 30 and 58 weeks post-urethane exposure developed lesions. **B:** Hemangiosarcoma from a *Trp53* $^{+/-}$ mouse (40X). Multiple large, blood-filled lakes are present, bordered by solid sheets of plump-to-spindle shaped endothelial cells (inset, 400X).

Discussion

The etiology of hepatic hemangiosarcoma is poorly understood, and, consequently, patients diagnosed with the disease face extremely poor prognoses. Weihrauch and colleagues previously reported that the $p14^{ARF}$ locus is frequently silenced in hemangiosarcomas of the liver (Weihrauch et al. 2002). Their work provided correlative but not causative evidence for tumor suppression by ARF in vascular neoplasia. Here we report evidence for a direct, causative role for ARF and its downstream signaling partner p53 in suppressing the formation and malignant progression of primary hepatic vascular tumors. Mice with homozygous deletion of *Arf* exhibited a significant predisposition for the development of hemangiomas and incipient hemangiosarcomas after carcinogen exposure, demonstrating that loss of *Arf* is sufficient to promote vascular neoplasia.

Many cancers are known to develop through a step-wise process, from hyperplastic to benign to malignant lesions. Evidence for this type of evolutionary progression, however, has not been established for hemangiosarcoma development (Cohen et al. 2009). Our study captured a tumor progression spectrum of hepatic vascular lesions. *Arf*-deficient mice developed lesions ranging from angiectasis to benign hemangiomas and incipient hemangiosarcomas in a time- and *Arf* gene-dose-dependent manner. In particular, $Arf^{+/-}$ mice displayed a dramatic disease progression between the 25 and 50-week time points. These findings elucidate the evolution of vascular tumors and, moreover, support the potential use of this mouse model in future investigations into the etiology of hemangiosarcoma.

An interesting finding from our study was that mouse genetic background strongly influenced susceptibility to the development of vascular tumors after urethane exposure. C57BL/6 *Arf* $^{-/-}$ mice presented with hepatic vascular lesions at a significantly higher frequency than NIH/Ola *Arf* $^{-/-}$ mice. The strain-specificity of this disease phenotype indicates the presence of genetic modifiers that differentially regulate vascular tumorigenesis between strains. Although a previous study of C57BL/6 *Trp53* $^{+/-}$ mice chronically exposed to urethane found a high susceptibility to hepatic vascular carcinogenesis (Carmichael et al. 2000), another study observed protection against hepatic vascular lesions in C57BL/6 strain *Vhl*-mutant mice compared to A/J and BALB/c strain mutants (Ma et al. 2003). Clearly, further investigation is warranted. Our model may lend itself to the future identification of additional genes involved in hemangiosarcoma susceptibility.

Vascular tumors are believed to result from the aberrant proliferation and transformation of endothelial cells (Budd 2002). ARF is required for the developmentally controlled regression of the hyaloid vasculature system in the mouse eye (McKeller et al. 2002), but the question of whether ARF contributes to vasculogenesis or angiogenesis in adults remains largely unanswered. Our finding that loss of *Arf* promotes the formation of vascular tumors indicates that ARF may, under defined circumstances, control endothelial cell proliferation in adult animals. However, an alternative hypothesis regarding hemangiosarcoma histogenesis posits that the cell of origin is a pluripotent mesenchymal stem cell (Thoolen et al. 2010). This hypothesis holds that although hemangiosarcomas present with an endothelial cell-like appearance, the tumors may in fact not be derived from mature endothelium but rather from a more primitive, progenitor cell.

Arf-deficient mice are prone to spontaneous sarcomagenesis (Kamijo et al. 1999), and there is mounting evidence that ARF suppresses the development of multiple sarcoma types in humans (Benassi et al. 2001; Takahira et al. 2004; Huang et al. 2005; Oda et al. 2005; Oh et al. 2006; Niini et al. 2011). This association between altered *ARF/INK4a* expression and the development of a wide range of sarcoma subtypes argues that the *CDKN2A* locus may play a critical role in arresting the growth of a transformed mesenchymal progenitor cell. Indeed, *CDKN2A* was found to be deleted in hTERT-transduced adult mesenchymal stem cells that exhibited anchorage independence and formed tumors when injected into mice (Serakinci et al. 2004; Burns et al. 2005). Taken together with these findings, our study supports the argument that the development of vascular tumors upon *Arf* loss reflects changes in mesenchymal stem cell differentiation and proliferation rather than a hyperproliferation of endothelial cells. In either case, the absence of vascular lesions in unexposed *Arf*-deficient mice indicates that for hemangiosarcoma development to occur, *Arf* loss must be accompanied by a cooperative "event" provided by urethane, presumably an oncogenic mutation.

The canonical function of ARF is to antagonize the MDM2 (HDM2 in humans) ubiquitin ligase in oncogene-stressed cells, thereby stabilizing cellular p53 levels and engaging an anti-proliferative response (Lin and Lowe 2001; Lowe et al. 2004). Urethane is known to cause oncogenic *Ras* mutations in rodents (Dragani et al. 1991; Maronpot et al. 1995; Horio et al. 1996), and mutant *RAS* has also been identified in human hepatic hemangiosarcoma (Marion et al. 1991; Przygodzki et al. 1997). In this study, we observed evidence of RAS-ERK

pathway activation in urethane-induced vascular lesions. Moreover, we have previously demonstrated that ARF suppresses the malignant progression of RAS-driven squamous cell carcinoma through a p53-dependent pathway (Kelly-Spratt et al. 2004), and other groups have shown that stabilization of p53 by ARF is required for cancer protection many weeks after exposure to genotoxins (Christophorou et al. 2006; Efeyan et al. 2006). Our findings here reveal a similar pattern. The ARF-p53 axis acts as an important, delayed barrier to carcinogen-induced hemangiosarcoma development.

Our study provides the first causative link between *Arf* loss and vascular neoplasia. Nevertheless, the specific contributions of *ARF* and *INK4a*, the two genes at the *CDKN2A* locus, to tumor suppression in humans remain controversial (Kamijo et al. 1997; Hahn and Weinberg 2002; Lowe and Sherr 2003; Gil and Peters 2006; Sherr 2006; Berger and Bardeesy 2007; Saporita et al. 2007). Deletion of the entire chromosomal region is frequent (Maher et al. 2001; Sharpless and Chin 2003; Conway et al. 2010), but it is clear that selective inactivation of *ARF* does occur in human cancer (Saporita et al. 2007). Weihrauch et al have published on the alterations of *INK4a* and *ARF* in human hepatic angiosarcoma (Weihrauch et al. 2002). Their findings show that loss of *INK4a* almost certainly contributes to hepatic vascular neoplasia, as 63% of tumors exhibited hypermethylation of *INK4a*. However, *ARF* was also found to be hypermethylated in human hepatic angiosarcoma (26%), and in 11% of patients hypermethylation was specific to *ARF* while *INK4a* remained unmethylated. Furthermore, the strong evidence that *p53* and *HDM2* are altered in human vascular neoplasia suggests that their functional partner ARF may also play a role in the disease (Hollstein et al. 1994; Naka et al. 1997; Zietz et al. 1998; Kosemehmetoglu et al. 2011). In summary, these

findings argue that there is selective pressure to inactivate both the ARF-HDM2-p53 pathway and the INK4a-RB pathway in human hepatic vascular neoplasia, as is seen in many other human malignancies (Sherr and McCormick 2002; Hanahan and Weinberg 2011).

The need for novel therapeutics to treat hemangiosarcoma patients is critical. Current standards of treatment are focused primarily on aggressive surgical resection, and the availability of adjuvant chemotherapies is limited, in part because few studies to date have elucidated the molecular pathways underlying vascular neoplasia (Budd 2002; Koch et al. 2008). Prognoses for patients diagnosed with hemangiosarcoma will likely not improve without significant advancement in our knowledge of the etiology of the disease. The identification of ARF as a suppressor of hepatic vascular lesion development illuminates the process of hemangiosarcomagenesis and suggests potential targets for future therapeutic intervention.

Acknowledgements

This work was supported by the NCI Mouse Models of Human Cancer Consortium, U01 CA141550, and by NIEHS 5 R01 ES020116. SEB was supported by Public Health Service, National Research Service Award, T32 GM007270 from the NIGMS.

Chapter Four

Understanding the Role of ARF in Cutaneous Squamous Cell Carcinoma Invasion and Metastasis

Stephanie E Busch[1,2,3], Karen S Kelly-Spratt[1,2], Susan C Tilton[2], Russell D Moser[2], Kay E Gurley[2], Nolwenn LeMeur[2], Robert Gentleman[2], Christopher J Kemp[2]

[1]The authors contributed equally to this work.

[2]Fred Hutchinson Cancer Research Center, Seattle, Washington 98109

[3]Molecular and Cellular Biology Graduate Program, University of Washington, Seattle, Washington 98195

Manuscript in Preparation

Summary

Understanding the process by which tumor cells invade and metastasize is a vitally important goal of cancer research. The two-step DMBA/TPA mouse skin carcinogenesis protocol provides an excellent model in which to study the malignant progression and metastatic spread of autochthonously arising cutaneous squamous cell carcinoma (SCC). We previously demonstrated that ARF, a tumor suppressor protein encoded from the *Cdkn2a* locus, inhibits the growth and invasion of DMBA/TPA-induced SCC. Herein we describe a novel role for ARF in directly suppressing the metastatic spread of carcinoma cells. Loss of *Arf* significantly increased the incidence of SCC metastases to proximal lymph nodes and to the lung, and a pro-invasion phenotype of *Arf*-deficient tumor cells was observed at the transcriptional level. Future efforts will focus on validation of key array targets, with particular emphasis on the up-regulation of E-cadherin and stem cell markers in metastatic carcinomas from *Arf*-deficient animals.

Introduction

The development of cancer is a multistep process, typically proceeding through discrete stages of tumor evolution. Although frequently asymptomatic and seldom detected in patients, many tumors of epithelial origin first present as hyperplastic or adenomatous lesions. The acquisition of additional genetic alterations drives tumor progression to malignancy (Fearon and Vogelstein 1990). Ultimately, the defining characteristics of malignant carcinoma are invasion and metastasis. Because metastatic disease is a critical determinant of patient survival (Chaffer and Weinberg 2011), arresting tumor growth at early stages and preventing the dissemination of neoplastic cells throughout the host are important goals of cancer research.

The two-step DMBA/TPA mouse skin carcinogenesis protocol provides an excellent model in which to study the natural history of tumor development (Kemp 2005). The initiating agent, DMBA, produces an oncogenic driving mutation, frequently *Hras* (Balmain et al. 1984; Nelson et al. 1992), in a small population of epidermal keratinocytes. After initiation, application of a promoting agent, such as TPA, causes the clonal expansion of the mutated cells. Cutaneous squamous cell tumors form and are readily visible on the dorsal surface of carcinogen-exposed mice (Abel et al. 2009). First to develop are exophytic squamous cell papillomas, neatly folded hyperplastic lesions that protrude from the skin surface. After a variable amount of time, depending on mouse strain and genotype (Sundberg et al. 1997; Abel et al. 2009), the papillomas begin to involute. The resultant endophytic tumors, referred to as squamous cell carcinomas (SCC), invade through the basement membrane and display cellular atypia and disorganized proliferation.

Our group has previously demonstrated that loss of ARF, a product of the *CDKN2A* locus and a key regulator of p53 activity (Sherr 2006), accelerates conversion of squamous cell papillomas to malignant carcinomas (Kelly-Spratt et al. 2004). Expression of ARF was increased in wild-type papillomas compared to normal skin but subsequently decreased in carcinomas. Moreover, tumors from *Arf* heterozygote animals were shown to lose their wild-type *Arf* allele during conversion to carcinoma. From these findings, we concluded that ARF suppresses malignant progression *in vivo*. Preliminary studies suggested that ARF might also inhibit the formation of metastases. However, study design precluded direct comparison of metastatic frequency between carcinomas of $Arf^{+/+}$ and $Arf^{-/-}$ mice. Herein we analyze the role of ARF in tumor invasion and metastasis, paying particular attention to the transcriptional changes that occur with *Arf* loss in malignant tumors.

Materials and Methods

Animal Experiments

All experiments were approved by the FHCRC Institutional Animal Care and Use Committee. The $Arf^{GFP/GFP}$ reporter mouse was generously provided by Charles Sherr (St. Jude's Research Hospital, Memphis, TN, USA) and backcrossed for three generations onto the NIH/Ola strain (Harlan Olac, Oxfordshire, United Kingdom). *DNA* for genotyping was isolated by digestion of ear tissue with proteinase K in InstaGene Matrix solution (Bio-Rad). Each mouse was genotyped as described (Kamijo et al. 1997). N4F1 $Arf^{GFP/GFP}$ (n = 50) and wild-type NIH/Ola (n = 26) animals were subjected to a single application of 7,12-dimethylbenz[*a*]anthracene (DMBA) followed one week later by a 15-week course of twice

weekly application of 12-*O*-tetradecanoylphorbol-13-acetate (TPA), as described (Kelly-Spratt et al. 2004). Mice were sacrificed following detection of carcinomas or when moribund. At necropsy, tissues were examined for green fluorescence using a Kramer GFP Illuminator attached to a Zeiss Stemi SV 11 Apo microscope. Skin tumors, lymph nodes, and lungs were frozen in liquid nitrogen and/or fixed in neutral buffered formalin (NBF).

Immunohistochemistry and Histopathology

Formalin-fixed, paraffin-embedded (FFPE) tissues were cut into 4µm sections, deparaffinized, rehydrated, and then stained with hematoxylin and eosin (H&E) or for specific proteins, cytokeratin 14 (Abcam) or GFP (Cell Signaling). Immunohistochemistry was performed using a standard three-step ABC method. Briefly, after antigen retrieval, using a pH 6.0 citrate buffer, sections were incubated with the specific primary antibody, followed by a biotinylated secondary (Vector, Southern Biotech), and then streptavidin-biotin peroxidase (Vectastain ABC Elite Kit, Vector). Slides were developed with diamino-benzidine/NiCl (Sigma) and counterstained with methyl green (Sigma) before dehydrating and mounting with Histomount (National Diagnostics).

RNA Isolation and cDNA Microarray

Tissues from NIH/Ola strain $Arf^{+/+}$ and $Arf^{-/-}$ littermates (Kamijo et al. 1997) were collected previously (Kelly-Spratt et al. 2004). Tissue RNA was extracted using the RNeasy kit (Qiagen) and subjected to amino-allyl reverse transcription labeling. cDNAs from normal skin (NS) and carcinomas (CA) of $Arf^{+/+}$ and $Arf^{-/-}$ mice (n = 4 each genotype, each condition)

were hybridized to a NIH/NIA mouse 15K spotted cDNA array containing genes from 52,374 ESTs. Hybridization results were scanned using GenePix Pro, and the data were pre-processed and normalized with Bioconductor. The *limma* package was used to search for differentially expressed genes (Smyth 2004), and *P*-values were adjusted for multiple testing with a False Discovery Rate correction (Benjamini and Hochberg 1995).

Functional Analysis of Transcriptional Signatures of SCC

The functional analyses and biological networks described were generated through the use of IPA (IngenuitySystems, www.ingenuity.com). Gene identifiers and corresponding expression values of differentially expressed genes (1.5-fold, $P < 0.05$) from $Arf^{+/+}$ and $Arf^{-/-}$ normal skin and carcinomas were uploaded into the application, and each identifier was mapped to its corresponding object in the Ingenuity Knowledge Base. Networks were then algorithmically generated based on their connectivity. IPA Core Analysis was performed to identify the biological functions, diseases, and canonical pathways that were most significant to the data set. The significance of the association between the data set and biological function and/or canonical pathway was measured in two ways: 1) A ratio of the number of molecules from the data set that map to the pathway divided by the total number of molecules that map to the biological functions and/or canonical pathway is displayed; 2) Fisher's exact test was used to calculate a *P*-value determining the probability that the association between the genes in the dataset and the biological function and/or canonical pathway is explained by chance alone. Significant functional categories and graphical representations of molecular biological relationships were then exported for generation of manuscript figures. In network maps, molecules are represented as nodes, and the biological relationship between two nodes is

represented as an edge (line). All edges are supported by at least one reference from the literature, from a textbook, or from canonical information stored in the Ingenuity Knowledge Base. The intensity of the node color indicates the degree of up- (red) or down- (green) regulation. Nodes are displayed using various shapes that represent the functional class of the gene product. The "pro-invasion and metastasis gene expression signature" described (56 genes) was curated from all differentially expressed genes (1.5 fold, $P < 0.05$) that were functionally categorized via IPA as genes involved in invasion and metastasis.

Statistical Methods

Time until development of a cutaneous carcinoma was graphically summarized for each genotype in a cumulative incidence plot. Differences in time to carcinoma development were analyzed for significance using the log-rank (Mantel-Cox) text. Animals euthanized for reasons other than the presentation of carcinomas were considered censored observations in the log-rank analysis. The incidence of metastases to the proximal lymph node and/or lung was compared between *Arf* $^{GFP/GFP}$ and *Arf* $^{+/+}$ animals; differences were analyzed for significance using a one-tailed chi-square test. *P*-values < 0.05 were considered significant. Statistical analyses were performed using GraphPad Prism software.

Results & Discussion

Our previous investigation of malignant progression in *Arf*-deficient and wild-type mice was terminated shortly after the incidence of carcinomas in *Arf* $^{-/-}$ animals reached 100%, 28 weeks post-initiation with DMBA (Kelly-Spratt et al. 2004). At this time point, only 25% of

Arf $^{+/+}$ mice had presented with at least one carcinoma. There also appeared to be an increased incidence of metastases in *Arf*-deficient animals compared to wild-type. However, as metastatic incidence is strongly correlated with tumor malignancy, and the majority of *Arf* $^{+/+}$ mice had not yet developed invasive carcinomas, we were unable to draw a definitive conclusion regarding the role of ARF in tumor metastasis. We therefore elected to repeat the DMBA/TPA protocol in *Arf* $^{+/+}$ and *Arf* $^{GFP/GFP}$ reporter mice, extending the experimental time course to allow for malignant carcinoma development in all animals. Our findings closely replicated those of the previous study, as 95% of *Arf* $^{GFP/GFP}$ animals developed at least one carcinoma by 29-weeks post-DMBA, versus less than 20% of *Arf* $^{+/+}$ mice (Fig. 4.1A; $P < 0.0001$). The onset of carcinoma development was also notably similar to our previous observations, with carcinomas first appearing 15 and 25 weeks after initiation in *Arf*-deficient and *Arf* $^{+/+}$ animals, respectively.

We next examined the incidence of metastatic spread to the proximal lymph node (LN) or lung in carcinoma-bearing animals. Although visible metastases were sometimes noted during necropsy, all tissues were examined by H&E for the presence of metastatic cells. 60.5% of *Arf* $^{GFP/GFP}$ animals examined (26 of 43) displayed LN metastases, compared to only 16.7% of *Arf* $^{+/+}$ animals (4 of 24; Fig. 4.1B; $P = 0.0003$). Metastasis to the lung was a less common occurrence in *Arf* $^{GFP/GFP}$ mice (13.3%; 6 of 45 examined), but the frequency was still statistically increased over *Arf* $^{+/+}$ animals (0 of 20 examined; Fig. 4.1C; $P = 0.0433$).

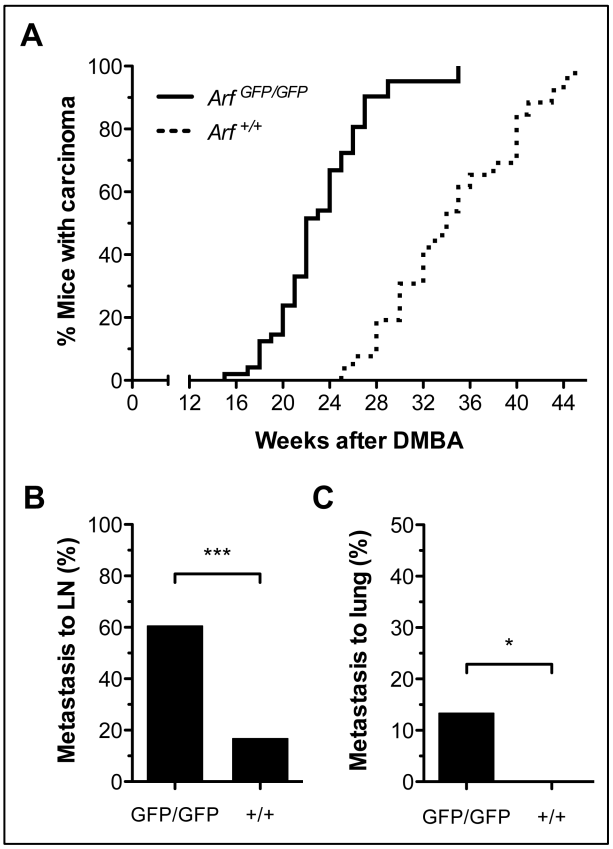

Figure 4.1: *Arf* loss facilitates malignant progression and metastatic spread. **(A)** Cumulative incidence plot summarizes the temporal development of carcinomas in *Arf* $^{GFP/GFP}$ and *Arf* $^{+/+}$ animals after DMBA/TPA exposure. **(B-C)** Percent of carcinoma-bearing mice with metastatic spread to nearby lymph nodes (B) or the lung (C), as visible on H&E stained tissue sections. *** $P = 0.0003$ and * $P = 0.0433$.

For this study, we utilized the *Arf* $^{GFP/GFP}$ reporter mouse, which is functionally *Arf* null but expresses GFP from an intact *Arf* promoter. Metastatic lesions from *Arf* $^{GFP/GFP}$ mice were visible under a fluorescence dissecting microscope (Fig. 4.2), and GFP immunoreactive cells were observed in sections from lymph node and lung tissues (Fig. 4.3). Notably, GFP^+ cells co-expressed the epidermal keratinocyte marker cytokeratin 14 (K14), providing evidence of their SCC origin. Taken together, our findings confirm that *Arf*-deficient mice experience greatly accelerated malignant progression of SCC and reveal, for the first time, that *Arf* loss enables metastasis to distant sites. Furthermore, these results demonstrate that the oncogenic signal driving ARF expression is retained throughout tumor development. Efforts to reintroduce ARF to late-stage tumors may therefore be therapeutically relevant.

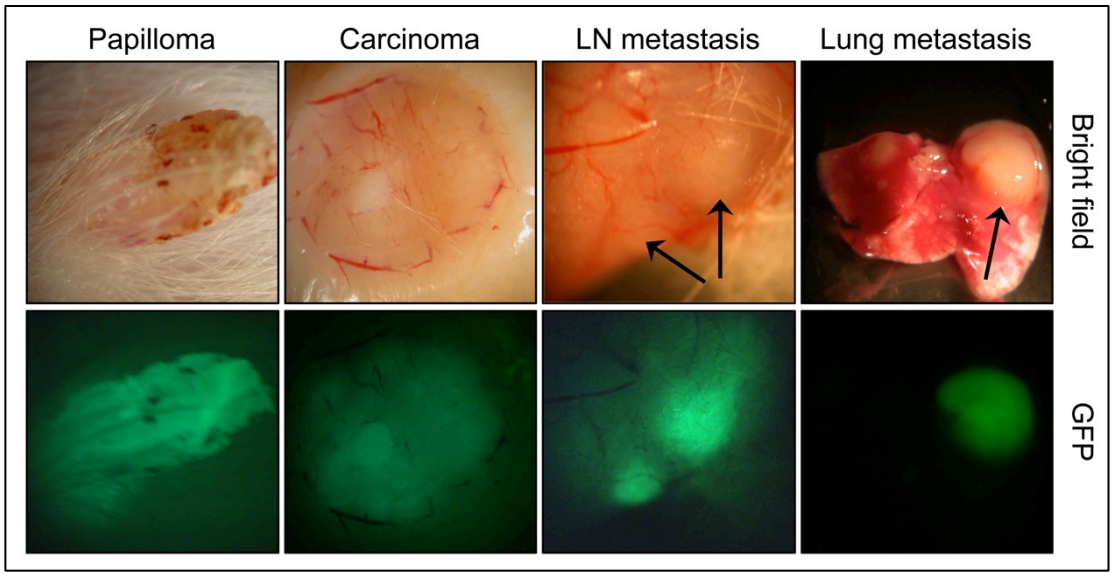

Figure 4.2: *Arf*-deficient squamous cell carcinomas metastasize to the lymph node and lung. Photomicrographs from a fluorescence dissecting scope reveal fluorescence emission from an exophytic papilloma, the underside of an invasive carcinoma, and an enlarged sentinel lymph node (arrows) and pulmonary metastasis (arrow) from a carcinoma-bearing $Arf^{GFP/GFP}$ mouse.

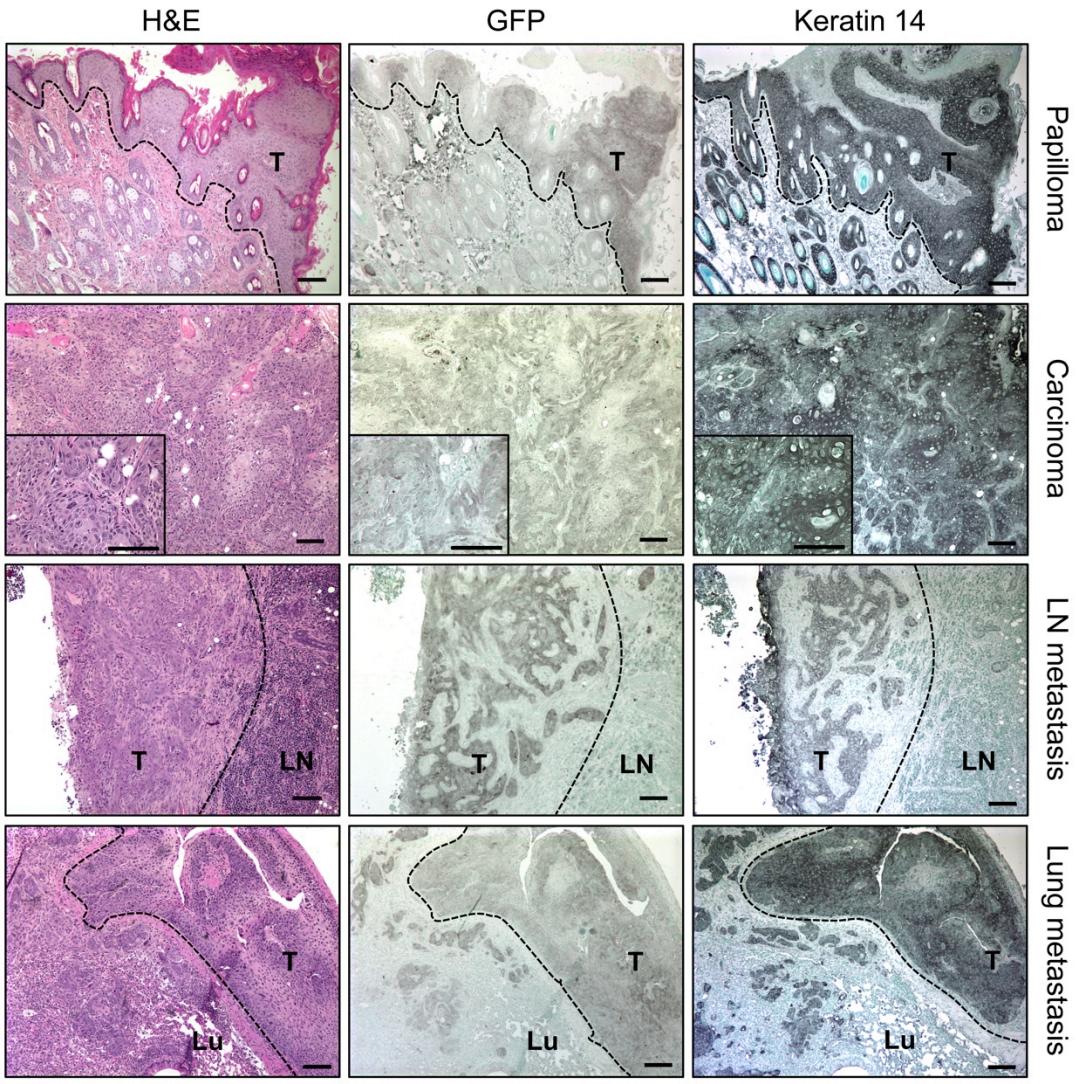

Figure 4.3: H&E staining and GFP and K14 immunohistochemistry of DMBA/TPA induced tumors from the *Arf* $^{GFP/GFP}$ reporter mouse (10X objective; scale bar = 100μm). GFP and K14 are expressed in the exophytic, proliferating keratinocytes of a benign papilloma and throughout the invasive front of a malignant carcinoma. Squamous cell carcinoma cells (T) continue to express both GFP and K14 markers after metastasizing to the lymph node (LN) and the lung (Lu).

In order to elucidate the molecular mechanism(s) by which ARF represses tumor cell invasion and metastasis, we performed transcriptional profiling on *Arf* $^{+/+}$ and *Arf* $^{-/-}$ carcinomas (CA) compared to normal skin (NS) of the corresponding genotype (Fig. 4.4A). 1881 genes were differentially expressed (1.5-fold change, $P < 0.05$) between *Arf* $^{+/+}$ CA and NS, 1580 genes between *Arf* $^{-/-}$ CA and NS, and 1126 genes between *Arf* $^{+/+}$ CA and *Arf* $^{-/-}$ CA. Compared to carcinomas from wild-type animals, *Arf* $^{-/-}$ carcinomas exhibited an expression signature indicative of loss of adhesion and increased cell migration (Fig. 4.4B). The transcriptome from *Arf* $^{-/-}$ carcinomas was highly enriched for components of the integrin signaling pathway and displayed up-regulation of the small GTPase *Rac1*, an important regulator of cell migration (Fig. 4.4C). We further identified a pro-invasion and metastasis gene expression signature in *Arf*-deficient SCC. The signature was comprised of 39 up-regulated and 17 down-regulated genes in *Arf* $^{-/-}$ CA compared to *Arf* $^{+/+}$ (Fig. 4.5). Interestingly, 10 of the up-regulated transcripts (i.e. *Adm*, *Ccnd1*, *Cd151*, *Ceacam1*, *Ctsd*, *Cttn*, *Gpi*, *Hras*, *Iqgap1*, *Tjp1*) highlighted in the pro-metastasis signature map to mouse Chromosome 7. Subsequent examination of the array dataset revealed that Chromosome 7 from *Arf* $^{-/-}$ CAs was significantly enriched in differentially expressed genes (Fig. 4.6). Copy number gain of Chromosome 7 frequently occurs during the malignant progression of DMBA/TPA-induced skin tumors (Aldaz et al. 1989), a phenomenon commonly believed to be related to *Hras* amplification. Although this chromosomal abnormality has historically been observed even in wild-type mice, our results suggest that *Arf* loss may accelerate the acquisition of an extra copy of Chr7. Moreover, our findings argue that gain of Chromosome 7 bestows additional, highly beneficial properties on carcinoma cells beyond simple amplification of RAS signaling.

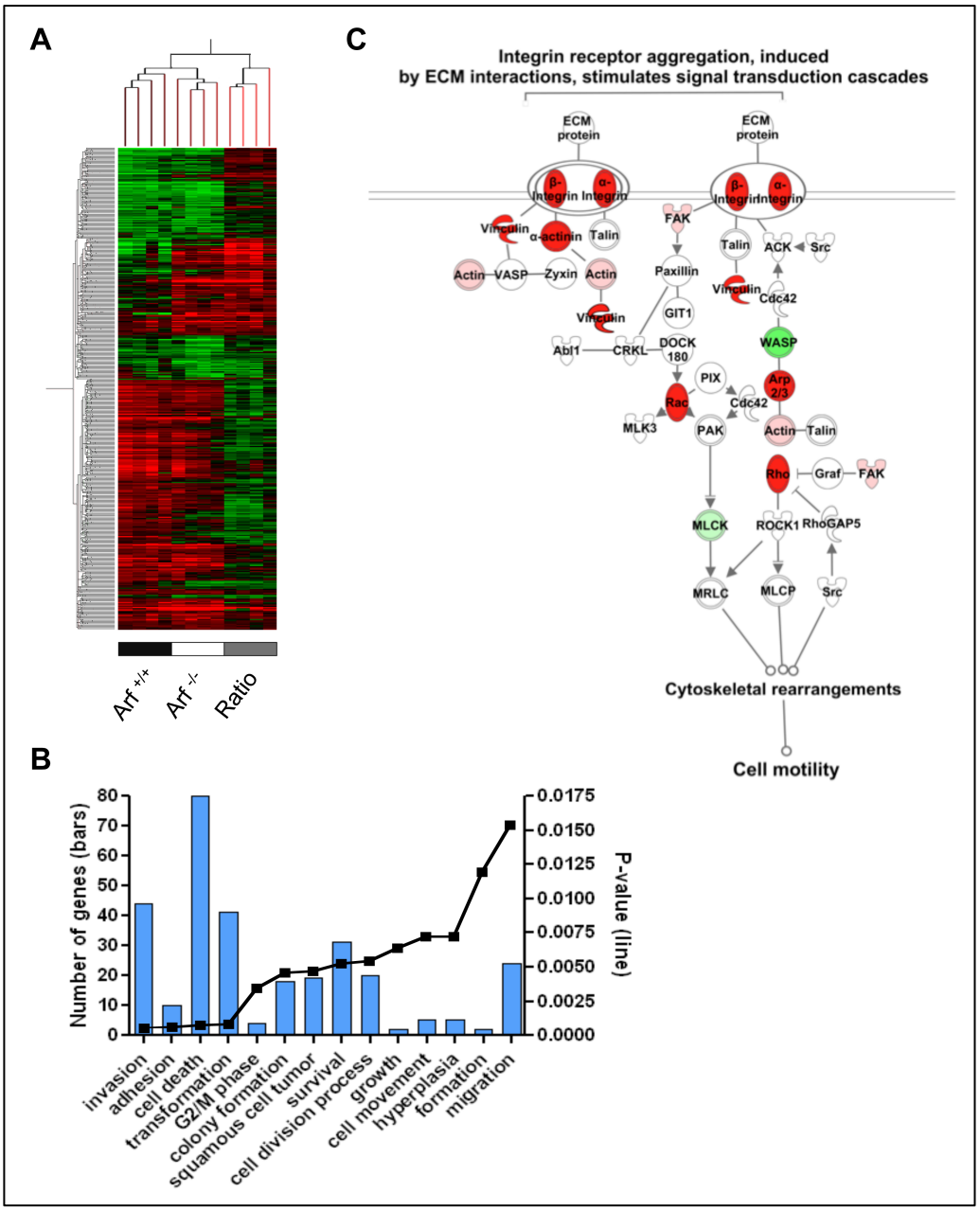

Figure 4.4: Transcriptional signature for DMBA/TPA induced squamous cell carcinomas. **(A)** Bidirectional hierarchical clustering of differentially expressed genes (1.5-fold, $P < 0.05$) in *Arf* $^{+/+}$ and *Arf* $^{-/-}$ skin tumors compared to normal skin of corresponding genotype. Ratio shown is *Arf* $^{-/-}$ carcinoma to *Arf* $^{+/+}$ carcinoma. Red indicates up-regulation, green down-regulation; tumors cluster by genotype. **(B)** Functional categorization of genes uniquely altered in *Arf* $^{-/-}$ carcinomas compared to *Arf* $^{-/-}$ normal skin. Compared to *Arf* $^{+/+}$ carcinomas, *Arf* $^{-/-}$ carcinomas exhibit an expression signature consistent with increased invasion, cell migration and metastasis. **(C)** The integrin signaling pathway is important in tumor suppression by Arf during skin carcinogenesis. Highlighted genes are those differentially regulated in *Arf* $^{-/-}$ carcinomas compared to normal skin; genes that are further dysregulated compared to *Arf* $^{+/+}$ carcinomas are indicated in darker red. Loss of *Arf* results in up-regulation of *Rho* and *Rac*, which are central regulators of signaling pathways important for invasion, migration, and metastasis.

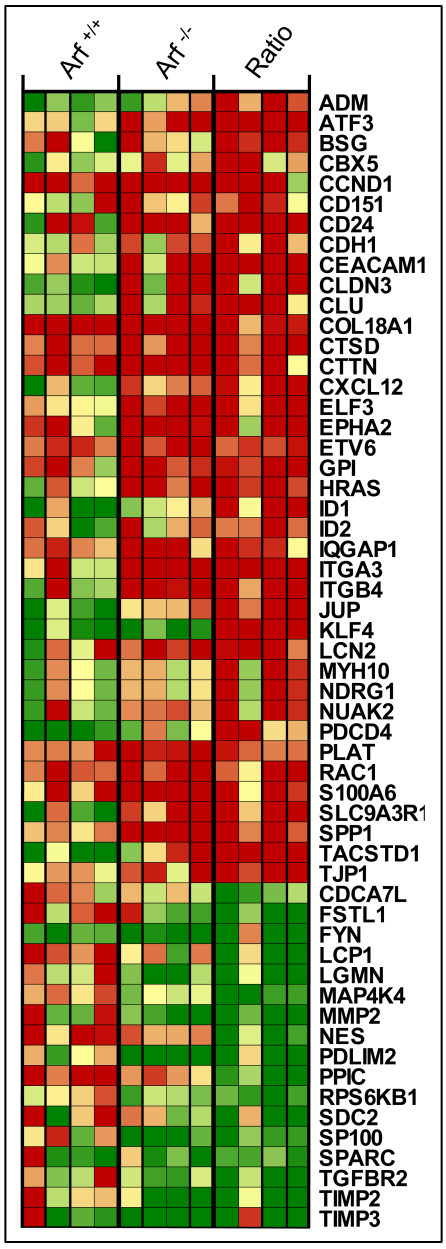

Figure 4.5: Pro-invasion and metastasis gene expression signature observed in Arf-deficient squamous cell carcinomas. Red indicates up-regulation, green down-regulation. All genes differentially regulated (1.5-fold, $p < 0.05$) in *Arf* $^{-/-}$ carcinomas compared to normal skin, *Arf* $^{+/+}$ carcinomas compared to normal skin, and *Arf* $^{-/-}$ carcinomas compared to *Arf* $^{+/+}$ carcinomas are represented.

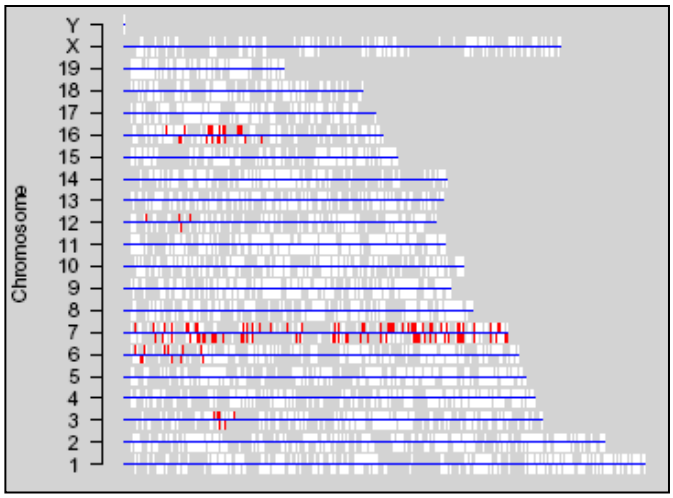

Figure 4.6: Differentially expressed genes (red) by chromosomal location in *Arf* -/- carcinomas. The mean of a hyper-geometric test was used to identify chromosomes having an over-representation of differentially expressed genes along their lengths. Transcriptional changes along chromosome 7 are highly over-represented.

Several genes associated with tumor cell invasion and metastasis exhibited unexpected patterns of expression in carcinomas from *Arf*-deficient animals (Fig. 4.5). *Col18a1*, otherwise known as endostatin, is a powerful inhibitor of angiogenesis and metastasis. Surprisingly, *Col18a1* expression was increased in carcinomas of both genotypes compared to normal skin, and was significantly higher in *Arf* $^{-/-}$ CAs than *Arf* $^{+/+}$. *Ndrg1* and *Pdcd4*, suppressors of invasion and migration, displayed similar counterintuitive increases in *Arf* $^{-/-}$ CAs, while pro-metastatic genes *Fyn*, *Lcp1*, *Lgmn*, *Map4k4*, *Nes*, *Rps6kb1*, *Sdc2*, and *Sparc* were unexpectedly decreased in *Arf* $^{-/-}$ compared to *Arf* $^{+/+}$ CAs. Perhaps the most notable findings from the array, however, were the down-regulation of *Mmp2* (matrix metalloproteinase 2) and the increased expression of *Cdh1* (E-cadherin) seen in *Arf*-deficient carcinomas. *Mmp2* expression strongly correlates with activation of the epithelial-mesenchymal transition (EMT) program and tumor invasion (Yokoyama et al. 2003; Bauvois 2012). The fact that aggressively invasive and metastatic tumors from *Arf*-deficient animals exhibit low expression of *Mmp2* is difficult to rationalize.

Even more conceptually challenging is our finding that E-cadherin expression is elevated in *Arf* $^{-/-}$ relative to *Arf* $^{+/+}$ CAs. Loss of E-cadherin expression is a defining feature of EMT (Nieto 2011) and has been consistently observed in DMBA/TPA SCC models (Navarro et al. 1991; Brouxhon et al. 2007; Abel et al. 2009) and other tumor types (Schmalhofer et al. 2009). Indeed, wild-type carcinomas from our study were found to significantly decrease *Cdh1* expression compared to normal skin, as would be predicted. High E-cadherin expression has been observed in established metastatic lesions, a finding that may reflect a mesenchymal-epithelial reverting transition (MErT) during the colonization process (Wells et al. 2008). To our knowledge, however, only one other group has observed high expression of E-cadherin in primary tumor cells. E-cadherin positive prostate carcinoma cells were shown to co-express the reprogramming transcription factors OCT3/4, SOX2, Nanog, c-MYC, and KLF4 (Bae et al. 2010). This cell population underwent asymmetrical division, formed spheroids under non-adherent tissue culture conditions, rapidly proliferated, and was highly tumorigenic. In short, CDH1 positivity appeared to label a population of stem-like prostate carcinoma cells. The CDH1^{+} cells were also shown to be highly invasive and to retain their stem cell characteristics after invasion (Bae et al. 2011). To explain their non-intuitive results, the authors presented evidence that stem-like carcinoma cells dynamically regulate CDH1 expression – turning off E-cadherin during the actual process of invasion, and switching it back on shortly thereafter. Thus, E-cadherin plasticity may be a marker of cancer cell stemness and invasive capacity. Notably, in addition to increased *Cdh1* expression, our transcriptional profiling revealed up-regulation of the stem cell markers *Oct3/4* and *Klf4* in *Arf* $^{-/-}$ compared to *Arf* $^{+/+}$ carcinomas. It is tempting to speculate that the increased invasion

and metastasis seen in *Arf*-deficient mice reflects the presence of an enhanced "stem-like" cell population.

In summary, loss of *Arf* generates highly mobile, highly metastatic cancer cells, and the pro-invasion phenotype of *Arf*-deficient carcinoma cells can be observed at the transcriptional level. Future efforts will focus on validation of key array targets by QPCR and protein expression analysis, with particular emphasis on the up-regulation of E-cadherin and stem cell markers in metastatic carcinomas from *Arf*-deficient animals.

Acknowledgements

This work was supported by PHS NRSA 2T32 GM007270 from NIHMS (SEB); NIH T32 CA8046 Interdisciplinary Training Grant in Cancer Research (KSK-S); and NCI R01 (CA099517) and NIEHS U01 (ES11045) grants to CJK.

Chapter Five

Conclusions and Future Directions

Since its discovery at the *CDKN2A* locus in 1995, *ARF* has been the source of endless debate. Does ARF suppress tumor development? How? Is the role of ARF completely dependent on p53, or does it exhibit a more promiscuous functionality? Do different organisms display varying requirements for *ARF*, with humans less reliant on the gene for tumor suppression than mice? To what extent is the expression of *ARF* entwined with that of its close neighbor, $p16^{INK4a}$? Why did *ARF* come into existence, what does it do for us, and what happens when we lose it? The overarching goal of the research described herein was to identify and elucidate tumor suppression by ARF in multiple mouse models of carcinogenesis. Contrary to previous reports (Feldser et al. 2010; Junttila et al. 2010; Young and Jacks 2010), I found that ARF suppresses the growth and malignant progression of *Kras*-driven lung adenocarcinoma. I showed that *Arf* loss dramatically sensitizes animals to hepatic vascular neoplasia after urethane exposure. Finally, I provided preliminary evidence that ARF acts as an inhibitor of metastasis in cutaneous squamous cell carcinoma. In this chapter, I will discuss several themes that arose during the course of my investigations and propose a series of follow-up experiments.

An interesting pattern that emerged from my studies was the effect of *Arf* loss on tumor malignancy. All three models exhibited accelerated malignant progression in the context of *Arf* deficiency, and there was strong evidence from the SCC (Kelly-Spratt et al. 2004) and NSCLC studies that ARF expression in wild-type animals created a barrier against tumor progression. In the lung, loss of ARF expression correlated with the formation of invasive adenocarcinomas; in the skin, squamous cell carcinomas. In both instances, the activity of ARF appeared to be p53-dependent, although my colleagues and I have not ruled out the

possibility of some p53-independent tumor suppression by ARF. Notably, *Arf* deficiency facilitated the development of sarcomatoid carcinomas in the lung and enabled metastatic spread from skin carcinomas. Pulmonary sarcomatoid carcinomas are believed to form through the activation of an epithelial-mesenchymal transition (EMT) program (Pelosi et al. 2010). EMT, first discovered as a critical feature of embryogenesis, is the process by which cells lose their epithelial differentiation and acquire migratory and invasive capabilities (Nieto 2011). In addition to normal development, EMT plays important roles in wound healing and tumorigenesis. Specifically, EMT is believed to be required for the invasion and metastasis of carcinoma cells (Chaffer and Weinberg 2011; Hanahan and Weinberg 2011). Thus, loss of *Arf* appears to be associated with EMT activation in two of the carcinogenesis models described in this work.

These results raise several important questions about ARF biology. First, does ARF directly regulate the EMT program? Embryogenesis is largely unaffected in *Arf*-deficient mice, so if ARF is controlling EMT, it must do so under a limited set of conditions in adult animals. To our knowledge, no group has examined the wound healing response in *Arf* $^{-/-}$ mice. However, *Trp53* loss has been shown to accelerate wound repair (Valencia et al. 2008), while *Mdm2* deficiency (i.e. p53-hyperactivity) impedes wound healing (Gannon et al. 2011). Given these findings, it would be informative to conduct standard wound healing assays in *Arf*-deficient animals compared to wild-type. Furthermore, the migratory capacity of human *ARF* $^{-/-}$ carcinoma cells should be assessed *in vitro*, using a Matrigel invasion assay or similar techniques. Does *ARF* loss increase cell migration? Will restoration of ARF expression in an *ARF*-deficient cell line (e.g. A549 lung adenocarcinoma cells) inhibit cell invasion? If so,

does this inhibition require p53 function? All of these experiments are important next steps in the investigation of *in vivo* tumor suppression by ARF.

Second, to address the potential mechanism(s) by which ARF regulates EMT, invasion, and metastasis, it will be critical to functionally validate the microarray data described in Chapter Four, by QPCR, Western blotting, and IHC. The up-regulation of E-cadherin and multiple stem cell markers observed in *Arf* $^{-/-}$ carcinomas hints at another possible role for ARF in tumorigenesis. Perhaps *Arf* loss confers a more "stem-like" phenotype on developing tumor cells. Indeed, it has been shown that the *CDKN2A/B* loci are epigenetically silenced in embryonic stem cells, and that silencing of the loci is a rate-limiting step in iPS cell reprogramming (Li et al. 2009). A reasonable hypothesis is that ARF-negative carcinoma cells constitute a population of pluripotent cancer stem cells, and that this population is responsible for invasive growth. However, it is worth noting that pulmonary sarcomatoid carcinomas have never (to our knowledge) been observed in wild-type mice, implying that *Arf* loss in later stages of tumor progression is insufficient to promote the development of said lesions. Do tumor cells with *ab initio* loss of *Arf* expression represent a unique and unnatural cell population? Can animals with germline deletion of *Arf* (or *Trp53*, *p21*^{Cip1}, etc.) reliably model tumor development in humans, where genetic alteration of tumor suppressors is typically a somatic event? Is, for example, oncogenic signaling unrestrained in an *ab initio Arf* null environment, thus altering the balance between proliferation, senescence, and apoptosis? Can a tumor arising in an *Arf* $^{-/-}$ mouse ever truly be considered "benign"? These intriguing questions can and should be addressed by examining tumorigenesis in models with targeted

Arf deletion (both spatial and temporal), and by directly investigating the behavior of ARF-negative carcinoma cells from human patients.

The other major theme that has emerged from my work and the work of my colleagues is the contribution of ARF to DNA damage signaling and genomic integrity. Lung adenocarcinomas (Chapter Two) and squamous cell carcinomas (Bailey et al. 2008) arising in *Arf* $^{-/-}$ mice exhibited increased levels of the DNA damage marker phospho-H2A.X compared to wild-type. Although ARF had long been thought to play a limited role in the DNA damage response through p53, recent studies have identified both p53-dependent and -independent functions of ARF in DNA damage signaling and repair (Khan et al. 2000; Sherr 2006). It will be important for follow-up investigations to address these proposed mechanisms of tumor suppression by ARF. Do *Arf* $^{-/-}$ carcinomas exhibit additional markers of DNA damage, e.g. activation of the ATM/ATR and CHK2/CHK1 pathway? Does *Arf* loss disrupt the G2/M cell cycle checkpoint by impairing function of the CDC25C phosphatase? Might the high levels of phosphorylated histone H2A.X indicate a defect in DNA repair in *Arf*-deficient animals, perhaps resulting from inhibition of the MRN complex by free MDM2? Increased Cyclin D1 expression was observed in both the NSCLC and SCC tumor models. Does *Arf* loss directly up-regulate nuclear Cyclin D1 expression, resulting in replication stress and DNA damage? Conversely, the mechanism linking *Arf* deficiency and increased DNA damage need not be direct. Elevated RAS-ERK pathway signaling was observed in *Arf* $^{-/-}$ lung adenocarcinomas and SCC. As described above, it remains plausible that the dominant effect of *Arf* loss is to enable unrestrained, no-holds-barred oncogenic signaling from the earliest stages of tumor development.

In summary, the findings described herein argue that ARF stands at a tumor suppression crossroads of genomic integrity, senescence, differentiation, and metastasis. It is my hope that future experiments will clarify these connections, with the ultimate goal of developing novel therapeutic strategies for cancer patients.

Bibliography

Abel, E. L., et al. 2009. Multi-stage chemical carcinogenesis in mouse skin: fundamentals and applications. *Nature protocols* 4 (9):1350-62.

Aggarwal, P., et al. 2007. Nuclear accumulation of cyclin D1 during S phase inhibits Cul4-dependent Cdt1 proteolysis and triggers p53-dependent DNA rereplication. *Genes Dev.* 21 (22):2908-22.

Aggarwal, P., et al. 2010. Nuclear cyclin D1/CDK4 kinase regulates CUL4 expression and triggers neoplastic growth via activation of the PRMT5 methyltransferase. *Cancer cell* 18 (4):329-40.

Agherbi, H., et al. 2009. Polycomb mediated epigenetic silencing and replication timing at the INK4a/ARF locus during senescence. *PloS one* 4 (5):e5622.

Ahrendt, S. A., et al. 2001. Cigarette smoking is strongly associated with mutation of the K-ras gene in patients with primary adenocarcinoma of the lung. *Cancer* 92 (6):1525-30.

Albanese, C., et al. 1995. Transforming p21ras mutants and c-Ets-2 activate the cyclin D1 promoter through distinguishable regions. *J. Biol. Chem.* 270 (40):23589-97.

Aldaz, C. M., et al. 1989. Sequential trisomization of chromosomes 6 and 7 in mouse skin premalignant lesions. *Mol. Carcinog.* 2 (1):22-6.

Aliouat-Denis, C. M., et al. 2005. p53-independent regulation of p21Waf1/Cip1 expression and senescence by Chk2. *Molecular cancer research : MCR* 3 (11):627-34.

Alt, J. R., et al. 2005. Mdm2 binds to Nbs1 at sites of DNA damage and regulates double strand break repair. *J. Biol. Chem.* 280 (19):18771-81.

Alt, J. R., et al. 2000. Phosphorylation-dependent regulation of cyclin D1 nuclear export and cyclin D1-dependent cellular transformation. *Genes Dev.* 14 (24):3102-14.

Andrique, L., et al. 2012. ErbB3(80 kDa), a nuclear variant of the ErbB3 receptor, binds to the Cyclin D1 promoter to activate cell proliferation but is negatively controlled by p14ARF. *Cell. Signal.* 24 (5):1074-85.

Aslanian, A., et al. 2004. Repression of the Arf tumor suppressor by E2F3 is required for normal cell cycle kinetics. *Genes Dev.* 18 (12):1413-22.

Bae, K. M., et al. 2011. E-cadherin plasticity in prostate cancer stem cell invasion. *Am J Cancer Res* 1 (1):71-84.

Bae, K. M., et al. 2010. Expression of pluripotent stem cell reprogramming factors by prostate tumor initiating cells. *J. Urol.* 183 (5):2045-53.

Bailey, S. L., et al. 2008. Tumor suppression by p53 in the absence of Atm. *Molecular cancer research : MCR* 6 (7):1185-92.

Balmain, A., et al. 1984. Activation of the mouse cellular Harvey-ras gene in chemically induced benign skin papillomas. *Nature* 307 (5952):658-60.

Barbin, A. 2000. Etheno-adduct-forming chemicals: from mutagenicity testing to tumor mutation spectra. *Mutat. Res.* 462 (2-3):55-69.

Bartkova, J., et al. 2005. DNA damage response as a candidate anti-cancer barrier in early human tumorigenesis. *Nature* 434 (7035):864-70.

Bartkova, J., et al. 2006. Oncogene-induced senescence is part of the tumorigenesis barrier imposed by DNA damage checkpoints. *Nature* 444 (7119):633-7.

Bates, S., et al. 1998. p14ARF links the tumour suppressors RB and p53. *Nature* 395 (6698):124-5.

Battaglia, R., et al. 1990. Ethyl carbamate (urethane) in alcoholic beverages and foods: a review. *Food Addit. Contam.* 7 (4):477-96.

Bauvois, B. 2012. New facets of matrix metalloproteinases MMP-2 and MMP-9 as cell surface transducers: outside-in signaling and relationship to tumor progression. *Biochim. Biophys. Acta* 1825 (1):29-36.

Beland, F. A., et al. 2005. Effect of ethanol on the tumorigenicity of urethane (ethyl carbamate) in B6C3F1 mice. *Food and chemical toxicology : an international journal published for the British Industrial Biological Research Association* 43 (1):1-19.

Belinsky, S. A., et al. 1992. Role of the alveolar type II cell in the development and progression of pulmonary tumors induced by 4-(methylnitrosamino)-1-(3-pyridyl)-1-butanone in the A/J mouse. *Cancer Res.* 52 (11):3164-73.

Benanti, J. A., et al. 2007. Epigenetic down-regulation of ARF expression is a selection step in immortalization of human fibroblasts by c-Myc. *Molecular cancer research : MCR* 5 (11):1181-9.

Benassi, M. S., et al. 2001. Involvement of INK4A gene products in the pathogenesis and development of human osteosarcoma. *Cancer* 92 (12):3062-7.

Benjamini, Y., and Y. Hochberg. 1995. Controlling the False Discovery Rate - a Practical and Powerful Approach to Multiple Testing. *J Roy Stat Soc B Met* 57 (1):289-300.

Berger, J. H., and N. Bardeesy. 2007. Modeling INK4/ARF tumor suppression in the mouse. *Curr. Mol. Med.* 7 (1):63-75.

Berkovich, E., et al. 2003. E2F and Ras synergize in transcriptionally activating p14ARF expression. *Cell cycle* 2 (2):127-33.

Blow, J. J., and P. J. Gillespie. 2008. Replication licensing and cancer--a fatal entanglement? *Nat. Rev. Cancer* 8 (10):799-806.

Brookes, S., et al. 2002. INK4a-deficient human diploid fibroblasts are resistant to RAS-induced senescence. *EMBO J.* 21 (12):2936-45.

Brouxhon, S., et al. 2007. Sequential down-regulation of E-cadherin with squamous cell carcinoma progression: loss of E-cadherin via a prostaglandin E2-EP2 dependent posttranslational mechanism. *Cancer Res.* 67 (16):7654-64.

Brummelkamp, T. R., et al. 2002. TBX-3, the gene mutated in Ulnar-Mammary Syndrome, is a negative regulator of p19ARF and inhibits senescence. *J. Biol. Chem.* 277 (8):6567-72.

Budd, G. T. 2002. Management of angiosarcoma. *Curr. Oncol. Rep.* 4 (6):515-9.

Buhrman, G., et al. 2010. Allosteric modulation of Ras positions Q61 for a direct role in catalysis. *Proc. Natl. Acad. Sci. U. S. A.* 107 (11):4931-6.

Burns, J. S., et al. 2005. Tumorigenic heterogeneity in cancer stem cells evolved from long-term cultures of telomerase-immortalized human mesenchymal stem cells. *Cancer Res.* 65 (8):3126-35.

Busch, S. E., et al. 2012. ARF Suppresses Hepatic Vascular Neoplasia in a Carcinogen-Exposed Murine Model. *J. Pathol.* 227 (3):298-305.

Cadranel, J. F., et al. 1993. Liver disease from surreptitious administration of urethane. *J. Clin. Gastroenterol.* 17 (1):52-6.

Carmichael, N. G., et al. 2000. The p53 heterozygous knockout mouse as a model for chemical carcinogenesis in vascular tissue. *Environ. Health Perspect.* 108 (1):61-5.

Cazorla, M., et al. 1998. Ki-ras gene mutations and absence of p53 gene mutations in spontaneous and urethane-induced early lung lesions in CBA/J mice. *Mol. Carcinog.* 21 (4):251-60.

Cha, C., et al. 2004. Long-term results with resection of radiation-induced soft tissue sarcomas. *Ann. Surg.* 239 (6):903-9; discussion 909-10.

Chaffer, C. L., and R. A. Weinberg. 2011. A perspective on cancer cell metastasis. *Science* 331 (6024):1559-64.

Chang, E. H., et al. 1982. Human genome contains four genes homologous to transforming genes of Harvey and Kirsten murine sarcoma viruses. *Proc. Natl. Acad. Sci. U. S. A.* 79 (16):4848-52.

Chen, H. Z., et al. 2009. Emerging roles of E2Fs in cancer: an exit from cell cycle control. *Nat. Rev. Cancer* 9 (11):785-97.

Christophorou, M. A., et al. 2006. The pathological response to DNA damage does not contribute to p53-mediated tumour suppression. *Nature* 443 (7108):214-7.

Clark, R., et al. 1985. Antibodies specific for amino acid 12 of the ras oncogene product inhibit GTP binding. *Proc. Natl. Acad. Sci. U. S. A.* 82 (16):5280-4.

Cohen, S. M., et al. 2009. Hemangiosarcoma in rodents: mode-of-action evaluation and human relevance. *Toxicological sciences : an official journal of the Society of Toxicology* 111 (1):4-18.

Collado, M., et al. 2005. Tumour biology: senescence in premalignant tumours. *Nature* 436 (7051):642.

Collado, M., and M. Serrano. 2010. Senescence in tumours: evidence from mice and humans. *Nat. Rev. Cancer* 10 (1):51-7.

Conway, C., et al. 2010. Deletion at chromosome arm 9p in relation to BRAF/NRAS mutations and prognostic significance for primary melanoma. *Genes. Chromosomes Cancer* 49 (5):425-38.

Cox, A. D., and C. J. Der. 2010. Ras history: The saga continues. *Small GTPases* 1 (1):2-27.

Creech, J. L., Jr., and M. N. Johnson. 1974. Angiosarcoma of liver in the manufacture of polyvinyl chloride. *Journal of occupational medicine. : official publication of the Industrial Medical Association* 16 (3):150-1.

D'Amico, M., et al. 2004. The inhibitor of cyclin-dependent kinase 4a/alternative reading frame (INK4a/ARF) locus encoded proteins p16INK4a and p19ARF repress cyclin D1 transcription through distinct cis elements. *Cancer Res.* 64 (12):4122-30.

Dacic, S., et al. 2002. Molecular pathogenesis of pulmonary carcinosarcoma as determined by microdissection-based allelotyping. *Am. J. Surg. Pathol.* 26 (4):510-6.

Damalas, A., et al. 2001. Deregulated beta-catenin induces a p53- and ARF-dependent growth arrest and cooperates with Ras in transformation. *EMBO J.* 20 (17):4912-22.

de Stanchina, E., et al. 1998. E1A signaling to p53 involves the p19(ARF) tumor suppressor. *Genes Dev.* 12 (15):2434-42.

Debies, M. T., et al. 2008. Tumor escape in a Wnt1-dependent mouse breast cancer model is enabled by p19Arf/p53 pathway lesions but not p16 Ink4a loss. *J. Clin. Invest.* 118 (1):51-63.

Der, C. J., et al. 1986. Biological and biochemical properties of human rasH genes mutated at codon 61. *Cell* 44 (1):167-76.

Der, C. J., et al. 1982. Transforming genes of human bladder and lung carcinoma cell lines are homologous to the ras genes of Harvey and Kirsten sarcoma viruses. *Proc. Natl. Acad. Sci. U. S. A.* 79 (11):3637-40.

Di Micco, R., et al. 2006. Oncogene-induced senescence is a DNA damage response triggered by DNA hyper-replication. *Nature* 444 (7119):638-42.

Di Tommaso, A., et al. 2004. The ink4a/arf locus evolution in primates: characterization of three ARF sequences. *DNA Cell Biol.* 23 (3):167-73.

Dimri, G. P., et al. 2000. Regulation of a senescence checkpoint response by the E2F1 transcription factor and p14(ARF) tumor suppressor. *Mol. Cell. Biol.* 20 (1):273-85.

Ding, L., et al. 2008. Somatic mutations affect key pathways in lung adenocarcinoma. *Nature* 455 (7216):1069-75.

Donehower, L. A., et al. 1992. Mice deficient for p53 are developmentally normal but susceptible to spontaneous tumours. *Nature* 356 (6366):215-21.

Dragani, T. A., et al. 1991. Incidence of mutations at codon 61 of the Ha-ras gene in liver tumors of mice genetically susceptible and resistant to hepatocarcinogenesis. *Oncogene* 6 (2):333-8.

Duro, D., et al. 1995. A new type of p16INK4/MTS1 gene transcript expressed in B-cell malignancies. *Oncogene* 11 (1):21-9.

Efeyan, A., et al. 2006. Tumour biology: Policing of oncogene activity by p53. *Nature* 443 (7108):159.

Efeyan, A., and M. Serrano. 2007. p53: guardian of the genome and policeman of the oncogenes. *Cell cycle* 6 (9):1006-10.

Eischen, C. M., et al. 1999. Disruption of the ARF-Mdm2-p53 tumor suppressor pathway in Myc-induced lymphomagenesis. *Genes Dev.* 13 (20):2658-69.

Ellis, R. W., et al. 1981. The p21 src genes of Harvey and Kirsten sarcoma viruses originate from divergent members of a family of normal vertebrate genes. *Nature* 292 (5823):506-11.

Esteller, M., et al. 2000. Hypermethylation-associated inactivation of p14(ARF) is independent of p16(INK4a) methylation and p53 mutational status. *Cancer Res.* 60 (1):129-33.

Eymin, B., et al. 2006. p14ARF activates a Tip60-dependent and p53-independent ATM/ATR/CHK pathway in response to genotoxic stress. *Mol. Cell. Biol.* 26 (11):4339-50.

Eymin, B., et al. 2002. Mdm2 overexpression and p14(ARF) inactivation are two mutually exclusive events in primary human lung tumors. *Oncogene* 21 (17):2750-61.

Eymin, B., et al. 2001. Human ARF binds E2F1 and inhibits its transcriptional activity. *Oncogene* 20 (9):1033-41.

Eymin, B., et al. 2003. p14ARF induces G2 arrest and apoptosis independently of p53 leading to regression of tumours established in nude mice. *Oncogene* 22 (12):1822-35.

Farago, A. F., et al. 2012. SnapShot: Lung cancer models. *Cell* 149 (1):246-246 e1.

Fearon, E. R., and B. Vogelstein. 1990. A genetic model for colorectal tumorigenesis. *Cell* 61 (5):759-67.

Feldser, D. M., et al. 2010. Stage-specific sensitivity to p53 restoration during lung cancer progression. *Nature* 468 (7323):572-5.

Feramisco, J. R., et al. 1984. Microinjection of the oncogene form of the human H-ras (T-24) protein results in rapid proliferation of quiescent cells. *Cell* 38 (1):109-17.

Ferbeyre, G., et al. 2002. Oncogenic ras and p53 cooperate to induce cellular senescence. *Mol. Cell. Biol.* 22 (10):3497-508.

Filmus, J., et al. 1994. Induction of cyclin D1 overexpression by activated ras. *Oncogene* 9 (12):3627-33.

Fisher, G. H., et al. 2001. Induction and apoptotic regression of lung adenocarcinomas by regulation of a K-Ras transgene in the presence and absence of tumor suppressor genes. *Genes Dev.* 15 (24):3249-62.

Forkert, P. G. 2010. Mechanisms of lung tumorigenesis by ethyl carbamate and vinyl carbamate. *Drug Metab. Rev.* 42 (2):355-78.

Freeman-Anderson, N. E., et al. 2009. Expression of the Arf tumor suppressor gene is controlled by Tgfbeta2 during development. *Development* 136 (12):2081-9.

Gannon, H. S., et al. 2011. Mdm2-p53 signaling regulates epidermal stem cell senescence and premature aging phenotypes in mouse skin. *Dev. Biol.* 353 (1):1-9.

Gao, N., et al. 2001. The exogenous wild-type p14ARF gene induces growth arrest and promotes radiosensitivity in human lung cancer cell lines. *J. Cancer Res. Clin. Oncol.* 127 (6):359-67.

Gautschi, O., et al. 2007. Cyclin D1 in non-small cell lung cancer: a key driver of malignant transformation. *Lung Cancer* 55 (1):1-14.

Ghanayem, B. I. 2007. Inhibition of urethane-induced carcinogenicity in cyp2e1-/- in comparison to cyp2e1+/+ mice. *Toxicol. Sci.* 95 (2):331-9.

Gibbs, J. B., et al. 1984. Intrinsic GTPase activity distinguishes normal and oncogenic ras p21 molecules. *Proc. Natl. Acad. Sci. U. S. A.* 81 (18):5704-8.

Gil, J., and G. Peters. 2006. Regulation of the INK4b-ARF-INK4a tumour suppressor locus: all for one or one for all. *Nat. Rev. Mol. Cell Biol.* 7 (9):667-77.

Gilley, J., and M. Fried. 2001. One INK4 gene and no ARF at the Fugu equivalent of the human INK4A/ARF/INK4B tumour suppressor locus. *Oncogene* 20 (50):7447-52.

Gonzalez, S., et al. 2006. Oncogenic activity of Cdc6 through repression of the INK4/ARF locus. *Nature* 440 (7084):702-6.

Gorgoulis, V. G., et al. 2005. Activation of the DNA damage checkpoint and genomic instability in human precancerous lesions. *Nature* 434 (7035):907-13.

Gromley, A., et al. 2009. Transient expression of the Arf tumor suppressor during male germ cell and eye development in Arf-Cre reporter mice. *Proc. Natl. Acad. Sci. U. S. A.* 106 (15):6285-90.

Gu, J., et al. 2006. Aberrant promoter methylation profile and association with survival in patients with non-small cell lung cancer. *Clin. Cancer Res.* 12 (24):7329-38.

Gunning, W. T., et al. 1991. Glyceraldehyde-3-phosphate dehydrogenase and other enzymatic activity in normal mouse lung and in lung tumors. *Exp. Lung Res.* 17 (2):255-61.

Hahn, W. C., et al. 1999. Creation of human tumour cells with defined genetic elements. *Nature* 400 (6743):464-8.

Hahn, W. C., and R. A. Weinberg. 2002. Modelling the molecular circuitry of cancer. *Nat. Rev. Cancer* 2 (5):331-41.

Haigis, K. M., et al. 2008. Differential effects of oncogenic K-Ras and N-Ras on proliferation, differentiation and tumor progression in the colon. *Nat. Genet.* 40 (5):600-8.

Hanahan, D., and R. A. Weinberg. 2011. Hallmarks of cancer: the next generation. *Cell* 144 (5):646-74.

Harvey, J. J. 1964. An Unidentified Virus Which Causes the Rapid Production of Tumours in Mice. *Nature* 204:1104-5.

Herbst, R. S., et al. 2008. Lung cancer. *N. Engl. J. Med.* 359 (13):1367-80.

Hollstein, M., et al. 1994. p53 mutations at A:T base pairs in angiosarcomas of vinyl chloride-exposed factory workers. *Carcinogenesis* 15 (1):1-3.

Horio, Y., et al. 1996. Ki-ras and p53 mutations are early and late events, respectively, in urethane-induced pulmonary carcinogenesis in A/J mice. *Mol. Carcinog.* 17 (4):217-23.

Hozo, I., et al. 2000. Liver angiosarcoma and hemangiopericytoma after occupational exposure to vinyl chloride monomer. *Environ. Health Perspect.* 108 (8):793-5.

Huang, H. Y., et al. 2005. Ewing sarcomas with p53 mutation or p16/p14ARF homozygous deletion: a highly lethal subset associated with poor chemoresponse. *Journal of clinical oncology : official journal of the American Society of Clinical Oncology* 23 (3):548-58.

Inai, K., et al. 1991. Quantitative risk assessment of carcinogenicity of urethane (ethyl carbamate) on the basis of long-term oral administration to B6C3F1 mice. *Japanese journal of cancer research : Gann* 82 (4):380-5.

Inoue, K., et al. 1999. Induction of ARF tumor suppressor gene expression and cell cycle arrest by transcription factor DMP1. *Proc. Natl. Acad. Sci. U. S. A.* 96 (7):3993-8.

Inoue, K., et al. 2000. Disruption of the ARF transcriptional activator DMP1 facilitates cell immortalization, Ras transformation, and tumorigenesis. *Genes Dev.* 14 (14):1797-809.

Jackson, E. L., et al. 2005. The differential effects of mutant p53 alleles on advanced murine lung cancer. *Cancer Res.* 65 (22):10280-8.

Jacobs, J. J., et al. 2000. Senescence bypass screen identifies TBX2, which represses Cdkn2a (p19(ARF)) and is amplified in a subset of human breast cancers. *Nat. Genet.* 26 (3):291-9.

Jacobs, J. J., et al. 1999. The oncogene and Polycomb-group gene bmi-1 regulates cell proliferation and senescence through the ink4a locus. *Nature* 397 (6715):164-8.

Janku, F., et al. 2010. Targeted therapy in non-small-cell lung cancer--is it becoming a reality? *Nature reviews. Clinical oncology* 7 (7):401-14.

Jemal, A., et al. 2011. Global cancer statistics. *CA. Cancer J. Clin.* 61 (2):69-90.

Johnson, L., et al. 1997. K-ras is an essential gene in the mouse with partial functional overlap with N-ras. *Genes Dev.* 11 (19):2468-81.

Johnson, L., et al. 2001. Somatic activation of the K-ras oncogene causes early onset lung cancer in mice. *Nature* 410 (6832):1111-6.

Jones, S. N., et al. 1995. Rescue of embryonic lethality in Mdm2-deficient mice by absence of p53. *Nature* 378 (6553):206-8.

Junttila, M. R., et al. 2010. Selective activation of p53-mediated tumour suppression in high-grade tumours. *Nature* 468 (7323):567-71.

Kamata, T., and J. R. Feramisco. 1984. Epidermal growth factor stimulates guanine nucleotide binding activity and phosphorylation of ras oncogene proteins. *Nature* 310 (5973):147-50.

Kamb, A., et al. 1994. A cell cycle regulator potentially involved in genesis of many tumor types. *Science* 264 (5157):436-40.

Kamijo, T., et al. 1999. Tumor spectrum in ARF-deficient mice. *Cancer Res.* 59 (9):2217-22.

Kamijo, T., et al. 1997. Tumor suppression at the mouse INK4a locus mediated by the alternative reading frame product p19ARF. *Cell* 91 (5):649-59.

Karnoub, A. E., and R. A. Weinberg. 2008. Ras oncogenes: split personalities. *Nat Rev Mol Cell Biol* 9 (7):517-31.

Kawagishi, H., et al. 2010. ARF suppresses tumor angiogenesis through translational control of VEGFA mRNA. *Cancer Res.* 70 (11):4749-58.

Kawamoto, S., et al. 1961. Influence of urethan on the development of spontaneous leukemia and on the induction of hemagiomas in the AKR and C58 strains of mice. *Cancer Res.* 21:71-4.

Kazianis, S., et al. 1999. Comparative structure and characterization of a CDKN2 gene in a Xiphophorus fish melanoma model. *Oncogene* 18 (36):5088-99.

Kelly-Spratt, K. S., et al. 2004. p19Arf suppresses growth, progression, and metastasis of Hras-driven carcinomas through p53-dependent and -independent pathways. *PLoS biology* 2 (8):E242.

Kelly-Spratt, K. S., et al. 2009. Inhibition of PI-3K restores nuclear p27Kip1 expression in a mouse model of Kras-driven lung cancer. *Oncogene* 28 (41):3652-62.

Kemp, C. J. 1995. Hepatocarcinogenesis in p53-deficient mice. *Mol. Carcinog.* 12 (3):132-6.

Kemp, C. J. 2005. Multistep skin cancer in mice as a model to study the evolution of cancer cells. *Semin. Cancer Biol.* 15 (6):460-73.

Khan, S. H., et al. 2000. Differential requirement for p19ARF in the p53-dependent arrest induced by DNA damage, microtubule disruption, and ribonucleotide depletion. *Proc. Natl. Acad. Sci. U. S. A.* 97 (7):3266-71.

Kim, C. F., et al. 2005. Identification of bronchioalveolar stem cells in normal lung and lung cancer. *Cell* 121 (6):823-35.

Kim, S. H., et al. 2003. Absence of p16INK4a and truncation of ARF tumor suppressors in chickens. *Proc. Natl. Acad. Sci. U. S. A.* 100 (1):211-6.

Kirsten, W. H., and L. A. Mayer. 1967. Morphologic responses to a murine erythroblastosis virus. *J. Natl. Cancer Inst.* 39 (2):311-35.

Kitaguchi, S., et al. 1998. Proliferative activity, p53 expression and loss of heterozygosity on 3p, 9p and 17p in atypical adenomatous hyperplasia of the lung. *Hiroshima J. Med. Sci.* 47 (1):17-25.

Koch, M., et al. 2008. Malignant tumors of blood vessels: angiosarcomas, hemangioendotheliomas, and hemangiopericytomas. *J. Surg. Oncol.* 97 (4):321-9.

Komori, H., et al. 2005. Distinct E2F-mediated transcriptional program regulates p14ARF gene expression. *EMBO J.* 24 (21):3724-36.

Korgaonkar, C., et al. 2002. ARF function does not require p53 stabilization or Mdm2 relocalization. *Mol. Cell. Biol.* 22 (1):196-206.

Kosemehmetoglu, K., et al. 2011. Morphological and immunohistochemical features of malignant vascular tumors with special emphasis on GLUT1, and FKBP12 expressions. *Turk Patoloji Derg* 27 (1):57-67.

Krimpenfort, P., et al. 2001. Loss of p16Ink4a confers susceptibility to metastatic melanoma in mice. *Nature* 413 (6851):83-6.

Kuo, M. L., et al. 2003. Arf induces p53-dependent and -independent antiproliferative genes. *Cancer Res.* 63 (5):1046-53.

Land, H., et al. 1983. Tumorigenic conversion of primary embryo fibroblasts requires at least two cooperating oncogenes. *Nature* 304 (5927):596-602.

Lavoie, J. N., et al. 1996. A temporal and biochemical link between growth factor-activated MAP kinases, cyclin D1 induction and cell cycle entry. *Prog. Cell Cycle Res.* 2:49-58.

Lee, F. I., et al. 1996. Occupationally related angiosarcoma of the liver in the United Kingdom 1972-1994. *Gut* 39 (2):312-8.

Li, H., et al. 2009. The Ink4/Arf locus is a barrier for iPS cell reprogramming. *Nature* 460 (7259):1136-9.

Li, Q., et al. 2011. Hematopoiesis and leukemogenesis in mice expressing oncogenic NrasG12D from the endogenous locus. *Blood* 117 (6):2022-32.

Lin, A. W., et al. 1998. Premature senescence involving p53 and p16 is activated in response to constitutive MEK/MAPK mitogenic signaling. *Genes Dev.* 12 (19):3008-19.

Lin, A. W., and S. W. Lowe. 2001. Oncogenic ras activates the ARF-p53 pathway to suppress epithelial cell transformation. *Proc. Natl. Acad. Sci. U. S. A.* 98 (9):5025-30.

Lindstrom, M. S., and K. G. Wiman. 2003. Myc and E2F1 induce p53 through p14ARF-independent mechanisms in human fibroblasts. *Oncogene* 22 (32):4993-5005.

Lingbeek, M. E., et al. 2002. The T-box repressors TBX2 and TBX3 specifically regulate the tumor suppressor gene p14ARF via a variant T-site in the initiator. *J. Biol. Chem.* 277 (29):26120-7.

Llanos, S., et al. 2001. Stabilization of p53 by p14ARF without relocation of MDM2 to the nucleolus. *Nature cell biology* 3 (5):445-52.

Lowe, S. W., et al. 2004. Intrinsic tumour suppression. *Nature* 432 (7015):307-15.

Lowe, S. W., and C. J. Sherr. 2003. Tumor suppression by Ink4a-Arf: progress and puzzles. *Curr. Opin. Genet. Dev.* 13 (1):77-83.

Lynch, T. J., et al. 2004. Activating mutations in the epidermal growth factor receptor underlying responsiveness of non-small-cell lung cancer to gefitinib. *N. Engl. J. Med.* 350 (21):2129-39.

Ma, W., et al. 2003. Hepatic vascular tumors, angiectasis in multiple organs, and impaired spermatogenesis in mice with conditional inactivation of the VHL gene. *Cancer Res.* 63 (17):5320-8.

Macleod, K. F., et al. 1995. p53-dependent and independent expression of p21 during cell growth, differentiation, and DNA damage. *Genes Dev.* 9 (8):935-44.

Maeda, T., et al. 2005. Role of the proto-oncogene Pokemon in cellular transformation and ARF repression. *Nature* 433 (7023):278-85.

Maestro, R., et al. 1999. Twist is a potential oncogene that inhibits apoptosis. *Genes Dev.* 13 (17):2207-17.

Maher, E. A., et al. 2001. Malignant glioma: genetics and biology of a grave matter. *Genes Dev.* 15 (11):1311-33.

Malkinson, A. M. 2001. Primary lung tumors in mice as an aid for understanding, preventing, and treating human adenocarcinoma of the lung. *Lung Cancer* 32 (3):265-79.

Mallakin, A., et al. 2006. Expression of Dmp1 in specific differentiated, nonproliferating cells and its regulation by E2Fs. *Oncogene* 25 (59):7703-13.

Manenti, G., et al. 1997. Genetic mapping of lung cancer modifier loci specifically affecting tumor initiation and progression. *Cancer Res.* 57 (19):4164-6.

Mao, L., et al. 1995. A novel p16INK4A transcript. *Cancer Res.* 55 (14):2995-7.

Marchetti, A., et al. 1996. p21 RNA and protein expression in non-small cell lung carcinomas: evidence of p53-independent expression and association with tumoral differentiation. *Oncogene* 12 (6):1319-24.

Marion, M. J., et al. 1991. Activation of Ki-ras gene by point mutation in human liver angiosarcoma associated with vinyl chloride exposure. *Mol. Carcinog.* 4 (6):450-4.

Mark, R. J., et al. 1996. Angiosarcoma. A report of 67 patients and a review of the literature. *Cancer* 77 (11):2400-6.

Maronpot, R. R., et al. 1995. Mutations in the ras proto-oncogene: clues to etiology and molecular pathogenesis of mouse liver tumors. *Toxicology* 101 (3):125-56.

Martelli, F., et al. 2001. p19ARF targets certain E2F species for degradation. *Proc. Natl. Acad. Sci. U. S. A.* 98 (8):4455-60.

Martin, A. C., et al. 2004. Pathogenesis of persistent hyperplastic primary vitreous in mice lacking the arf tumor suppressor gene. *Invest. Ophthalmol. Vis. Sci.* 45 (10):3387-96.

Mason, R. J., et al. 2000. Surfactant protein C expression in urethane-induced murine pulmonary tumors. *Am. J. Pathol.* 156 (1):175-82.

Mason, S. L., et al. 2002. p14(ARF) regulates E2F activity. *Oncogene* 21 (27):4220-30.

McKeller, R. N., et al. 2002. The Arf tumor suppressor gene promotes hyaloid vascular regression during mouse eye development. *Proc. Natl. Acad. Sci. U. S. A.* 99 (6):3848-53.

Midgley, C. A., et al. 2000. An N-terminal p14ARF peptide blocks Mdm2-dependent ubiquitination in vitro and can activate p53 in vivo. *Oncogene* 19 (19):2312-23.

Montes de Oca Luna, R., et al. 1995. Rescue of early embryonic lethality in mdm2-deficient mice by deletion of p53. *Nature* 378 (6553):203-6.

Moore, L., et al. 2003. Cooperativity of p19ARF, Mdm2, and p53 in murine tumorigenesis. *Oncogene* 22 (49):7831-7.

Mori, S., et al. 2004. p53 apoptotic pathway molecules are frequently and simultaneously altered in nonsmall cell lung carcinoma. *Cancer* 100 (8):1673-82.

Mounawar, M., et al. 2007. Patterns of EGFR, HER2, TP53, and KRAS mutations of p14arf expression in non-small cell lung cancers in relation to smoking history. *Cancer Res.* 67 (12):5667-72.

Mulcahy, L. S., et al. 1985. Requirement for ras proto-oncogene function during serum-stimulated growth of NIH 3T3 cells. *Nature* 313 (5999):241-3.

Naka, N., et al. 1997. Mutations of p53 tumor-suppressor gene in angiosarcoma. *International journal of cancer. Journal international du cancer* 71 (6):952-5.

Navarro, P., et al. 1991. A role for the E-cadherin cell-cell adhesion molecule during tumor progression of mouse epidermal carcinogenesis. *J. Cell Biol.* 115 (2):517-33.

Nelson, M. A., et al. 1992. Detection of mutant Ha-ras genes in chemically initiated mouse skin epidermis before the development of benign tumors. *Proc. Natl. Acad. Sci. U. S. A.* 89 (14):6398-402.

Nicholson, S. A., et al. 2001. Alterations of p14ARF, p53, and p73 genes involved in the E2F-1-mediated apoptotic pathways in non-small cell lung carcinoma. *Cancer Res.* 61 (14):5636-43.

Nieto, M. A. 2011. The ins and outs of the epithelial to mesenchymal transition in health and disease. *Annu. Rev. Cell Dev. Biol.* 27:347-76.

Niini, T., et al. 2011. Array comparative genomic hybridization reveals frequent alterations of G1/S checkpoint genes in undifferentiated pleomorphic sarcoma of bone. *Genes. Chromosomes Cancer* 50 (5):291-306.

Nikitin, A. Y., et al. 2004. Classification of proliferative pulmonary lesions of the mouse: recommendations of the mouse models of human cancers consortium. *Cancer Res.* 64 (7):2307-16.

Nobori, T., et al. 1994. Deletions of the cyclin-dependent kinase-4 inhibitor gene in multiple human cancers. *Nature* 368 (6473):753-6.

Normand, G., et al. 2005. p14ARF induces G2 cell cycle arrest in p53- and p21-deficient cells by down-regulating p34cdc2 kinase activity. *J. Biol. Chem.* 280 (8):7118-30.

Oda, Y., et al. 2005. Frequent alteration of p16(INK4a)/p14(ARF) and p53 pathways in the round cell component of myxoid/round cell liposarcoma: p53 gene alterations and reduced p14(ARF) expression both correlate with poor prognosis. *The Journal of pathology* 207 (4):410-21.

Oh, J. H., et al. 2006. Aberrant methylation of p14ARF gene correlates with poor survival in osteosarcoma. *Clin. Orthop.* 442:216-22.

Okamoto, A., et al. 1995. Mutations in the p16INK4/MTS1/CDKN2, p15INK4B/MTS2, and p18 genes in primary and metastatic lung cancer. *Cancer Res.* 55 (7):1448-51.

Olivier, M., et al. 2010. TP53 mutations in human cancers: origins, consequences, and clinical use. *Cold Spring Harbor perspectives in biology* 2 (1):a001008.

Packenham, J. P., et al. 1995. Homozygous deletions at chromosome 9p21 and mutation analysis of p16 and p15 in microdissected primary non-small cell lung cancers. *Clin. Cancer Res.* 1 (7):687-90.

Paez, J. G., et al. 2004. EGFR mutations in lung cancer: correlation with clinical response to gefitinib therapy. *Science* 304 (5676):1497-500.

Palmero, I., et al. 2002. Activation of ARF by oncogenic stress in mouse fibroblasts is independent of E2F1 and E2F2. *Oncogene* 21 (19):2939-47.

Palmero, I., et al. 1998. p19ARF links the tumour suppressor p53 to Ras. *Nature* 395 (6698):125-6.

Pao, W., et al. 2004. EGF receptor gene mutations are common in lung cancers from "never smokers" and are associated with sensitivity of tumors to gefitinib and erlotinib. *Proc. Natl. Acad. Sci. U. S. A.* 101 (36):13306-11.

Pao, W., et al. 2005. KRAS mutations and primary resistance of lung adenocarcinomas to gefitinib or erlotinib. *PLoS medicine* 2 (1):e17.

Papageorge, A., et al. 1982. Comparative biochemical properties of p21 ras molecules coded for by viral and cellular ras genes. *J. Virol.* 44 (2):509-19.

Parada, L. F., et al. 1982. Human EJ bladder carcinoma oncogene is homologue of Harvey sarcoma virus ras gene. *Nature* 297 (5866):474-8.

Parisi, T., et al. 2002. Transcriptional regulation of the human tumor suppressor p14(ARF) by E2F1, E2F2, E2F3, and Sp1-like factors. *Biochem. Biophys. Res. Commun.* 291 (5):1138-45.

Park, M. J., et al. 2003. Pathogenetic and biologic significance of TP14ARF alterations in nonsmall cell lung carcinoma. *Cancer Genet. Cytogenet.* 141 (1):5-13.

Pelosi, G., et al. 2010. Review article: pulmonary sarcomatoid carcinomas: a practical overview. *International journal of surgical pathology* 18 (2):103-20.

Philipp-Staheli, J., et al. 2002. Pathway-specific tumor suppression. Reduction of p27 accelerates gastrointestinal tumorigenesis in Apc mutant mice, but not in Smad3 mutant mice. *Cancer cell* 1 (4):355-68.

Pomerantz, J., et al. 1998. The Ink4a tumor suppressor gene product, p19Arf, interacts with MDM2 and neutralizes MDM2's inhibition of p53. *Cell* 92 (6):713-23.

Pontano, L. L., et al. 2008. Genotoxic stress-induced cyclin D1 phosphorylation and proteolysis are required for genomic stability. *Mol. Cell. Biol.* 28 (23):7245-58.

Pontano, L. L., and J. A. Diehl. 2008. Speeding through cell cycle roadblocks: Nuclear cyclin D1-dependent kinase and neoplastic transformation. *Cell division* 3:12.

Potenza, N., et al. 2005. Replacement of K-Ras with H-Ras supports normal embryonic development despite inducing cardiovascular pathology in adult mice. *EMBO reports* 6 (5):432-7.

Przygodzki, R. M., et al. 1997. Sporadic and Thorotrast-induced angiosarcomas of the liver manifest frequent and multiple point mutations in K-ras-2. *Laboratory investigation; a journal of technical methods and pathology* 76 (1):153-9.

Pylayeva-Gupta, Y., et al. 2011. RAS oncogenes: weaving a tumorigenic web. *Nat. Rev. Cancer* 11 (11):761-74.

Quelle, D. E., et al. 1993. Overexpression of mouse D-type cyclins accelerates G1 phase in rodent fibroblasts. *Genes Dev.* 7 (8):1559-71.

Quelle, D. E., et al. 1997. Cancer-associated mutations at the INK4a locus cancel cell cycle arrest by p16INK4a but not by the alternative reading frame protein p19ARF. *Proc. Natl. Acad. Sci. U. S. A.* 94 (2):669-73.

Quelle, D. E., et al. 1995. Alternative reading frames of the INK4a tumor suppressor gene encode two unrelated proteins capable of inducing cell cycle arrest. *Cell* 83 (6):993-1000.

Radfar, A., et al. 1998. p19(Arf) induces p53-dependent apoptosis during abelson virus-mediated pre-B cell transformation. *Proc. Natl. Acad. Sci. U. S. A.* 95 (22):13194-9.

Randerson-Moor, J. A., et al. 2001. A germline deletion of p14(ARF) but not CDKN2A in a melanoma-neural system tumour syndrome family. *Hum. Mol. Genet.* 10 (1):55-62.

Regala, R. P., et al. 2011. Matrix metalloproteinase-10 promotes Kras-mediated bronchio-alveolar stem cell expansion and lung cancer formation. *PloS one* 6 (10):e26439.

Rizos, H., et al. 2007. p14ARF regulates E2F-1 ubiquitination and degradation via a p53-dependent mechanism. *Cell cycle* 6 (14):1741-7.

Robertson, K. D., and P. A. Jones. 1998. The human ARF cell cycle regulatory gene promoter is a CpG island which can be silenced by DNA methylation and down-regulated by wild-type p53. *Mol. Cell. Biol.* 18 (11):6457-73.

Robinson, D. A., et al. 1987. Magnetic resonance imaging of the solitary hepatic mass: direct correlation with pathology and computed tomography. *Clin. Radiol.* 38 (6):559-68.

Rodenhuis, S., et al. 1988. Incidence and possible clinical significance of K-ras oncogene activation in adenocarcinoma of the human lung. *Cancer Res.* 48 (20):5738-41.

Rowland, B. D., et al. 2002. E2F transcriptional repressor complexes are critical downstream targets of p19(ARF)/p53-induced proliferative arrest. *Cancer cell* 2 (1):55-65.

Ruas, M., and G. Peters. 1998. The p16INK4a/CDKN2A tumor suppressor and its relatives. *Biochim. Biophys. Acta* 1378 (2):F115-77.

Ruley, H. E. 1983. Adenovirus early region 1A enables viral and cellular transforming genes to transform primary cells in culture. *Nature* 304 (5927):602-6.

Sanchez-Cespedes, M., et al. 1999. Inactivation of the INK4A/ARF locus frequently coexists with TP53 mutations in non-small cell lung cancer. *Oncogene* 18 (43):5843-9.

Santos, E., et al. 1982. T24 human bladder carcinoma oncogene is an activated form of the normal human homologue of BALB- and Harvey-MSV transforming genes. *Nature* 298 (5872):343-7.

Saporita, A. J., et al. 2007. Therapeutic targets in the ARF tumor suppressor pathway. *Curr. Med. Chem.* 14 (17):1815-27.

Scheffzek, K., et al. 1997. The Ras-RasGAP complex: structural basis for GTPase activation and its loss in oncogenic Ras mutants. *Science* 277 (5324):333-8.

Schmalhofer, O., et al. 2009. E-cadherin, beta-catenin, and ZEB1 in malignant progression of cancer. *Cancer Metastasis Rev.* 28 (1-2):151-66.

Schmeltz, I., et al. 1978. Formation and Determination of Ethyl Carbamate in Tobacco and Tobacco-Smoke. *J. Anal. Toxicol.* 2 (6):265-268.

Schreiber, E., et al. 1989. Rapid detection of octamer binding proteins with 'mini-extracts', prepared from a small number of cells. *Nucleic Acids Res* 17 (15):6419.

Scolnick, E. M., et al. 1979. Guanine nucleotide-binding activity as an assay for src protein of rat-derived murine sarcoma viruses. *Proc. Natl. Acad. Sci. U. S. A.* 76 (10):5355-9.

Scolnick, E. M., and W. P. Parks. 1974. Harvey sarcoma virus: a second murine type C sarcoma virus with rat genetic information. *J. Virol.* 13 (6):1211-9.

Scolnick, E. M., et al. 1973. Studies on the nucleic acid sequences of Kirsten sarcoma virus: a model for formation of a mammalian RNA-containing sarcoma virus. *J. Virol.* 12 (3):458-63.

SEER Cancer Statistics Review, 1975-2008. ed N. A. Howlader N, Krapcho M, Neyman N, Aminou R, Waldron W, Altekruse SF, Kosary CL, Ruhl J, Tatalovich Z, Cho H, Mariotto A, Eisner MP, Lewis DR, Chen HS, Feuer EJ, Cronin KA, Edward BK. Bethesda, MD: National Cancer Institute. http://seer.cancer.gov/csr/1975_2008/ (accessed 2011).

Selamat, S. A., et al. 2011. DNA methylation changes in atypical adenomatous hyperplasia, adenocarcinoma in situ, and lung adenocarcinoma. *PloS one* 6 (6):e21443.

Serakinci, N., et al. 2004. Adult human mesenchymal stem cell as a target for neoplastic transformation. *Oncogene* 23 (29):5095-8.

Serrano, M., et al. 1993. A new regulatory motif in cell-cycle control causing specific inhibition of cyclin D/CDK4. *Nature* 366 (6456):704-7.

Serrano, M., et al. 1996. Role of the INK4a locus in tumor suppression and cell mortality. *Cell* 85 (1):27-37.

Serrano, M., et al. 1997. Oncogenic ras provokes premature cell senescence associated with accumulation of p53 and p16INK4a. *Cell* 88 (5):593-602.

Sharpless, E., and L. Chin. 2003. The INK4a/ARF locus and melanoma. *Oncogene* 22 (20):3092-8.

Sharpless, N. E., et al. 2001. Loss of p16Ink4a with retention of p19Arf predisposes mice to tumorigenesis. *Nature* 413 (6851):86-91.

Sherr, C. J. 2006. Divorcing ARF and p53: an unsettled case. *Nat. Rev. Cancer* 6 (9):663-73.

Sherr, C. J., and R. A. DePinho. 2000. Cellular senescence: mitotic clock or culture shock? *Cell* 102 (4):407-10.

Sherr, C. J., and F. McCormick. 2002. The RB and p53 pathways in cancer. *Cancer cell* 2 (2):103-12.

Silva, R. L., et al. 2005. Arf-dependent regulation of Pdgf signaling in perivascular cells in the developing mouse eye. *The EMBO journal* 24 (15):2803-14.

Slebos, R. J., et al. 1991. Relationship between K-ras oncogene activation and smoking in adenocarcinoma of the human lung. *J. Natl. Cancer Inst.* 83 (14):1024-7.

Smyth, G. K. 2004. Linear models and empirical bayes methods for assessing differential expression in microarray experiments. *Statistical applications in genetics and molecular biology* 3:Article3.

Sreeramaneni, R., et al. 2005. Ras-Raf-Arf signaling critically depends on the Dmp1 transcription factor. *Mol. Cell. Biol.* 25 (1):220-32.

Stacey, D. W., and H. F. Kung. 1984. Transformation of NIH 3T3 cells by microinjection of Ha-ras p21 protein. *Nature* 310 (5977):508-11.

Stone, S., et al. 1995. Complex structure and regulation of the P16 (MTS1) locus. *Cancer Res.* 55 (14):2988-94.

Sundberg, J. P., et al. 1997. Comparison of chemical carcinogen skin tumor induction efficacy in inbred, mutant, and hybrid strains of mice: morphologic variations of induced tumors and absence of a papillomavirus cocarcinogen. *Mol. Carcinog.* 20 (1):19-32.

Sweet, R. W., et al. 1984. The product of ras is a GTPase and the T24 oncogenic mutant is deficient in this activity. *Nature* 311 (5983):273-5.

Takahashi, T., et al. 1989. p53: a frequent target for genetic abnormalities in lung cancer. *Science* 246 (4929):491-4.

Takahira, T., et al. 2004. Alterations of the p16INK4a/p14ARF pathway in clear cell sarcoma. *Cancer Sci.* 95 (8):651-5.

Tam, A. S., et al. 2003. Perturbations of the Ink4a/Arf gene locus in aflatoxin B1-induced mouse lung tumors. *Carcinogenesis* 24 (1):121-32.

Tannenbaum, A., and C. Maltoni. 1962. Neoplastic response of various tissues to the administration of urethan. *Cancer Res.* 22:1105-12.

Tannenbaum, A., and H. Silverstone. 1958. Urethan (ethyl carbamate) as a multipotential carcinogen. *Cancer Res.* 18 (10):1225-31.

Tao, W., and A. J. Levine. 1999. P19(ARF) stabilizes p53 by blocking nucleo-cytoplasmic shuttling of Mdm2. *Proc. Natl. Acad. Sci. U. S. A.* 96 (12):6937-41.

Thaete, L. G., and A. M. Malkinson. 1991. Cells of origin of primary pulmonary neoplasms in mice: morphologic and histochemical studies. *Exp. Lung Res.* 17 (2):219-28.

Thompson, L., et al. 1996. Monoclonal origins of malignant mixed tumors (carcinosarcomas). Evidence for a divergent histogenesis. *Am. J. Surg. Pathol.* 20 (3):277-85.

Thoolen, B., et al. 2010. Proliferative and nonproliferative lesions of the rat and mouse hepatobiliary system. *Toxicol. Pathol.* 38 (7 Suppl):5S-81S.

Thornton, J. D., et al. 2005. The Arf tumor suppressor regulates platelet-derived growth factor receptor beta signaling: a new view through the eyes of Arf(-/-) mice. *Cell cycle* 4 (10):1316-9.

To, M. D., et al. 2008. Kras regulatory elements and exon 4A determine mutation specificity in lung cancer. *Nat. Genet.* 40 (10):1240-4.

Travis, W. D., et al. 2011. International association for the study of lung cancer/american thoracic society/european respiratory society international multidisciplinary

classification of lung adenocarcinoma. *Journal of thoracic oncology : official publication of the International Association for the Study of Lung Cancer* 6 (2):244-85.

Valencia, C., et al. 2008. Human papillomavirus E6/E7 oncogenes promote mouse ear regeneration by increasing the rate of wound re-epithelization and epidermal growth. *J. Invest. Dermatol.* 128 (12):2894-903.

Vesselinovitch, S. D., and N. Mihailovich. 1968a. The development of neurogenic neoplasms, embryonal kidney tumors, harderian gland adenomas, anitschkow cell sarcomas of the heart, and other neoplasms in urethan-treated newborn rats. *Cancer Res.* 28 (5):888-97.

Vesselinovitch, S. D., and N. Mihailovich. 1968b. The induction of benign and malignant liver tumors by urethan in newborn rats. *Cancer Res.* 28 (5):881-7.

Vonlanthen, S., et al. 1998. Expression of p16INK4a/p16alpha and p19ARF/p16beta is frequently altered in non-small cell lung cancer and correlates with p53 overexpression. *Oncogene* 17 (21):2779-85.

Voorhoeve, P. M., and R. Agami. 2003. The tumor-suppressive functions of the human INK4A locus. *Cancer cell* 4 (4):311-9.

Wang, Y. C., et al. 2005. Wild-type p53 overexpression and its correlation with MDM2 and p14ARF alterations: an alternative pathway to non-small-cell lung cancer. *J. Clin. Oncol.* 23 (1):154-64.

Wang, Y., et al. 2006. A mouse model for tumor progression of lung cancer in ras and p53 transgenic mice. *Oncogene* 25 (8):1277-80.

Watanabe, T., et al. 2003. Deregulation of the TP53/p14ARF tumor suppressor pathway in low-grade diffuse astrocytomas and its influence on clinical course. *Clin. Cancer Res.* 9 (13):4884-90.

Weber, J. D., et al. 2000a. p53-independent functions of the p19(ARF) tumor suppressor. *Genes Dev.* 14 (18):2358-65.

Weber, J. D., et al. 2000b. Cooperative signals governing ARF-mdm2 interaction and nucleolar localization of the complex. *Mol. Cell. Biol.* 20 (7):2517-28.

Weber, J. D., et al. 1999. Nucleolar Arf sequesters Mdm2 and activates p53. *Nature cell biology* 1 (1):20-6.

Wei, W., et al. 2001. Role of p14(ARF) in replicative and induced senescence of human fibroblasts. *Mol. Cell. Biol.* 21 (20):6748-57.

Weihrauch, M., et al. 2002. Abnormalities of the ARF-p53 pathway in primary angiosarcomas of the liver. *Hum. Pathol.* 33 (9):884-92.

Wells, A., et al. 2008. E-cadherin as an indicator of mesenchymal to epithelial reverting transitions during the metastatic seeding of disseminated carcinomas. *Clin. Exp. Metastasis* 25 (6):621-8.

Westra, W. H. 2000. Early glandular neoplasia of the lung. *Respiratory research* 1 (3):163-9.

Westra, W. H., et al. 1996. K-ras oncogene activation in atypical alveolar hyperplasias of the human lung. *Cancer Res.* 56 (9):2224-8.

Westra, W. H., et al. 1993. K-ras oncogene activation in lung adenocarcinomas from former smokers. Evidence that K-ras mutations are an early and irreversible event in the development of adenocarcinoma of the lung. *Cancer* 72 (2):432-8.

Wick, M. R., and P. E. Swanson. 1993. Carcinosarcomas: current perspectives and an historical review of nosological concepts. *Semin. Diagn. Pathol.* 10 (2):118-27.

Xiong, Y., et al. 1993. Subunit rearrangement of the cyclin-dependent kinases is associated with cellular transformation. *Genes Dev.* 7 (8):1572-83.

Xu, X., et al. 2012. Evidence for type II cells as cells of origin of K-Ras-induced distal lung adenocarcinoma. *Proc. Natl. Acad. Sci. U. S. A.* 109 (13):4910-5.

Xue, Q., et al. 2002. Aberrant expression of pRb, p16, p14ARF, MDM2, p21 and p53 in stage I adenocarcinomas of the lung. *Pathol. Int.* 52 (2):103-9.

Yanagi, S., et al. 2007. Pten controls lung morphogenesis, bronchioalveolar stem cells, and onset of lung adenocarcinomas in mice. *J. Clin. Invest.* 117 (10):2929-40.

Yokoyama, K., et al. 2003. Increased invasion and matrix metalloproteinase-2 expression by Snail-induced mesenchymal transition in squamous cell carcinomas. *Int. J. Oncol.* 22 (4):891-8.

You, M., et al. 1989. Activation of the Ki-ras protooncogene in spontaneously occurring and chemically induced lung tumors of the strain A mouse. *Proc. Natl. Acad. Sci. U. S. A.* 86 (9):3070-4.

Young, N. P., and T. Jacks. 2010. Tissue-specific p19Arf regulation dictates the response to oncogenic K-ras. *Proc. Natl. Acad. Sci. U. S. A.* 107 (22):10184-9.

Zeng, Y., et al. 2011. p53 binds to and is required for the repression of Arf tumor suppressor by HDAC and polycomb. *Cancer Res.* 71 (7):2781-92.

Zerrouqi, A., et al. 2012. P14ARF inhibits human glioblastoma-induced angiogenesis by upregulating the expression of TIMP3. *J. Clin. Invest.* 122 (4):1283-95.

Zhang, B., et al. 2011. Cigarette smoking and p16INK4alpha gene promoter hypermethylation in non-small cell lung carcinoma patients: a meta-analysis. *PloS one* 6 (12):e28882.

Zhang, H. J., et al. 2010a. p14ARF interacts with E2F factors to form p14ARF-E2F/partner-DNA complexes repressing E2F-dependent transcription. *J. Cell. Biochem.* 109 (4):693-701.

Zhang, W., et al. 2010b. Comparison of the inhibitory effects of three transcriptional variants of CDKN2A in human lung cancer cell line A549. *J. Exp. Clin. Cancer Res.* 29:74.

Zhang, Y., and Y. Xiong. 1999. Mutations in human ARF exon 2 disrupt its nucleolar localization and impair its ability to block nuclear export of MDM2 and p53. *Mol. Cell* 3 (5):579-91.

Zhang, Y., et al. 1998. ARF promotes MDM2 degradation and stabilizes p53: ARF-INK4a locus deletion impairs both the Rb and p53 tumor suppression pathways. *Cell* 92 (6):725-34.

Zhang, Z., et al. 2002. A strong candidate gene for the Papg1 locus on mouse chromosome 4 affecting lung tumor progression. *Oncogene* 21 (38):5960-6.

Zheng, S., et al. 2007. A genetic mouse model for metastatic lung cancer with gender differences in survival. *Oncogene* 26 (48):6896-904.

Zhu, C. Q., et al. 2008. Role of KRAS and EGFR as biomarkers of response to erlotinib in National Cancer Institute of Canada Clinical Trials Group Study BR.21. *J. Clin. Oncol.* 26 (26):4268-75.

Zietz, C., et al. 1998. MDM-2 oncoprotein overexpression, p53 gene mutation, and VEGF up-regulation in angiosarcomas. *The American journal of pathology* 153 (5):1425-33.

Zimmerli, B., and J. Schlatter. 1991. Ethyl carbamate: analytical methodology, occurrence, formation, biological activity and risk assessment. *Mutat. Res.* 259 (3-4):325-50.

Zindy, F., et al. 1998. Myc signaling via the ARF tumor suppressor regulates p53-dependent apoptosis and immortalization. *Genes Dev.* 12 (15):2424-33.

Zindy, F., et al. 2003. Arf tumor suppressor promoter monitors latent oncogenic signals in vivo. *Proc. Natl. Acad. Sci. U. S. A.* 100 (26):15930-5.

CURRICULUM VITAE

Stephanie E Busch

EDUCATION

Ph.D., Molecular and Cellular Biology
University of Washington, Seattle, WA, 2012

B.A., Biological Sciences
University of Chicago, Chicago, IL, 2006

RESEARCH

Graduate Research Assistant, Fred Hutchinson Cancer Research Center; Seattle, WA
Division of Human Biology, June 2007 – May 2012
Advisor: Dr. Christopher Kemp
Dissertation Title: "Tumor Suppression by ARF in Carcinogen-Exposed Mice."

Summer Research Intern, Sanford Research; Sioux Falls, SD
Cardiovascular Health Research Center, June – September 2005, March – August 2006
Advisor: Dr. Qiangrong Liang

Undergraduate Researcher, University of Chicago; Chicago, IL
Department of Organismal Biology and Anatomy, October 2004 – March 2006
Advisor: Dr. Urs Schmidt-Ott

Microbiology Intern, South Dakota Department of Health; Pierre, SD
Public Health Laboratory, June – September 2004

PUBLICATIONS

1. **Busch SE**, Gurley KE, Moser RD, Kemp CJ. ARF suppresses hepatic vascular neoplasia in a carcinogen-exposed murine model. *J Pathol* 227, 298-305. 2012.
2. Lemke S, **Busch SE**, Antonopoulos DA, Meyer F, Domanus MH, Schmidt-Ott U. Maternal activation of gap genes in the hover fly Episyrphus. *Development* 137, 1709-19. 2010.
3. **Busch SE,** Gurley KE, Moser RD, Kelly-Spratt KS, Kemp CJ. ARF inhibits the growth and malignant progression of non-small cell lung carcinoma. In Preparation.
4. Kemp CJ, Moore JM, Moser RD, Smith LE, Rabaia N, **Busch SE**, Gurley KE, Lobanenkov VV, Liggett D, Filippova GN. The epigenetic regulator CTCF is a haploinsufficient tumor suppressor. In Preparation.